

Pyroclastic Geology of Towada Volcano

Yukio HAYAKAWA

Earthquake Research Institute, University of Tokyo

(Received October 21, 1985)

Abstract

The eruptive activity of Towada Volcano is documented by the tephrostratigraphic study. More than 20 eruptive episodes are described in detail with isopach maps and isograde maps of maximum pumice size, maximum lithic size, and median diameter for the individual fallout deposits.

The activity of the volcano started about 200,000 years ago along the NE-SW trending line crossing the present lake Towadako and relatively small-scale volcanoes were formed. A caldera 11 km \times 11 km wide was formed as a result of several eruptive episodes during the period about 55,000 to 13,000 years ago, three of which included voluminous pyroclastic flow eruptions. The post-caldera activity occurred at a rate of one eruptive episode every 1,000 to 2,000 years and a stratovolcano and two lava domes were formed in the caldera. The latest eruptive episode was dated 1,250 y B.P. by the radiocarbon method.

Rocks of Towada Volcano cover a wide range from basaltic andesite to rhyodacite (SiO₂: 51-70 wt. %) with phenocrysts of plagioclase, augite, hypersthene, and magnetite with occasional olivine. Hornblende is characteristically found in the pyroclastic deposits of 13,000 years old and in some earlier deposits.

Volumes, V , of two plinian deposits are determined by the crystal method: 6.7 km³ for the Chuseri deposit and 2.2 km³ for the Nambu deposit. Then an empirical formula, $V=12.2 TS$, is obtained for the practical volume estimation, where T is the thickness of an isopach and S is the area enclosed by the isopach. Application of the formula to the fallout deposits of Towada Volcano suggests that the total magma erupted during the past 55,000 years amounts to 1.5×10^{17} g. This corresponds to the discharge rate of dense rock equivalent to 1.1 km³ per thousand years.

The cross-wind range, R_c , of the pyroclasts of a given size may be a good indicator of the maximum height reached by the pyroclasts in the eruption column. It is found that the R_c is relatively large for those deposits whose erupted masses are relatively large. The

dispersal of a fallout deposit is also seriously affected by winds. A plausible solution of the eruption condition for the Nambu deposit is that 4 mm size lithic fragments reached the maximum height of 15 km in the eruption column, then they were detached from the column and displaced by winds having an average velocity of 30 m/s. After a 20 min flight, they fell upon the ground 48 km east of the source.

Whole-deposit grain size populations are determined for the Chuseri and Nambu plinian deposits. The Chuseri population is similar to the New Zealand examples. However, the Nambu population is distinctly coarser than the others.

Contents

1. Introduction	508
2. Geologic history	510
Basement and Early Pleistocene volcanoes	510
Towada Volcano	513
Pre-caldera volcanism	515
Formation of the Towadako caldera.....	517
Post-caldera volcanism	518
3. Petrography	518
4. Pyroclastic deposits	524
5. Volume and mass of fallout deposits.....	566
Crystal method	566
Empirical formula for volume estimation of a fallout deposit	573
6. Factors governing the dispersal of fallout deposits	578
Height reached by the pyroclasts.....	578
Wind velocity and direction.....	582
Grain size population of the eruption column	584
7. Conclusions	586
References	587

1. Introduction

Towada Volcano near the northern end of Honshu (Fig. 1) is one of the late Quaternary caldera volcanoes in Japan. Like others a large amount of pyroclastic deposits are distributed around the caldera. The deposits are freshly preserved and exposures are common in numerous road cuttings and banks of new fields on the mountainside, as well as in occasional stream sections. The tephrostratigraphy of Towada Volcano has been studied by Oike and his colleagues (*e.g.* OIKE, 1972; OIKE and NAKAGAWA, 1979). However, it can be more than simple stratigraphy because the measurement of thickness, grain size, and constitution of the deposits which are necessary for correlative purposes are of great volcan-

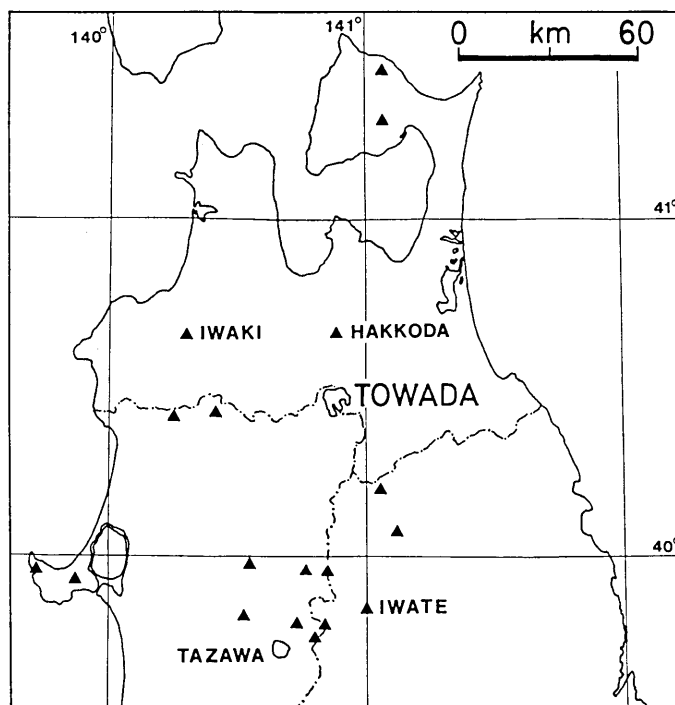


Fig. 1. Index map of Towada Volcano. Solid triangles are Quaternary volcanoes.

ological value in studying explosive volcanic eruptions. Recently, many volcanological studies of pyroclastic deposits have been performed from this point of view; they are those in the Azores (WALKER and CROASDALE, 1971; BOOTH *et al.*, 1978), New Zealand (WALKER, 1980, 1981a, b), Iceland (SPARKS *et al.*, 1981), and Mexico (WALKER *et al.*, 1981a).

In this paper, the geologic history and petrography of Towada Volcano are described first. Then, a description of pyroclastic deposits is presented, which documents the explosive volcanic activity over the past 50,000 years of the volcano's history, and the magnitude and dispersal of the pyroclastic fallout deposits are discussed.

Localities are expressed by three numbers in parentheses, *e.g.* (145: 8.6 km, 40°). They are the locality No., the distance and the azimuth from the center of the Nakanoumi crater, about 2 km SSE of the center of the caldera (Fig. 2).

2. Geologic history

KAWANO (1939), KUNO *et al.* (1964), and TANIGUCHI (1972) studied the geology of Towada Volcano and published the geologic maps. A new map (Fig. 2) is prepared from the author's own field work and the geologic history of Towada Volcano and adjacent areas is revealed. The result is summarized as a block diagram in Fig. 3.

Basement and Early Pleistocene volcanoes

The basement of this area is Miocene volcanic rocks and sediments, which are exposed on the lower parts of the western, northern, and eastern caldera walls (KAWANO, 1939). They are composed mostly of light green rhyolitic tuffs and associated with subordinate mudstone and lavas of andesite and dacite. They have undergone intense hydrothermal alteration and in some places embrace Kuroko ore deposits. The Namariyama mine on the western wall of the caldera is an example.

During the Early Pleistocene epoch, at least five volcanoes were formed in this area; namely, the Zakura Misaki, Minami Hakkoda, Towadayama, Towariyama, and Heraidake volcanoes (Fig. 4). The Zakura Misaki

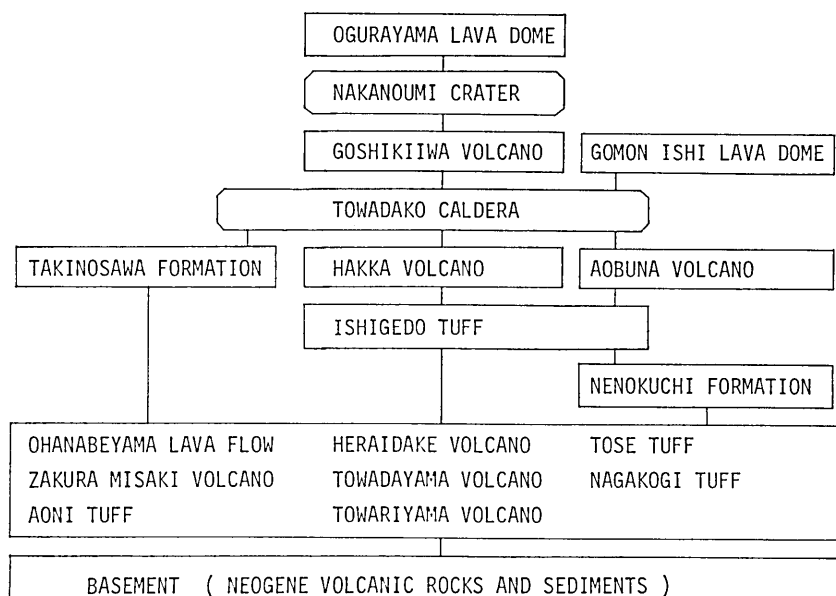


Fig. 3. Block diagram showing the geologic history of the Towada area.
Above the Ishigedo tuff is Towada Volcano.

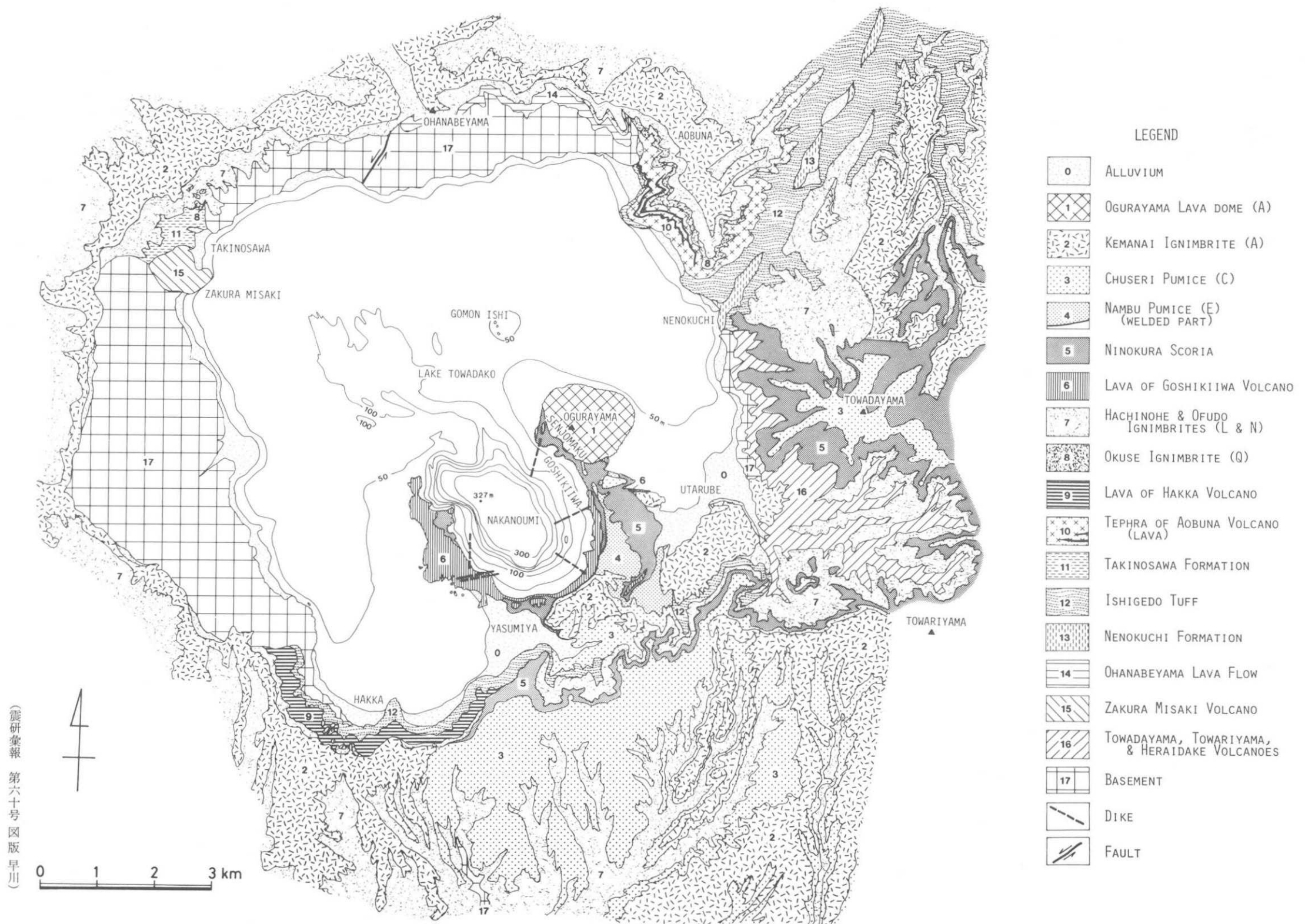


Fig. 2. Geologic map of Towada Volcano.

volcano, exposed on the northwestern corner of the caldera, is made up predominantly of andesite lava flows. The Minami Hakkoda volcano on the north of the caldera is a cluster of several cones mostly made up of lava flows. The Ohanabeyama lava flow on the middle part of the northern caldera wall is one of the constituents. The latter three volcanoes showing nearly conical shapes are situated to the east of the caldera. They are thickly covered by younger pyroclastic deposits and scarcely expose the andesite lava flows.

Three units of subaqueous tuffs of the early Pleistocene epoch are seen in places under thick accumulations of pyroclastic deposits of Towada Volcano. They are the Aoni tuff (1.6 ± 0.8 , 1.3 ± 0.8 Ma; MURAOKA and HASE, 1981), the Tose tuff (HAYAKAWA, 1983a), and the Nagakogi tuff (possibly the same as the Aoni tuff). Their type sections are listed in Table 6.

A lacustrine sediment, named the Nenokuchi formation, is exposed along the lower parts of the gorge of the Oirase river which drains the lake water to the north. It is composed predominantly of subhorizontally bedded silt at the lower part and conglomerate at the upper part. Fine tuff beds associated with fallout pumice beds (rhyolitic) are occasionally intercalated. Although the base is not exposed, the total thickness is estimated at about 100 m.

In the lower part of the Nenokuchi formation a section of a scoria cone crops out 3.5 km NNE of Nenokuchi ($145:8.6$ km, 40°). This, named the Oirase scoria cone, measures more than 340 m across and more than 18 m high. A bedded structure is seen and equant-shaped angular scoria lapilli are the main constituents. Fines ($<1/16$ mm) are mostly removed and ballistic lithic blocks up to 43 cm across are embedded. The scoria lapilli are moderately vesiculated but rimmed with water-chilled glassy surfaces. It is suggested that this eruption occurred under shallow-water conditions and the cone was formed under the water. At the marginal parts, the Oirase subaqueous scoria cone is directly overlain by a water-laid rhyolitic fine tuff bed.

The lake which had deposited the Nenokuchi formation was buried by voluminous ignimbrites erupted from the Tashirota caldera ($10 \text{ km} \times 7 \text{ km}$) about 20 km north of the Towadako caldera (KUNO *et al.*, 1964). They are named the Ishigedo tuff together with the intercalated fallout deposits and soil beds. The Ishigedo tuff is exposed not only along the Oirase river but on the lower parts of the southern wall of the Towadako caldera (Fig. 2). From this distribution it is supposed that the lake had

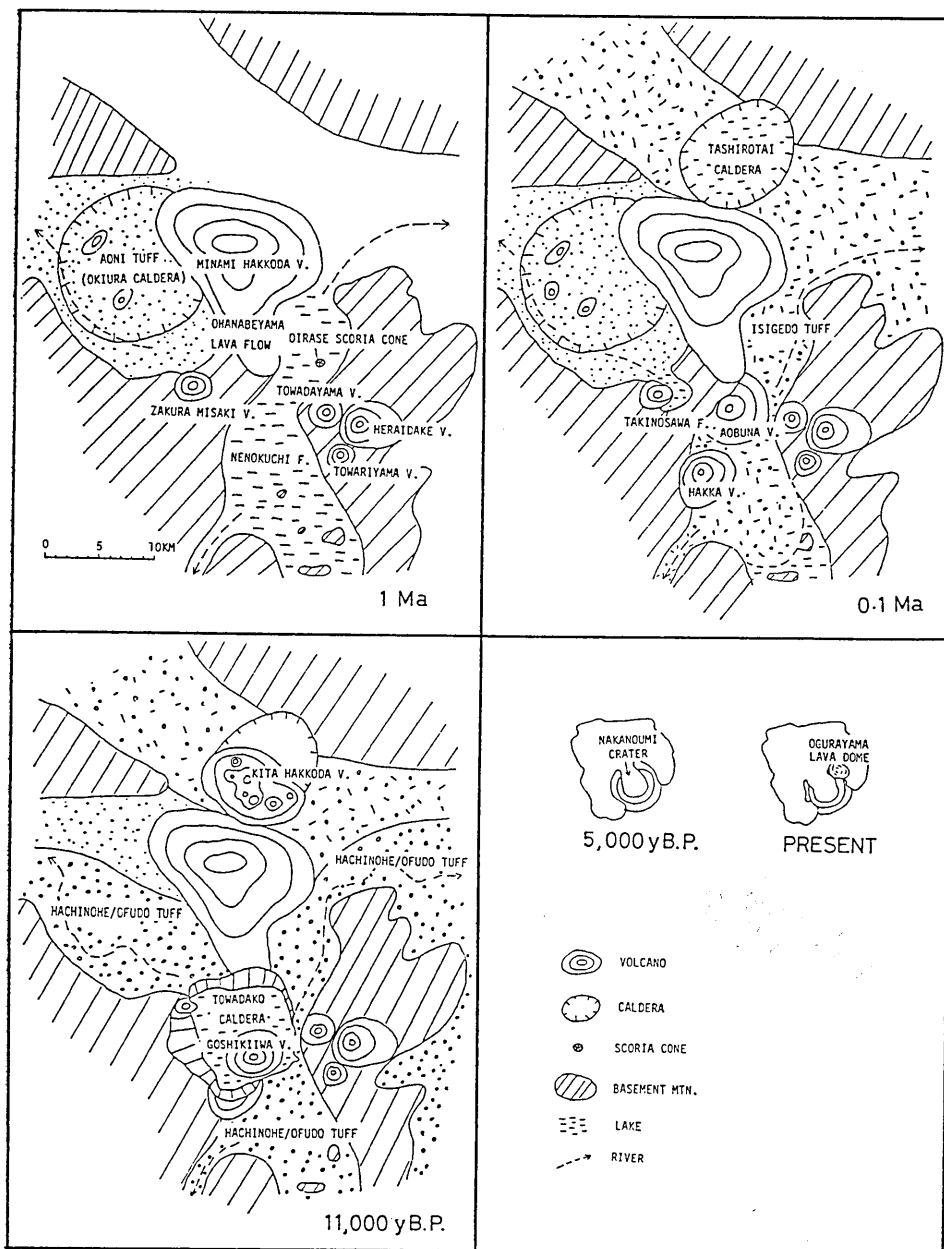


Fig. 4. Sketch maps showing the development of the paleogeography of the Towada area.

extended over the southeastern half of the present Towadako caldera before the eruption of the Ishigedo tuff.

Towada Volcano

Volcanic edifices younger than the Ishigedo tuff are collectively called here Towada Volcano. Table 1 is a summary of the eruptive history of

Table 1. Summary of the eruptive episodes and stratigraphy of Towada Volcano. Age of W is from MACHIDA (1983).

AGE (y.B.P.)	ERUPTIVE EPISODE	TEPHRA MASS ($\times 10^{15}$ g)	STRATIGRAPHY		VOLCANIC EDIFICE
1,250	A	~4.5 1.18	top soil (including TOMAKOMAI ash from Baegdusan Volcano) KEMANAI OYU	flood / ash flow ash fall, pumice fall	OGURAYAMA lava dome
	B	0.79 0.09	A/B soil SOBE MAYOGATAI	ash fall pumice fall	
5,400	C	1.49 0.81 4.01	B/C soil UTARUBE KANEKASAWA CHUSERI	ash surge, ash fall pumice fall pumice fall	NAKANOUIMI crater
	D	0.20	C/D soil OGUNI	(including D' ash) pumice fall, ash fall	
8,500	E	0.39 0.97	D/E soil KAIMORI NAMBU	ash fall pumice fall, ash fall	
	F	0.34 0.57	E/F soil KABAYAMA NATSUZAKA	ash fall scoria fall	
	G	0.25	F/G soil SHINGO	pumice fall	
	H I J K	6.3	NINOKURA	scoria fall, ash fall, lava flow, dike, scoria flow, soil	GOSHIKIWA volcano (GOMON ISHI lava dome) ?
13,000	L	~40 10.9	Ninokura/L soil HACHINOHE HACHINOHE	flood / ash flow ash fall, pumice fall	TOWADAKO caldera
	M	~6	L/M soil MAITA	ash fall / pumice fall	
25,000	N	~40 4.7	M/N soil OFUDO KIRIDA	flood / ash flow ash fall, pumice fall	
	O	~3.5	N/O soil	pumice fall, ash fall	
	P	3.0	O/P soil	pumice fall	
	Q	~10 1.9	P/Q soil OKUSE	flood / ash flow scoria fall / pumice fall	
	R S T U V			pumice fall, scoria fall, ash fall, lava flow, soil	AOBUNA volcano HAKKA volcano
110,000*	W			ash fall from Toya Volcano	
	X Y Z ...			pumice fall, ash fall, block & ash flow, lava flow, soil	

the volcano obtained by studies of tephrostratigraphy. The eruptive history of Towada Volcano can be best described by a concept of an eruptive episode, which is a succession of eruptions separated by apparently dormant intervals inferred from buried soils and the absence of eruptive deposits. More than 20 eruptive episodes are identified from the examination of hundreds of pyroclastic sections on the slopes of the volcano. An alphabetical code is assigned to each eruptive episode in a downward sequence (Table 1 and Fig. 5); the pre-caldera volcanism is older than Q and the

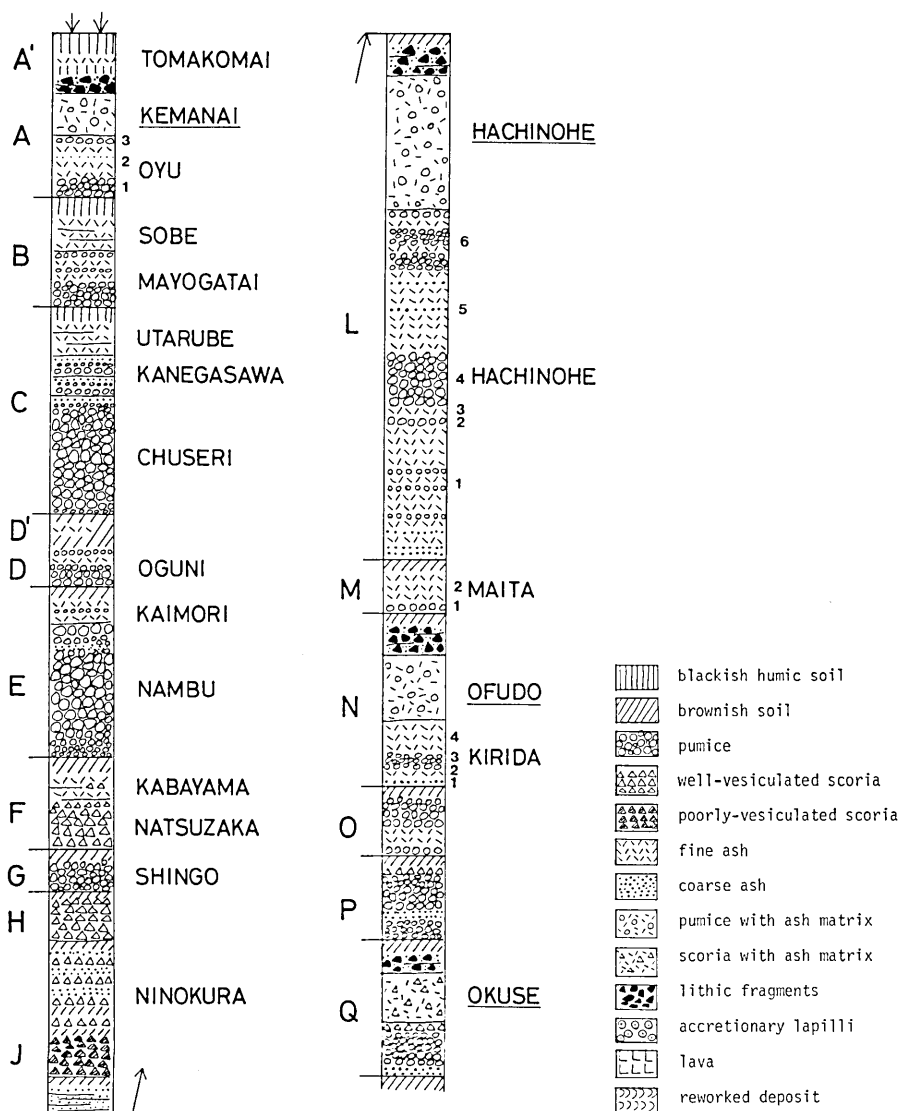


Fig. 5. Idealized columnar section (not to scale). Those underlined are ignimbrites.

stage of the caldera formation is between Q and L. Those episodes younger than L are the post-caldera volcanism. Results of radiocarbon-age determinations for eruptive episodes A, C, E, L, and N are listed in Table 2.

Pre-caldera volcanism

The activity of Towada Volcano started upon the NE-SW trending border line between the Ishigedo tuff plain and the basement mountains. At least two stratovolcanoes, Aobuna and Hakka, were formed and their remnants are now exposed on the caldera walls. The former on the northeastern corner of the caldera is composed predominantly of a nearly horizontal accumulation of pyroclastic deposits up to 200 m thick (Fig. 6).

Table 2. Radiocarbon ages. All ages based on Libby half-life (5570 y), referenced to A.D. 1950. Analyzed at Gakushuin University by K. KIGOSHI.

Episode	GaK No.	Age (y \pm 1 σ)	Remarks
A	548	1,280 \pm 90	HIRAYAMA & ICHIKAWA, 1966
A	10045	1,470 \pm 100	40°21'35"N, 140°51'38"E
A	10046	1,090 \pm 100	40°21'35"N, 140°51'38"E
C	9761	5,390 \pm 140	HAYAKAWA, 1983b
E	2613	8,600 \pm 250	OIKE, 1970
E	10650	8,370 \pm 170	40°25'59"N, 140°55'04"E
L	205	12,700 \pm 260	OIKE, 1964
L	385	12,000 \pm 250	SATOH, 1966
L	460	10,400 \pm 200	SATOH, 1966
L	550	12,200 \pm 250	ISSHIKI <i>et al.</i> , 1965
L	5995	13,960 \pm 510	OIKE & SHOJI, 1977
L	5996	13,770 \pm 510	OIKE <i>et al.</i> , 1977
L	9515	13,050 \pm 320	40°32'36"N, 141°11'56"E
L	9516	13,120 \pm 260	40°32'36"N, 141°11'56"E
L	9517	13,450 \pm 320	40°30'39"N, 140°46'49"E
L	9518	12,630 \pm 320	40°18'52"N, 140°14'08"E
L	10043	12,460 \pm 520	40°21'29"N, 140°51'10"E
L	10044	10,680 \pm 360	40°29'32"N, 140°49'55"E
L	10649	13,190 \pm 300	40°15'59"N, 140°48'14"E
N	549	25,700 \pm 900	ISSHIKI <i>et al.</i> , 1965
N	551	28,300 \pm 1500	ISSHIKI <i>et al.</i> , 1965
N	1593	>33,000	SOTOH, 1969
N	6725	25,560 \pm 1340	OIKE, 1978
N	6726	23,140 \pm 1020	OIKE, 1978
N	9514	19,450 \pm 780	40°32'31"N, 141°11'45"E
N	9762	30,130 \pm 2590	40°21'22"N, 141°10'01"E

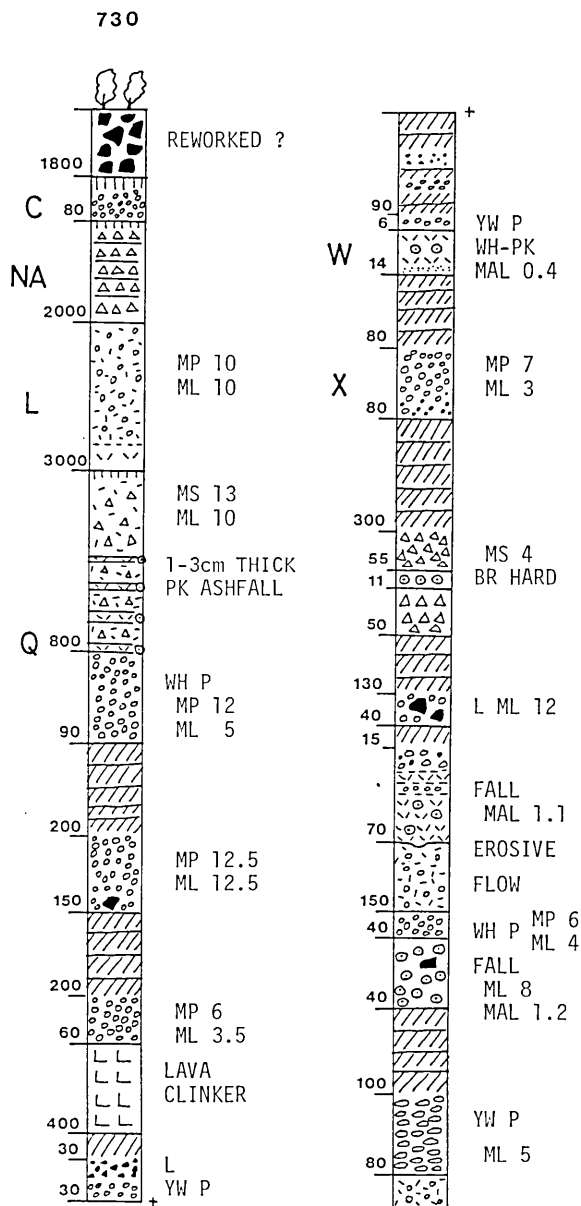


Fig. 6. Columnar section on the northeastern wall of the Towadako caldera (Aobunayama; 730: 6.8 km, 24°). Thicknesses are in cm. Symbols are as in Fig. 5.

P: Pumice, S: Scoria, L: Lithics, C: Crystals; BL: Blue, BR: Brown, OR: Orange, PK: Pink, PU: Purple, YW: Yellow; c: coarse, m: medium, f: fine; MP: Maximum pumice size (cm), MS: Maximum scoria size (cm), ML: Maximum lithic size (cm), MAL: Maximum accretionary lapilli size (cm).

Thick soil beds develop on a number of horizons and two sheets of andesite lava flow are intercalated. The explosion index (RITTMAN, 1962), the percentage of pyroclastic materials in the total volcanic products, is about 90. A 110,000 years-old ash bed, W, from Toya Volcano (MACHIDA, 1983) is found in the middle of the section. It is therefore supposed that the activity of the Aobuna volcano started about 200,000 years ago.

Another volcano, Hakka, is exposed on the opposite side of the caldera wall. In contrast to the Aobuna volcano, it is composed predominantly of andesite lava flows and a small amount of scoria flow deposits. The explosion index is about 10.

A contemporaneous lacustrine sediment, named the Takinosawa formation, is exposed on the northwestern corner of the caldera wall. It is composed of silt and mud beds, which are in parts strongly folded by the slumping probably caused by the caldera subsidence. Lenses of conglomerate beds are occasionally seen.

KUNO *et al.* (1964) believed that a single large stratovolcano had been formed before the caldera collapse, however, there is no evidence supporting this idea. It is concluded that only a part of the area presently occupied by the Towadako caldera was covered by a few relatively small-scale pre-caldera volcanoes.

Formation of the Towadako caldera

The prevailing view of the caldera formation is a catastrophic event being formed by a single of large-scale explosive eruption. The Towadako caldera, however, seems to have grown incrementally in response to several moderate-scale eruptive episodes. As many as six eruptive episodes, Q to L, may be responsible for the caldera's formation. The time span extends about 40,000 years, during which three voluminous pyroclastic flow eruptions are included: the Okuse (Q; *ca.* 10 km³), Ofudo N; *ca.* 40 km³), and Hachinohe (L; *ca.* 40 km³) pyroclastic flow eruptions.

The caldera is 11 km×11 km wide and mostly occupied by Lake Towadako. The northern, western, and southern rims are well defined as crests of inward-dipping steep slopes and outward-dipping gentle slopes, but the rim of the eastern part is hard to define being occupied by Early Pleistocene volcanoes. The volume lost by the formation of the caldera is estimated at 30 km³. It amounts to about two thirds of the total magma erupted during this stage; the mass is calculated at 1.2×10^{17} g (see Fig. 43) which equals the equivalent of 48 km³ of dense rock having a density of 2.5 g/cm³.

Post-caldera volcanism

As soon as the caldera had been fully developed during the eruptive episode L (13,000 y B.P.), post-caldera activities started about 2 km SSE of the center of the caldera, where the Goshikiwa volcano appeared and grew into a stratocone 4.5 km across. Then the central crater was progressively enlarged by several plinian eruptions and during the eruptive episode C it was finally connected to the lake water outside. The crater is named the Nakanoumi crater. Except for the northern part it is surrounded by the 40°-dipping steep cliffs up to 200 m high, where inner structures of the Goshikiwa volcano is exposed well; in the western part it is composed predominantly of basaltic andesite lava flows and in the eastern part of pyroclastic materials. A number of radial dikes, 5-6 m wide, are seen. Striking developments of iron-oxidation, crude columnar jointing in the pyroclastic materials, and apparently conformable relations between the lava flows all prove that the Goshikiwa volcano grew in a short period.

Two lava domes extruded inside the caldera. The northern one, the Gomon Ishi, has its top near the level of lake surface (Fig. 7a) and measures 650 m across and 60 m high standing on the lake floor. It seems that the eruptive activity was not accompanied by pyroclastic eruptions, thus the age cannot be assigned by tephrochronology.

The other dome, the Ogurayama (Fig. 7b), lies on the northeastern slopes of the Goshikiwa volcano. Because the lava dome is not covered by any pyroclastic deposits, it is evident that it was emplaced at the end of the latest eruptive episode A. The dome is 1,500 m across and 360 m high. The columnar jointing on the Senjomaku cliff, which is perpendicular to the upper and lower surfaces, suggests that the greater part may well be called a thick lava flow or coulee.

No sign of fumarolic activity or hot springs is presently observed in the area of Towada Volcano.

3. Petrography

Petrographic descriptions of the volcanic rocks in the Towada region have been given by CHIBA (1966) and TANIGUCHI (1972). Rocks analyzed by them are reclassified in Table 3 according to the stratigraphy presently established.

A microscopic description of the rocks collected by the present author is shown in Table 4. The rocks of the basement are more or less altered: phenocrysts replaced by chlorite and/or carbonate, groundmass suffered

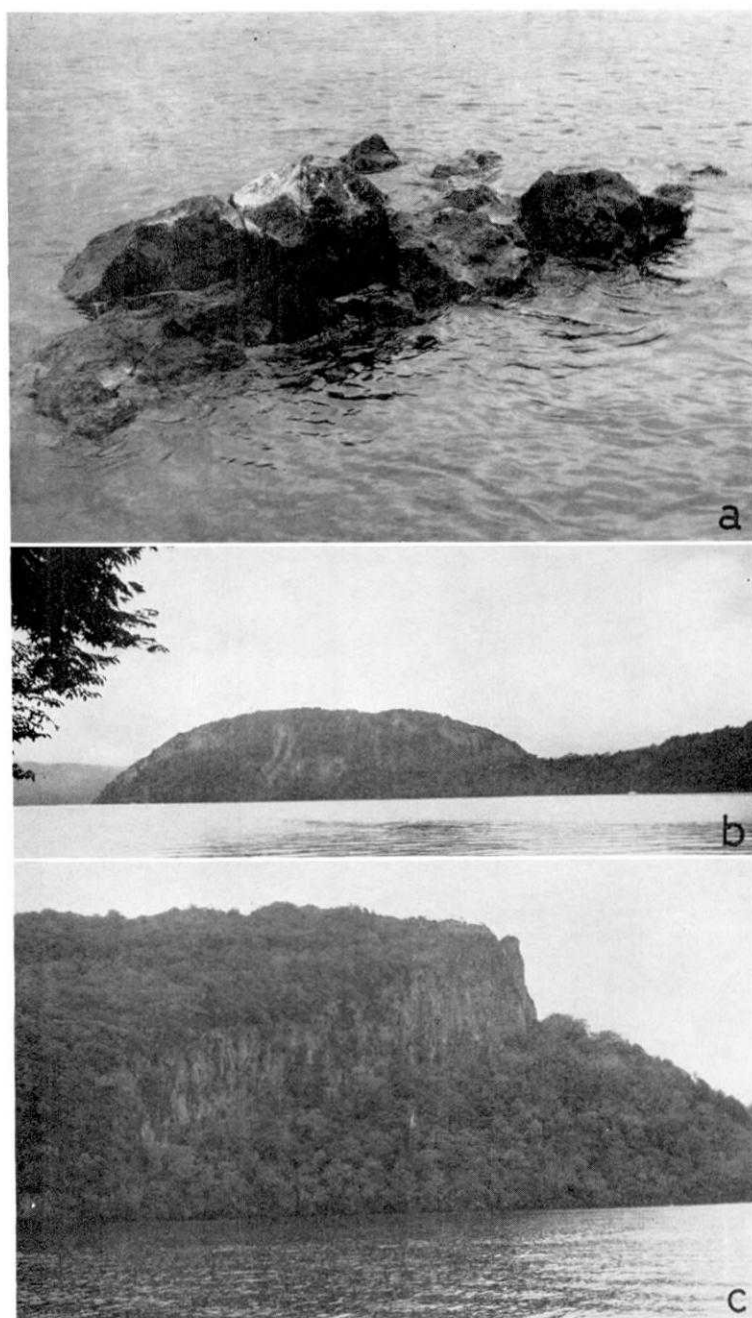


Fig. 7. Lava domes. (a) Top of the Gomon Ishi lava dome on the lake surface (3 m long). (b) Ogurayama lava dome viewed from Uranaiba. (c) Vertical columnar jointing on the Senjomaku cliff, Ogurayama lava dome. Lower right is the Goshikiwa volcano.

Table 3. Rocks chemically analyzed by CHIBA (1966) and TANIGUCHI (1972).
 They are reclassified according to the stratigraphy made by the author.
 Rocks analyzed by CHIBA (1966) are identified by "C-" with original
 analyses number and those by TANIGUCHI (1972) are by "T-".

Geologic unit	Rock	% SiO ₂	Remarks
Ogurayama dome	C-36	68.38	lava
Nambu pumice	C-31	63.49	welded tuff
	C-33	63.98	obsidian
	T-9	63.30	welded tuff
	T-10	64.03	welded tuff
A-G	T-11	62.24	pumice
	T-12	58.44	pumice
	T-13	62.87	pumice
Ninokura scoria	T-6	52.60	scoria
	T-7	55.86	scoria
	T-8	57.78	scoria
Goshikiwa v.	C-23	50.79	lava
	C-24	53.53	lava
	C-25	53.71	lava
	C-26	54.49	lava
	C-27	54.57	dike
	C-28	56.01	lava
	C-29	57.93	lava
	T-5	54.96	lava
Gomon Ishi dome	C-35	65.42	lava
	T-14	65.43	lava
Hachinohe ign.	C-17	66.85	pumice
	C-18	68.21	pumice
	C-19	68.80	pumice
	C-21	68.47	pumice
	C-22	70.40	pumice
	T-3	69.86	pumice glass
	T-4	69.30	pumice glass
Aobuna v.	C-1	51.90	lava
	C-5	55.46	lava
	C-6	55.65	lava
	C-11	60.19	lava
	C-12	60.35	lava
	C-13	60.44	lava
	C-14	62.23	lava
	C-15	63.66	lava
	C-16	64.45	lava
Hakka v.	C-2	52.63	lava
	C-7	56.25	lava
	C-8	58.85	scoria
	C-9	59.30	lava
Zakura Misaki v.	C-3	54.73	lava
	T-2	54.20	lava
Heraidake v.	T-1	60.82	lava

v: volcano.

Table 4. Microscopic description of rocks.

Geologic unit	Sample	Locality	Rock type
Ogurayama dome	672-1	Ogurayama	Hyp-aug dacite
Nambu pumice	146-2	Kankodai	Hyp-aug dacite
Goshikiwa v.	631-1	Utarube	Hyp-aug andesite
	792-1	NW of Ogurayama	Aug-hyp andesite
	797-1	Byobuiwa	Ol-hyp-aug andesite
	801	Omaegahama	Hyp-aug andesite
	830	Nakanoumi	Ol-hyp-aug andesite
	831	Nakanoumi	Aug-hyp andesite
	832	Nakanoumi	Aug-hyp andesite
	833	Nakanoumi	Hyp-aug andesite
	147-1	Jigomoriwa	Ol-hyp-aug andesite
	793-1	Higurashiiwa	Aug-hyp andesite
	796-1	Eboshiiwa	Ol-hyp-aug andesite
	798-1	Sarukozaki	Ol-hyp-aug andesite
	800	Nakayama pen.	Ol-hyp-aug andesite
Gomon Ishi dome	791-1	Gomon Ishi	Aug-hyp dacite
Aobuna v.	730-6	the upper lava	Hyp-aug andesite
	201	the lower lava	Ol-bg hyp-aug andesite
	522-1	the lower lava	Ol-bg hyp-aug andesite
	528-1	the lower lava	Ol-bg hyp-aug andesite
	835-1	the lower lava	Ol-hyp-aug andesite
Hakka v.	999-1	Hakka pass	Ol-bg hyp andesite
Ishigedo tuff	177	Oirasegawa	Hyp-aug-Qz dacite
	190	Tochikubo	Hyp-aug-Qz dacite
	678-1	Takayama	Qz-aug-hyp dacite
	998-1	Hakka	Aug-hyp-Qz dacite
	837-1	Kodatamiishi	Hyp-aug-Qz dacite
Zakura Misaki v.	549-1	Zakura Misaki	Hyp-aug andesite
Towadayama v.	677-1	Nenokuchi	Pyx-Qz dacite
Heraidake v.	851-1	Myogaeshigawa	Qz-hyp-aug andesite
M. Hakkoda v.	371-1	Matsuminotaki	Hyp-Qz dacite
Basements	217-1	Yodonomisaki	heavily altered rock
	371-3	Matsuminotaki	muddy sandstone
	498-1	Akuyagawa	Qz-hyp-aug andesite
	566-1	Hiromorigawa	Hb-Qz dacite
	666-1	Higashinosawa	Hb-Qz dacite
	789-1	Kabayama Eboshi	Qz-hyp-aug andesite
	803-1	N. lakeshore	Aug-hyp dacite
	804-1	N. lakeshore	Hb-bg hyp-aug andesite
	805-1	N. lakeshore	Hyp-aug andesite
	807-1	N. lakeshore	Hyp-aug andesite
	808-1	N. lakeshore	Hyp-aug andesite
	838	S of Nenokuchi	Aug dacite

aug: augite, hb: hornblende, hyp: hypersthene, ol: olivine, pyx: pyroxene, Qz: quartz, bg: bearing.

albitization. Some rocks of the Early Pleistocene volcanoes are also replaced by chlorite and/or carbonate. The others are relatively fresh carrying phenocrysts of plagioclase, pyroxene, and magnetite with occasional quartz. The welded ignimbrites of the Ishigedo tuff carries plagioclase, quartz, augite, hypersthene, and magnetite. Eutaxitic texture is seen in the matrix.

Lavas of the Hakka, Aobuna, and Goshikiwa volcanoes are fresh hypersthene-augite andesite. Corroded quartz phenocrysts are occasionally found and augite is generally surrounded by a reaction rim of hypersthene. Glomeroporphyritic aggregates are common. Lavas of the Gomon Ishi and Ogurayama domes are augite-hypersthene dacite without quartz phenocryst.

Tephra of Towada Volcano are dacite to andesite with crystals of plagioclase, augite, hypersthene, and magnetite. Hornblende is characteristically found in the Hachinohe deposits (L) and in some older deposits. Products of a single eruptive episode are generally homogeneous in petrography. However, there are some exceptions; juvenile clasts of the fallout deposits of Q change upward from pumice to scoria and the overlying Okuse ignimbrite carries three types of juvenile clasts: white pumice, black scoria, and a streaky mixture of the two. A small amount (<1 wt. %) of dark-colored juvenile clasts are also found in the Chuseri (C) and Nambu (E) pumice deposits where most of the juvenile clasts are yellowish white pumice.

A time-dependent compositional change is distinct in the post-caldera volcanism. Silica contents of lavas of the oldest Goshikiwa volcano are 51-58 wt. % and that of the latest lava of the Ogurayama dome (A) is 68 wt. % (Table 3). This means that the present magma underneath the volcano has almost the same chemical composition as that of the magma which produced the voluminous Hachinohe deposits (L) 13,000 years ago.

Fig. 8 shows vertical variations of the crystal contents of pumice fragments observed in the deposits of C and E. It seems that crystals larger than 1/2 mm are concentrated toward the top of the deposits probably due to the crystal settling in the magma chamber. The crystal contents of large juvenile clasts of representative deposits are shown in Table 5. The largest crystals measure about 2 mm long and only a minor portion is finer than 1/8 mm. The total crystal contents vary between 4.9 and 27.2 wt. % irrespective of the stratigraphic sequence or chemical composition.

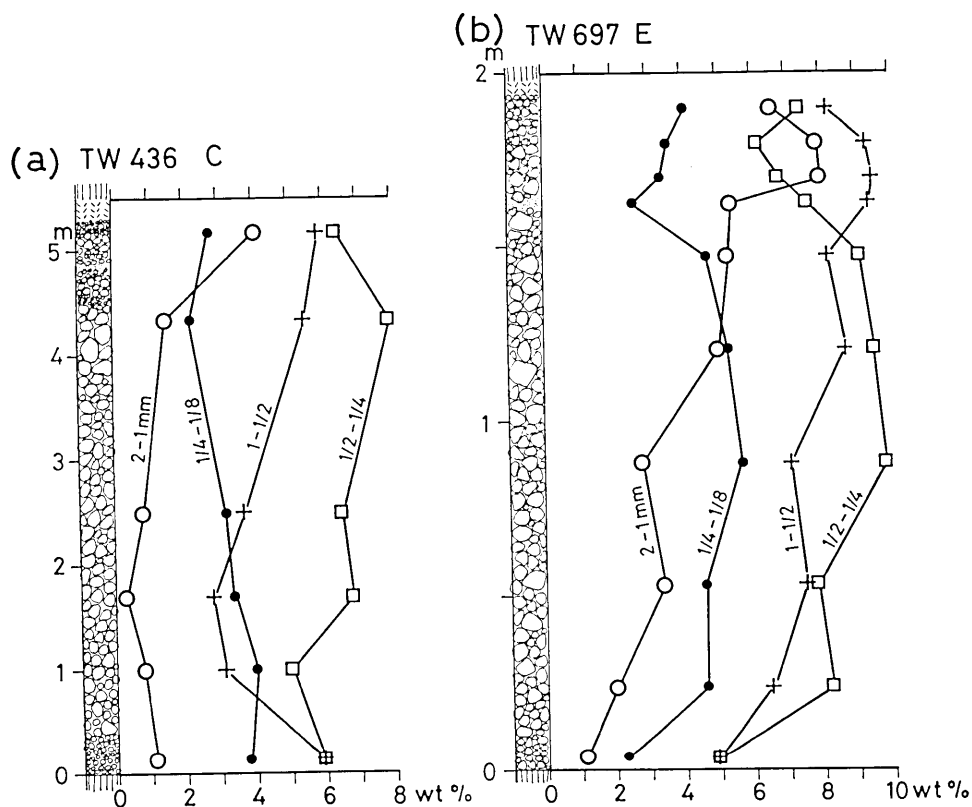


Fig. 8. (a) Section through the C deposits showing vertical variations of crystal contents for each size class in pumice fragments, at Sobegawa (436: 9.2 km, 52°) (b) The same for the E deposits, at Januma (697: 22.5 km, 103°).

Table 5. Crystal contents (wt. %) for large juvenile fragments of representative pyroclastic deposits of Towada Volcano.

	Sample	wt. (g)	2-1 mm	1-1/2	1/2-1/4	1/4-1/8 mm	Total
Kemanai i.	823-1	10.50	0.2	2.5	4.2	2.1	9.0
Mayogatai	790-2	19.00	0.6	1.9	2.1	0.7	5.3
Kanegasawa	436-7	8.88	4.1	5.9	6.4	2.8	19.1
Chuseri		143.80	0.45	3.3	6.8	4.0	14.5
Oguni	718-1	7.24	2.3	2.8	2.8	1.2	9.1
Nambu		177.66	3.7	7.9	8.0	3.7	23.3
Natsuzaka	718-2	11.78	0.5	1.7	1.8	0.9	4.9
Hachinohe i.	197-3	14.57	0.07	2.2	6.0	2.7	11.0
Ofudo i.	199-2	13.72	2.0	5.9	3.9	1.2	13.1
Okuse i. (p)	728-P	9.50	5.5	8.9	9.2	3.6	27.2

i.: ignimbrite, p: pumice.

4. Pyroclastic deposits

The succession of pyroclastic deposits has been previously shown in Table 1 and Fig. 5. The lithology of each deposit is described here referring to the established type section(s) (Table 6). The dispersal is shown by isopach maps and by grain size isograde maps of maximum pumice size (MP), maximum lithic size (ML), and median diameter (Md). In practice, following WALKER (1980), MP and ML are taken as the average maximum diameter of the three largest fragments of each type seen at each exposure.

Table 7 shows the age of each eruptive episode and a correlation to pyroclastic deposits described by OIKE and NAKAGAWA (1979). For simplicity, an alphabetical code which was assigned to each eruptive episode is also used for the deposits. Fig. 9 demonstrates the areal correlation of the post-caldera pyroclastic deposits, younger than L. Each of the soil layers separating the pyroclastic deposits does not thicken toward Towada Volcano and they have nearly an identical thickness irrespective of their distances from the volcano (Fig. 10). The rate of accumulation of soil is in the order of 0.1 mm/year.

A' (ca. 1,000 y B.P.)

The youngest pyroclastic deposit distributed in the Towada area is the Tomakomai ash (MACHIDA *et al.*, 1981) which is intercalated in the black humic soil about 10 cm below the present surface. The type section is a roadcut at Tsutsumigashira (859: 23.6 km, 71°) where the thickness is 2 cm and its orange color exhibits a striking contrast to the white of the Oyu ash below. It is composed mainly of micropumice of fine ash size (<1/16 mm). MACHIDA *et al.* (1981) considered that the source of this ash is not the Towada but Baegdusan Volcano, 1,100 km west of Towada. The ash is also found in Hokkaido and Sea of Japan (MACHIDA *et al.*, 1981).

A (1,250 y B.P.; A.D. 915 ?)

This latest eruptive episode of Towada Volcano produced thin but widespread pyroclastic deposits all around the source, the position of the Ogurayama lava dome. At Ochiai Bashi (575: 10.3 km, 168°) a whole succession of A is exposed:

- 200 cm white fine ash with scattered pumice lapilli (Kemanai ignimbrite)
- 3 cm Iron-stained small pumice lapilli; MP 0.8 cm, ML 0.5 cm (Oyu 3 pumice)
- 12 cm yellowish white fine ash enclosing air bubbles and accretionary

Table 6. Type section(s) of pyroclastic deposits.

	Type section(s)
A' Tomakomai	859
A Kemanai	753, 575
Oyu 1-3	575
B Sobe	827, 799
Mayogatai	827, 799
C Utarube	609, 264
Kanegasawa	609
Chuseri	609
D'	849, 834
D Oguni	718
E Kaimori	602, 697, 849
Nambu	602, 697, 849
F Kabayama	718, 845, 852
Natsuzaka	718, 845
G Shingo	391
Ninokura	151, 219, 873, 389, 717, 857, 688, 825
H	828, 219
I	828, 389
J	842, 389
K	873
L Hachinohe i	132, 197
Hachinohe 1-6	345
M Maita 1-2	868, 866
N Ofudo	199, 710
Kirida 1-4	699, 709, 378
O	871
P	709, 699, 200, 871
Q Okuse	710, 862, 728
(fall)	862, 699, 200, 871
R	193, 200, 871
S	193, 200, 871
T	193, 200, 871
U	193, 200, 871
V	193, 200, 871
W Toya	871, 193
X	193, 871
Y	704
Z	704
Tose	485
Aoni	775
Nagakogi	162, 709, 698

(continued to be next page)

Locality index. Sites are shown by distance and azimuth from the center of the Nakanoumi crater.

Loc.	Distance	Azimuth	Name
132	23.5 km	95°	Yokozawa
151	9.7	151	Tashirotai
162	16.4	91	Nagakogi
193	27.0	60	Kirida
197	28.4	66	Kiyose
199	31.2	67	Maita
200	29.8	66	Maita
219	4.5	102	E of Takayama
345	45.4	79	Shiriuchi
378	9.4	51	Sobegawa
389	14.6	98	W of Ninokura dam
391	17.1	92	Hainai
485	23.2	137	Tose
575	10.3	168	Ochiai Bashi
602	7.0	122	Tashirogawa
609	23.4	83	Kanegasawa
688	13.6	68	Odaibokuya
697	22.5	103	Januma
698	23.8	105	Kaimori
699	24.4	71	Tsutsumigashira
704	28.2	63	Kirida
709	23.0	49	Okuse
710	21.7	45	Okuse
717	19.8	117	Shimizugashira
718	14.6	124	NW of Okuromori
728	6.8	20	Aobunayama
753	16.2	196	Oyu
775	16.7	301	Kuzukawa Bashi
799	3.1	95	Utarube
825	6.0	200	S of Hakka pass
827	5.6	116	W of Towariyama
828	5.2	112	W of Towariyama
834	8.6	14	Aobunayama
842	11.2	110	E of Mayogatai
845	12.0	105	E of Mayogatai
849	10.7	97	S of Heraidake
852	15.1	96	Ninokura dam
857	18.0	82	Kawashiro
859	23.6	71	Tsutsumigashira
862	18.3	46	Okuse
866	31.2	67	Maita
868	25.5	69	Kobayashi
871	34.4	74	Kawaramachi
873	17.7	108	Sugisawa

Table 7. Ages of the eruptive episodes and a correlation to pyroclastic deposits described by OIKE and NAKAGAWA (1979). Ages in parentheses are estimated by interpolations using soil thicknesses.

Age (y)	Eruptive episode	OIKE & NAKAGAWA (1979)
(1,000)	A'	—
1,250	A	Kemanai/To-a
(3,000)	B	To-b
5,400	C	Chuseri
(6,000)	D'	—
(7,000)	D	"unnamed pumice"
8,500	E	Nanbu
(9,500)	F	} Ninokura
(10,500)	G	
	Ninokura	
13,000	L	Hachinohe/Hachinohe
(17,000)	M	BP ₂
25,000	N	Ofudo/BP ₁
(35,000)	O	GP
(45,000)	P	Kb
(55,000)	Q	Okuse/RP
	R	—
	S	SP
	T	OPII
	U	AP
	V	CP
110,000*	W	WT
	X	ZP ₂
	Y	—
	Z	NP

* MACHIDA (1983)

lapilli; compact; intercalating a thin layer of coarse ash (Oyu 2 ash)

7 cm yellowish white pumice lapilli with abundant obsidian; MP 3.5 cm, ML 0.8 cm (Oyu 1 pumice).

Fig. 11 shows a schematic columnar section of A. The dispersal of each member is shown in Fig. 12. The southwestward dispersal of the Oyu 1 and 3 plinian pumice deposits is exceptional among other plinian pumice deposits of Towada Volcano whose dispersal axes mostly extend eastward. The Oyu 1 pumice does not thicken toward the source. About 3 km WSW of Nakataki (506:9.8 km, 201°), the Oyu 2 and 3 deposits are completely missing and the Kemanai ignimbrite directly overlies the Oyu

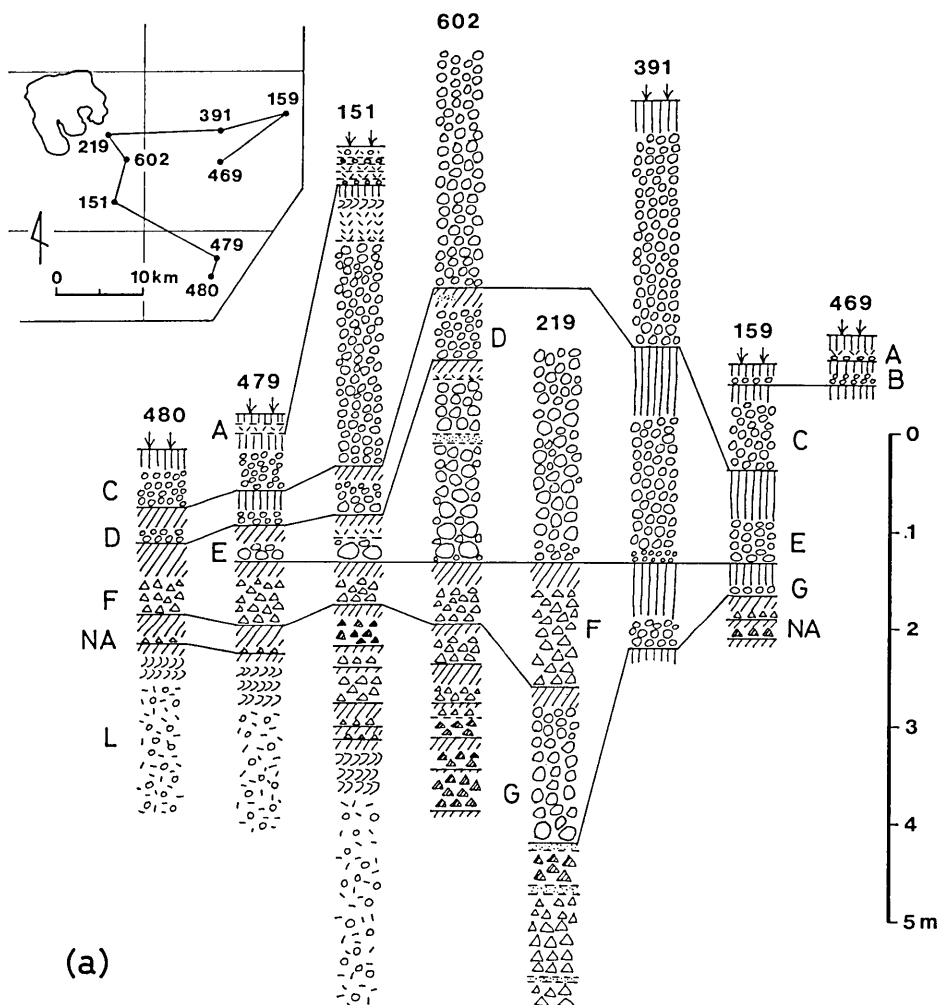


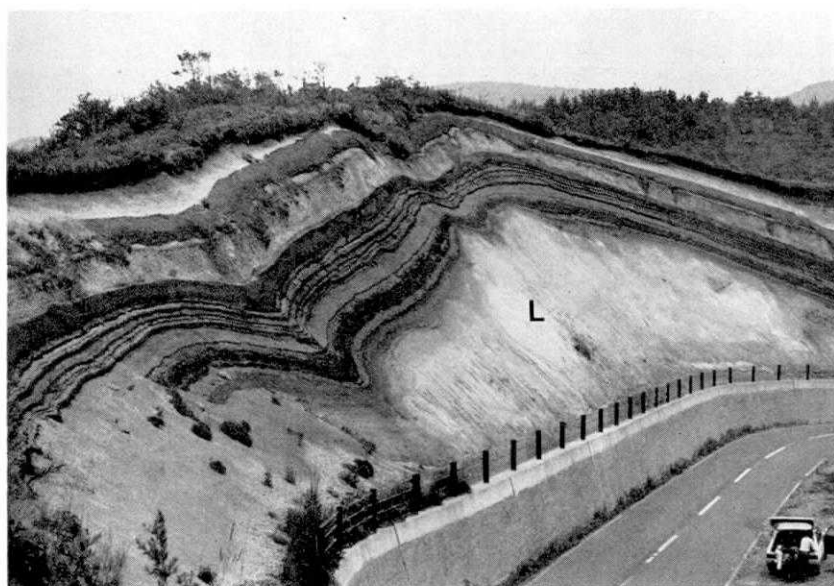
Fig. 9(a) (a) Correlation of post-caldera pyroclastic sections. Symbols are as in Fig. 5. NA: Ninokura.

1 pumice. This succession implies that a pyroclastic flow had already been generated before the deposition of the Oyu 2 ash. Therefore, it is suggested that the Oyu 2 ash is a co-ignimbrite fallout of the Kemanai ignimbrite eruption. The Oyu 3 pumice may be a product from a reestablished high plinian column.

Two distinctly different depositional facies exist in the Kemanai ignimbrite: thickly accumulated valley-pond type and thin veneer type. Outcrops of the former type are seen along river valleys (Fig. 12): the Oyu river to the south, Gonohe river to the east, and Oirase river to the north. There is no evidence of the distribution to the northwest along the Asaseishi river. The deposit nearest the vent is seen at Utarube



(b)



(c)

Fig. 9. (b) Roadcut at Kotashirogawa (576: 9.9 km, 150°) showing post-caldera fallout deposits. Spade (in circle) is 80 cm long. (c) Roadcut west of the Ninokura dam (389: 14.6 km, 98°) showing the Hachinohe ignimbrite (L) and overlying post-caldera fallout deposits.

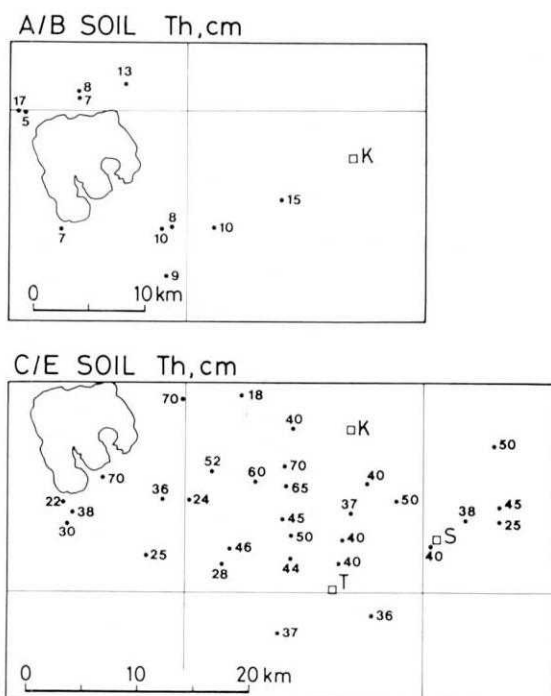


Fig. 10. Thickness map of the A/B soil bed and C/E soil bed. Note that they do not thicken toward Towada Volcano. Vertical and horizontal lines are 1:50,000 map boundaries. K: Kanegasawa, S: Sannohe, T: Takko.

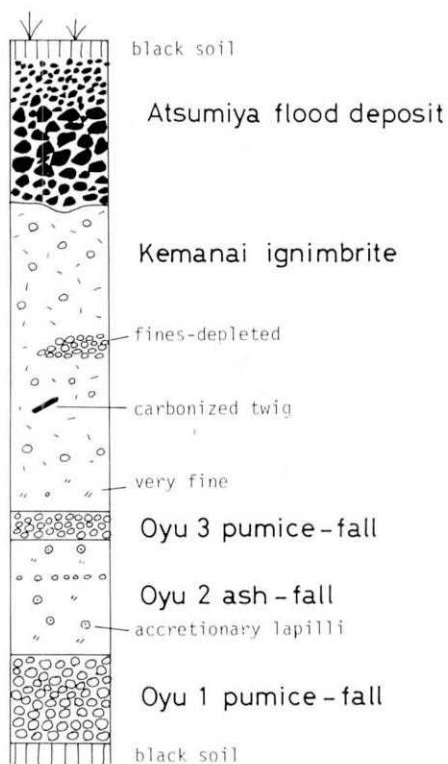


Fig. 11. Schematic columnar section of A (not to scale).

(799:3.1 km, 95°), where it contains more than 20 wt. % fine ash (Fig. 13), a very high content when compared to other ignimbrites. The latter type is seen in outcrops located topographically high. It is usually thinner than a few tens of cm (Fig. 12). Several mm size lithic fragments, mainly obsidian chips, are scattered in the fine ash matrix. A remarkable cross stratification is seen near the Hakka pass (563:5.0 km, 216°) where charred wood is found. It is seen at Oyu (759:17.7 km, 202°) that the veneer type passes into the vally-pond type. These depositional facies are superficially similar to those of the Taupo ignimbrite, New Zealand (WALKER *et al.*, 1981b).

A flood was generated along the Oyu river immediately after the Kemanai pyroclastic flow eruption. The deposit directly covers the eroded surface of the Kemanai ignimbrite. It is named the Atsumiya flood deposit which is composed of clast-supported lithic fragments with a small amount of fine ash matrix. Obsidian chips are abundant. A good exposure is seen at Oyu (753:16.2 km, 196°).

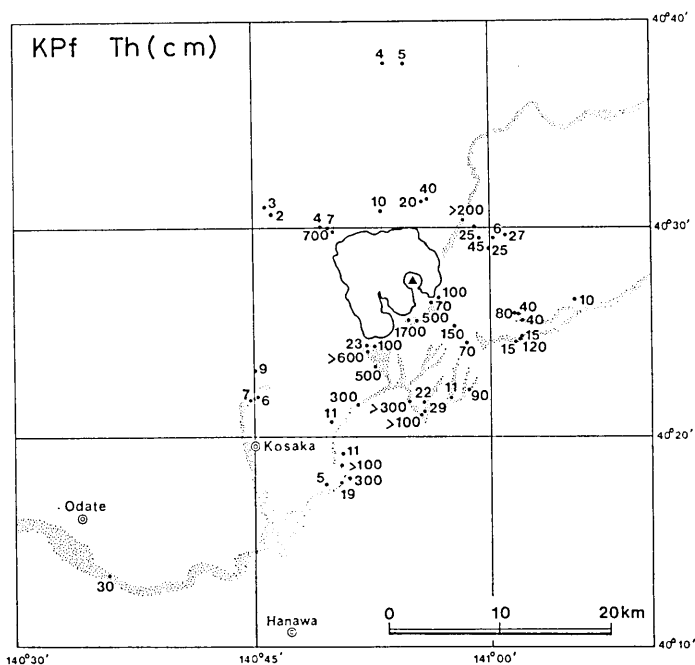


Fig. 12. Dispersal maps of A. KPf: Kemanai ignimbrite, OY: Oyu fallout deposit. Th: thickness (in cm), MP: maximum pumice size (in mm), ML: maximum lithic size (in mm), Md: median diameter (in ϕ units; $\phi = -\log_2 n$, where n is the grain size in mm). MP and ML are taken as the average maximum diameter of the three largest fragments of each type seen at each exposure.

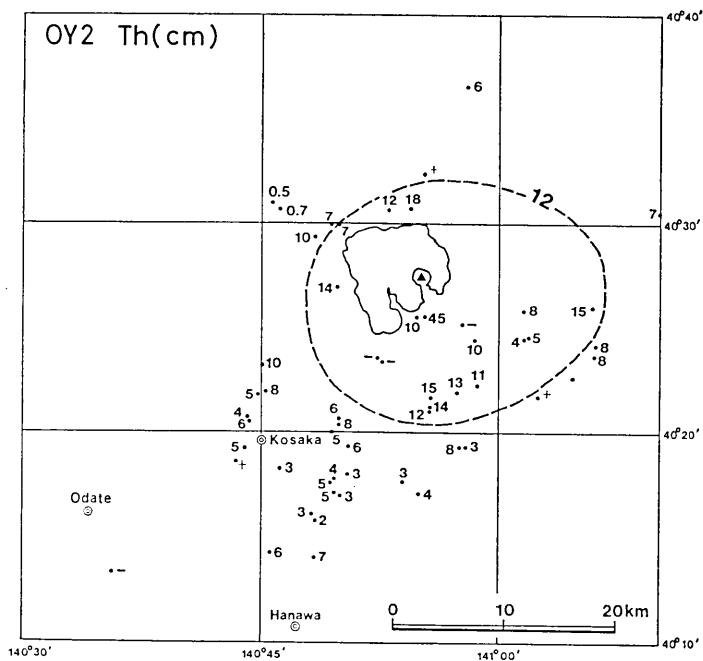
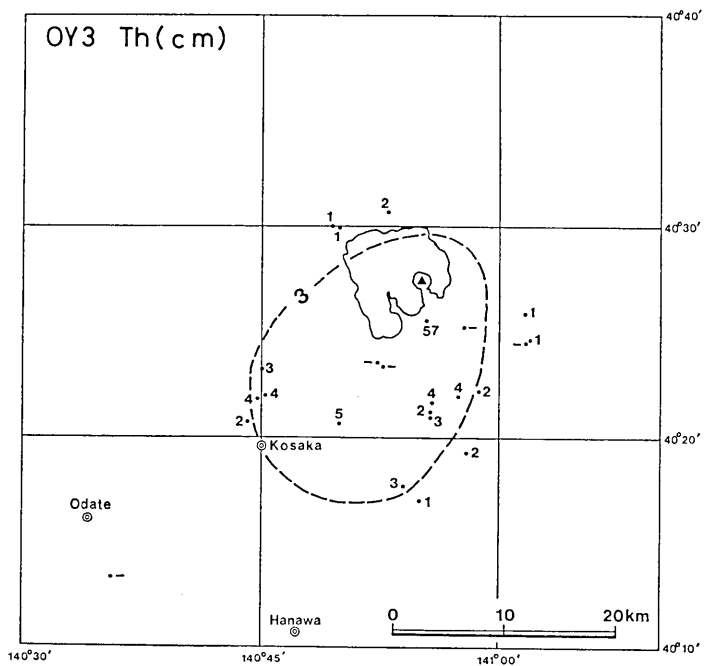


Fig. 12. (continued)

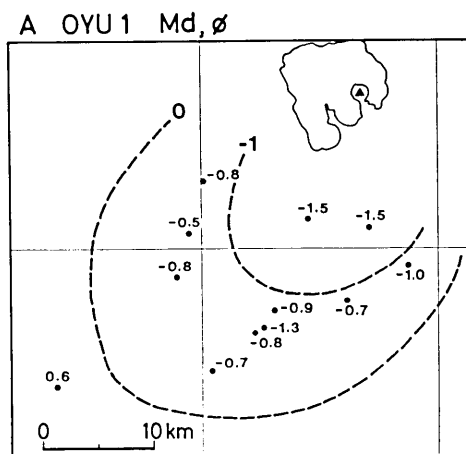
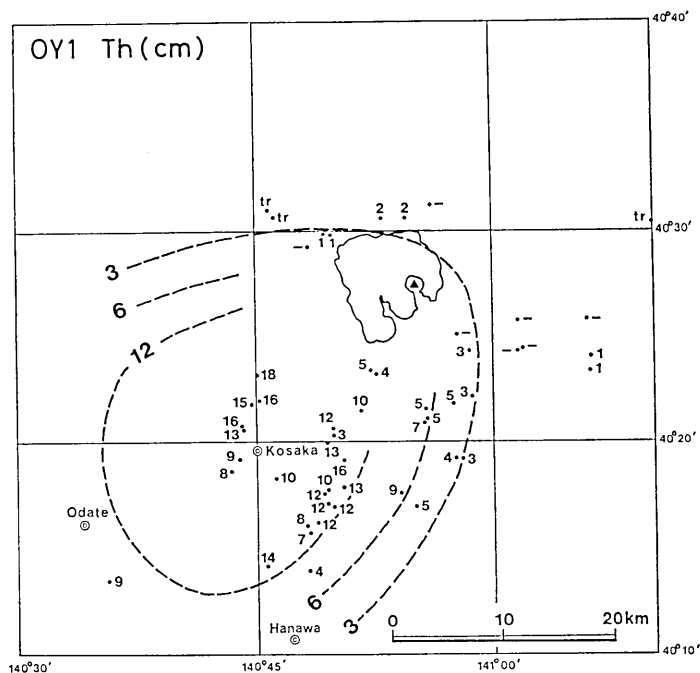


Fig. 12. (continued)

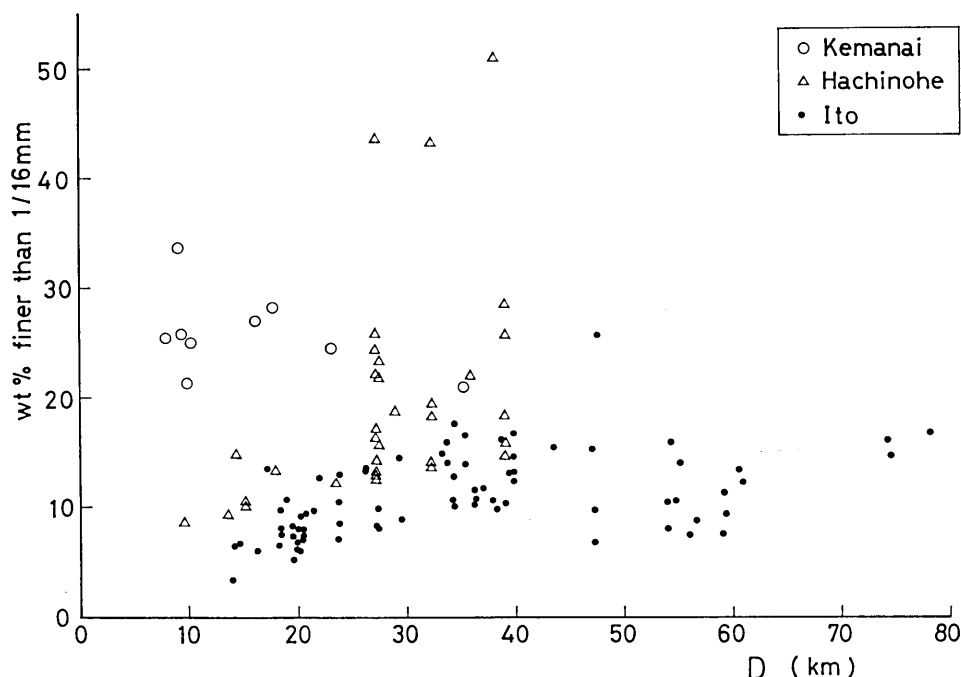


Fig. 13. Plots of weight percentages of the fraction finer than 1/16 mm against distance from the source for the Kemanai, Hachinohe, and Ito ignimbrites. Note that the Kemanai ignimbrite contains fines more than 20 wt. % even in the proximal area. The data on Hachinohe and Ito are from Aramaki and Hayakawa (unpublished).

MACHIDA *et al.* (1981) reported that an ash bed correlatable to A extends as far as Mt. Iide, 300 km south of Towada. However, its precise correlation with the above-mentioned members is yet to be made.

The date of the eruption could be assigned to August 17, 915 (the Heian era) according to an old document, Fuso Ryakki (Machida, personal communication, 1984). Fig. 14 is a series of schematic diagrams showing the development of the eruptive episode A.

B (ca. 3,000 y B.P.)

The second youngest eruptive episode, B, is represented by two members: the Mayogatai pumice and Sobe ash. About 2.5 km west of Towariyama (827: 5.6 km, 116°), the 90 cm thick Sobe ash overlies the 36 cm thick Mayogatai pumice:

- 90 cm thinly bedded dark blue ash; hard; trapping air bubbles
- 4 cm white pumice lapilli
- 1.5 cm ash

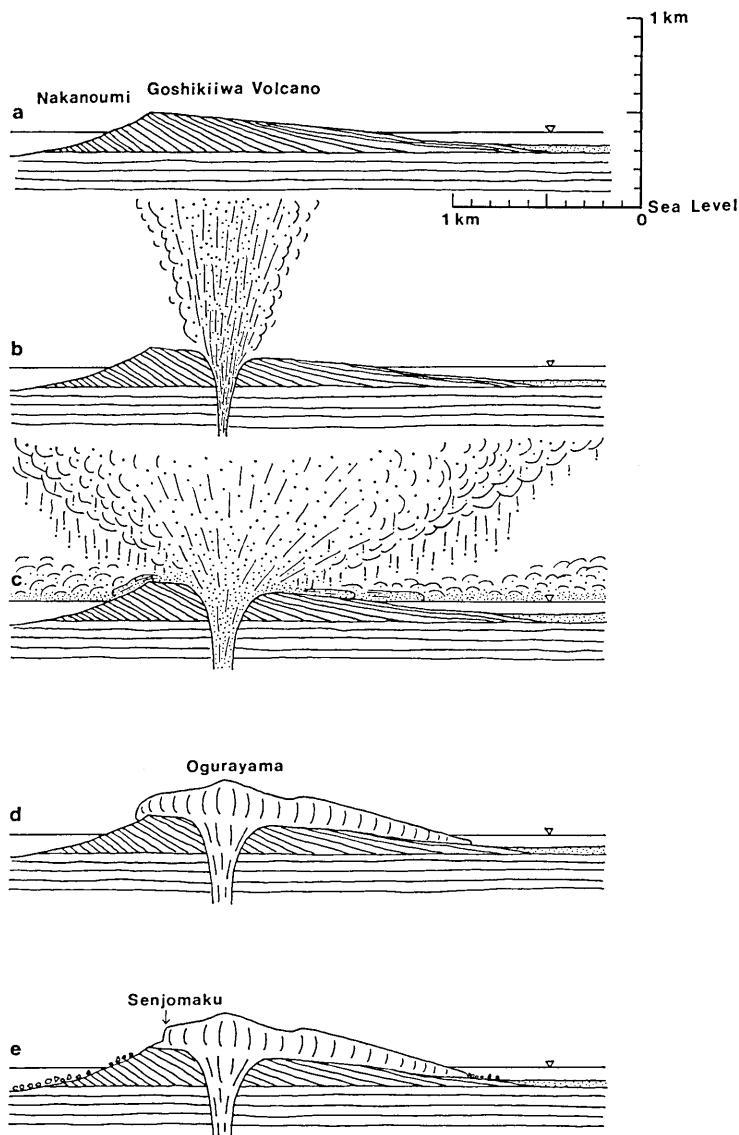


Fig. 14. Schematic diagrams showing the development of the eruptive episode A (a) Before the eruption. The Nakanoumi crater had been formed at the central part of the Goshikiwa volcano during the eruptive episode C. (b) Beginning of the eruption. A plinian column producing the Oyu 1 fallout pumice was sustained for a short period. (c) Climax of the eruption. The vent was engulfed enough to form the Kemanai pyroclastic flow and associated Oyu 2 ash fall. (d) End of the eruption. The Ogurayama lava dome was extruded and flowed down the gentle slopes of the Goshikiwa volcano. (e) Ogurayama today. Lava of the flow front has collapsed and the columnar jointing is exposed on the Senjomaku cliff.

18 cm finer white pumice lapilli

12 cm coarser white pumice lapilli; MP 5.7 cm, ML 3.7 cm.

The main constituents of the Mayogatai pumice are finely vesiculated white pumice with a smaller amount of gray pumice and obsidian chips. It extends to N110°E in a narrow dispersal fan from the Nakanoumi crater (Fig. 15), and it is represented as a one-particle-layer deposit at localities more than about 20 km distant from the source. The 6 cm isopach covers an area of 152 km².

The dispersal fan of the Sobe ash is far broader than that of the Mayogatai pumice; the 12 cm isopach covers an area of 397 km². The ash bed is therefore useful as a key bed for the correlation purpose in proximal areas. At Utarube (799: 3.1 km, 95°) it is 75 cm thick and shows evidences of water-flushed origin: lenticular microbedding (WALKER, 1981b), gullies, accretionary lapilli, and air bubbles. Intercalated thin layers of silt may indicate the presence of small water pools on the earth surfaces during short pauses during eruptions. The thinly laminated structure suggests a

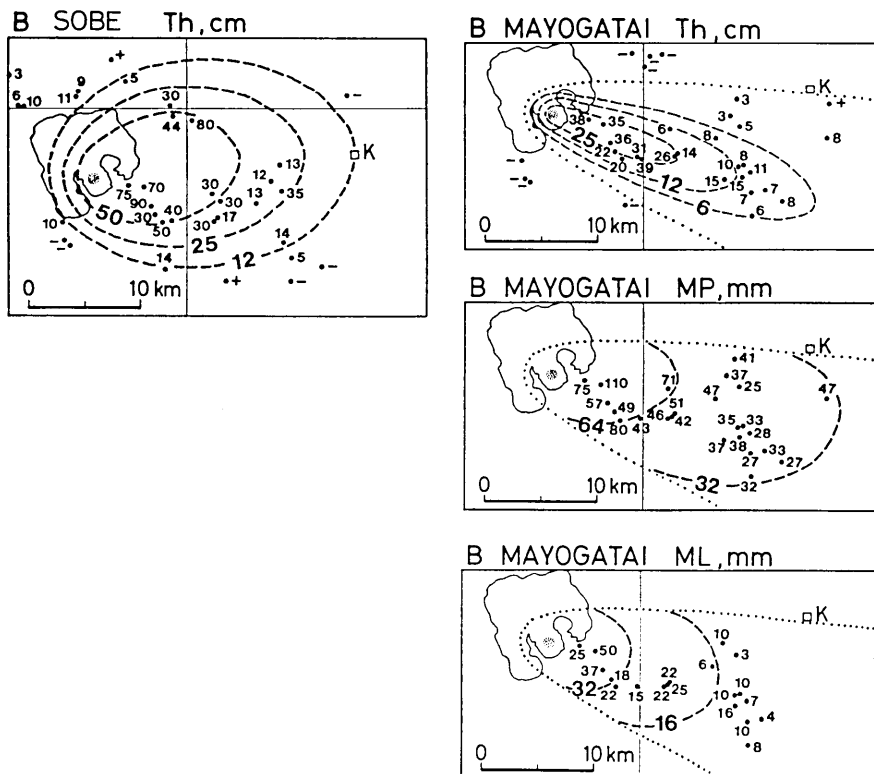


Fig. 15. Dispersal maps of B.

relatively long eruption duration, say, a week or a month. However, it could not have exceeded a year because no layer of fallen leaves or soil is found. Orientations of decomposed log holes laied down probably by the eruptive activity point to the center of the Nakanoumi crater.

C (5,400 y B.P.)

This is the largest-volume eruptive episode of Towada Volcano in the Holocene epoch (HAYAKAWA, 1983b). One of the best exposures of C is a roadcut at Kanegasawa (609:23.4 km, 83°), where the deposits are well preserved because they were covered by reworked debris immediately after the eruption:

- >50 cm reworked debris
- 9 cm bedded brown fine ash with scattered accretionary lapilli (Utarube ash)
- 25 cm pumice with a large amount of lithic fragments; composed of two beds showing normal grading (Kanegasawa pumice)
- 91 cm pale yellow coarse pumice with isolated crystals; a small amount of banded pumice and scoria; MP 3.8 cm, ML 0.3 cm; faint reverse grading through the whole section besides the uppermost finer bedded layer (Chuseri pumice).

The Chuseri pumice may be a product of a typical plinian eruption and the volume is the largest of all plinian deposits of Towada Volcano. Its isopachs are nearly circular but the centers of thinner isopachs are successively offset eastward (Fig. 16). This may be attributed to a down-wind drifting of the eruptive column. The outermost 25 cm isopach encloses an area of 1,636 km² and it is obvious that the overall dispersal area is far larger than 2,000 km². The maximum thickness of 17 m is attained at Kanda (619:2.2 km, 143°) 280 m south of the rim of the Nakanoumi crater, where the top part is missing due to erosion. The original thickness may well have exceeded 20 m. The distance plots of thicknesses yield an extrapolated maximum thickness of 33 m just above the vent (HAYAKAWA, 1983b, Fig. 6).

The MP, ML, and Md all decrease more or less exponentially with distance from the source as is characteristic of plinian fallout deposits (WALKER, 1980). However, ML values within 3 km from the vent are several times larger than the values derived from the extrapolation of the distant data. It is explained that the measured values are obtained from ballistic lithic fragments. BOOTH *et al.* (1978) has shown that ballistic lithic fragments exceeding about 10 cm across typically extend out to 2 to 5 km from the vent, which is useful to determine the vent

position. The maximum size of ballistic lithic fragments measured 80 cm \times 60 cm \times 30 cm at Kanda (261 : 2.0 km, 139°).

Fig. 17 shows the grain size characteristics of the Chuseri pumice deposit. It does not contain a substantial amount of fine ash, at least, as far as 45 km from the source. The concentration of free crystals occurs outward from the vent due to the fact, as stated by WALKER (1981c), that the assemblage of crystals covers a limited size range, and crystals are concentrated at a distance from the source where the fall velocity of the crystals equals the fall velocity of the deposits. A proximal deposit

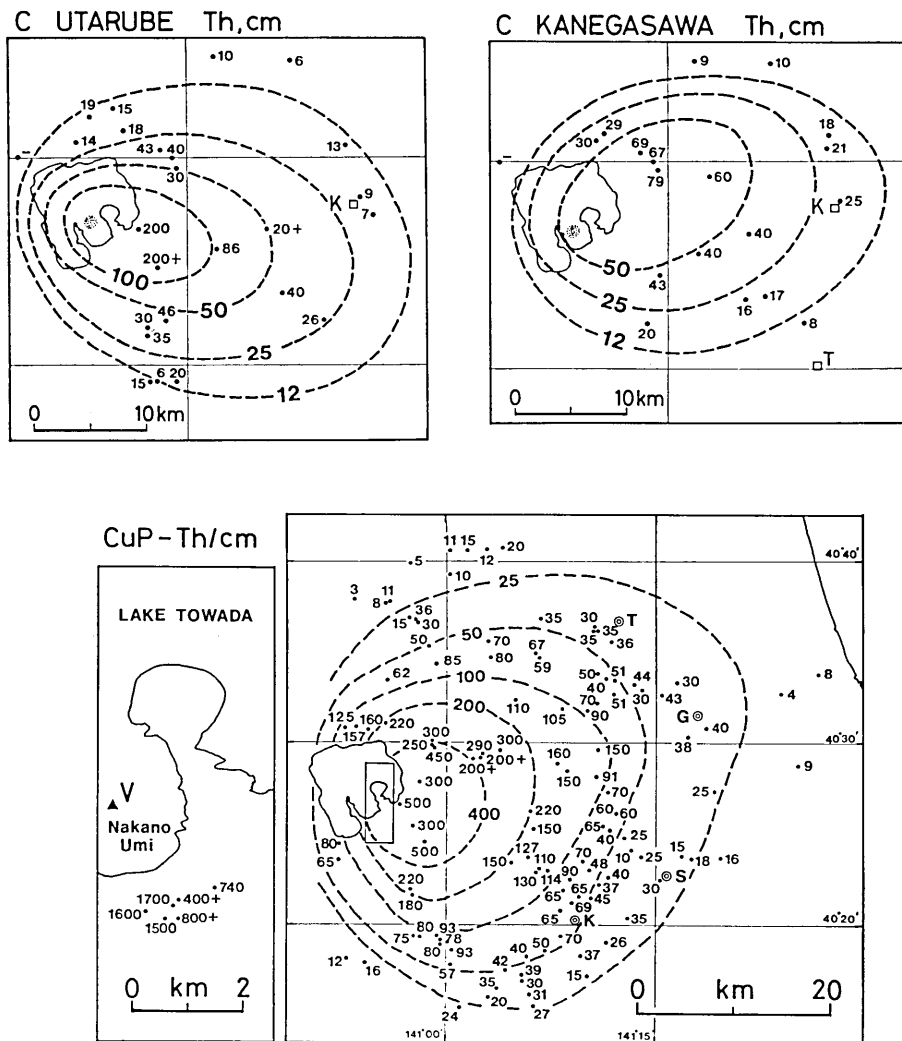


Fig. 16. Dispersal maps of C. CuP: Chuseri pumice.

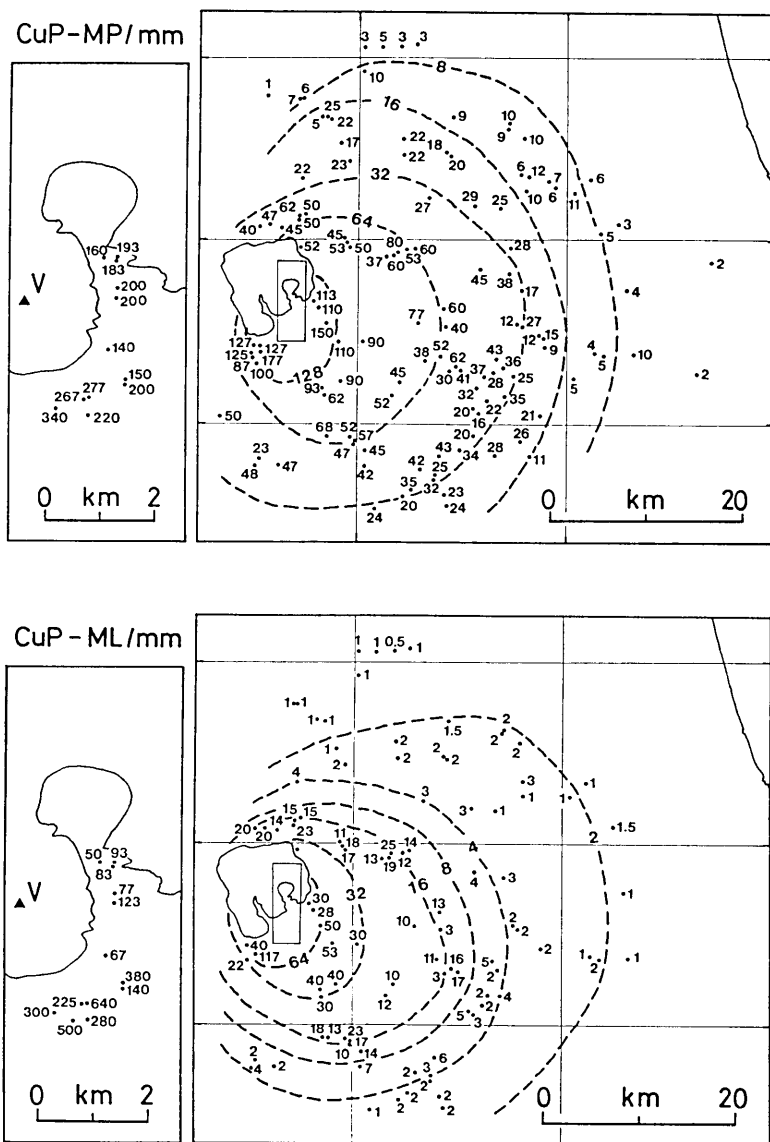


Fig. 16. (continued)

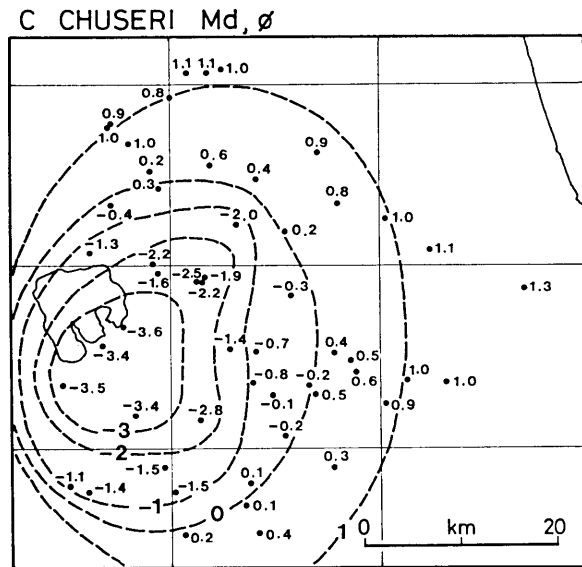


Fig. 16. (continued)

at Kanda (261:2.0 km, 139°) is poorly sorted and contains fine ash more than 2 wt. %. This character is used as a diagnostic criterion to distinguish between the Chuseri and Nambu pumice deposits at proximal exposures; the latter is well sorted and contains fine ash less than 2 wt. %.

A coarser pumice deposit of the Chuseri plinian eruption is overlain by finer and better stratified Kanegasawa pumice deposit. It is interpreted that, at the end of the Chuseri eruption, the eruption column diminished the dispersive power and changed its nature from a sustained eruption to an intermittent one. The high content of lithic fragments in the Kanegasawa deposit implies that the vent was widened during the explosions, which may have been partly phreatic, possibly caused by the access of lake water into the vent.

The violent Kanegasawa explosions finally removed the northwestern part of the Goshikiwa volcano, when copious lake water rushed into the vent gully the lake bottom. Then, the Utarube ash eruption took place by the magma-cold water interaction. At Utarube (264:4.3 km, 86°) a 2 m thick pyroclastic surge deposit is exposed and intercalated with thin fallout ash beds containing abundant accretionary lapilli. The distribution of the pyroclastic surge deposits is limited in the caldera, whereas the fallout ash occurs over a wide area outside the caldera (Fig. 16). The Taal 1965 eruption (MOORE *et al.*, 1966) may be a historical analogue to the Utarube ash eruption.

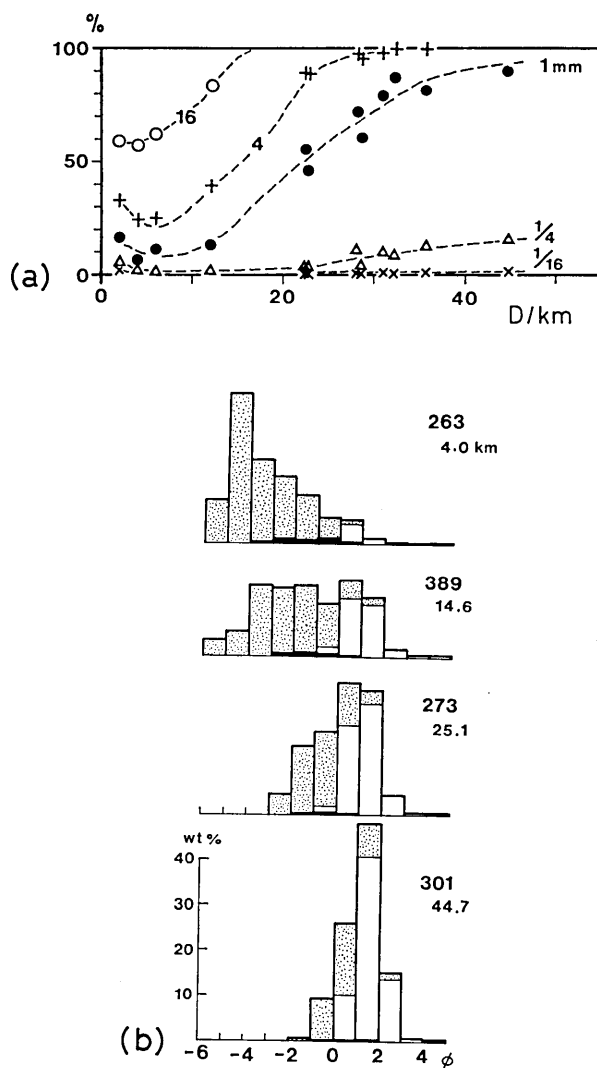


Fig. 17. (a) Cumulative weight percentage of materials finer than the selected grain size of the Chuseri pumice deposit plotted against distance from the source. (b) Size frequency histograms of the Chuseri pumice deposit. The bars on the histograms are subdivided according to their contents of pumice (stippled), lithics (solid), and crystals (blank). Figures on the right hand are the locality No. and distance from the source. Note that crystals increase in amount as they get farther from the source.

D' (ca. 6,000 y B.P.)

D' was a very weak eruptive episode. At a roadcut south of Mt. Heraidake (849:10.7 km, 97°), the deposit is represented as a laminated, 6 cm thick, dark blue ash bed. No plinian pumice deposit is found in D'.

D (ca. 7,000 y B.P.)

The type section of D is established at a roadcut northwest of Okuromori (718:14.6 km, 124°), where a 34 cm thick Oguni pumice crops out. The description is:

- 6 cm yellow pumice
- 2 cm pale yellow ash
- 26 cm reversely graded yellow pumice; MP 3.7 cm, ML 0.8 cm.

The intercalated thin ash is distinctive and is used as a key to the identification among other plinian pumice deposits. The narrow dispersal fan extends to N131°E. The 12 cm isopach covers an area of 213 km² (Fig. 18).

E (8,500 y B.P.)

E comprises the Nambu pumice, the second largest plinian deposit in the Holocene epoch, and the overlying Kaimori ash. A description of E at a roadcut south of Mt. Heraidake (849:10.7 km, 97°) is:

Kaimori ash

- 22 cm laminated brown ash; hard
- 6 cm pumice lapilli
- 16 cm laminated brown ash; hard

Nambu pumice

- 42 cm reddish yellow pumice lapilli; finer at the top
- 5 cm fine and medium brown ash;

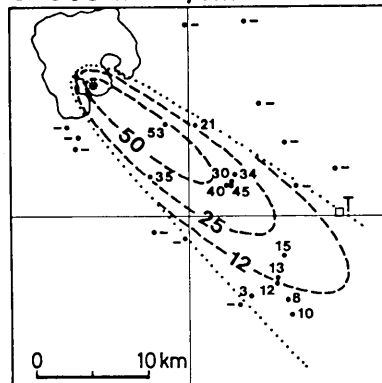
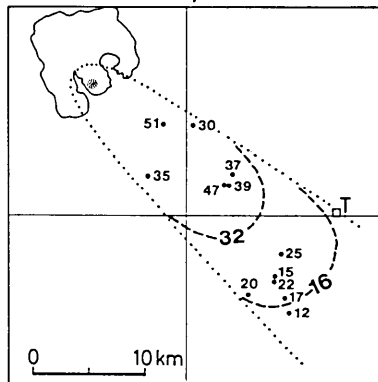
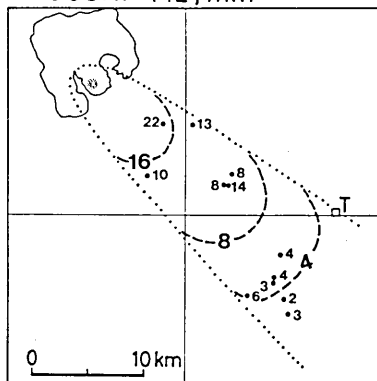
D OGUNI Th, cm**D OGUNI MP, mm****D OGUNI ML, mm**

Fig. 18. Dispersal maps of D.

loose

213 cm reddish yellow pumice lapilli; finer and bedded at the bottem;
MP 17.7 cm, ML 3.5 cm.

The Nambu deposit consists predominantly of dacitic pumice fragments and a smaller amount of lithic fragments and isolated crystals. Near-planer surfaces on many of the large pumice fragments suggest breakage on impact with the ground. A pink thermal coloration produced by oxidation of iron occurs inside the largest pumice fragments. In the upper half of the deposit, the pumice fragments are coated with fine ash (*e.g.* at Januma; 697:22.5 km, 103°). A thin layer of brown ash intercalated at about three quarters from the base suggests an event in which the high plinian column was once lowered during the eruption. The dispersal fan is remarkably elongated toward N103°E and the 12 cm isopach encloses an area of 1,426 km² (Fig. 19).

The Nambu pumice is thickly accumulated up to 40 m at Kankodai (146:1.5 km, 103°), a lookout place on the Nakanoumi crater, where the lower 5 m are composed of an alternation of densely welded beds and partly welded beds. A densely welded massive bed 6 m thick is exposed at Kanda (617:2.4 km, 158°). The welding can be attributed to a high accumulation rate of scarcely cooled pumice fragments from a relatively lower eruption column. SPARKS and WRIGHT (1979) have shown that the accumulation rate for the documented Askja 1875 welded tuff was about 20 cm/min. Assuming this rate, a duration of 30 min may be estimated for the lower welded part of the Nambu pumice.

The overlying Kaimori ash is a water-flushed deposit containing accretionary lapilli. It implies that the eruptive episode E terminated in a phreatomagmatic eruption as C did. This is also the case with F.

F (*ca.* 9,500 y B.P.)

The type section of F is a roadcut northwest of Okuromori (718:14.6 km, 124°), where the 14 cm thick Kabayama ash is underlain by the 65 cm thick Natsuzaka scoria:

- 3 cm accretionary lapilli-bearing brown ash
- 4 cm dark brown scoria, MS (maximum scoria size) 1.3 cm
- 7 cm accretionary lapilli-bearing brown ash
- 65 cm dark brown scoria with abundant large lithic fragments; MS 4.9 cm, ML 4.0 cm.

The dark blue color inside the large scoria fragments is probably due to the crystallization of magnetite microcrystals. Although isopachs of the Natsuzaka scoria are less constrained, it seems that the dispersal axis

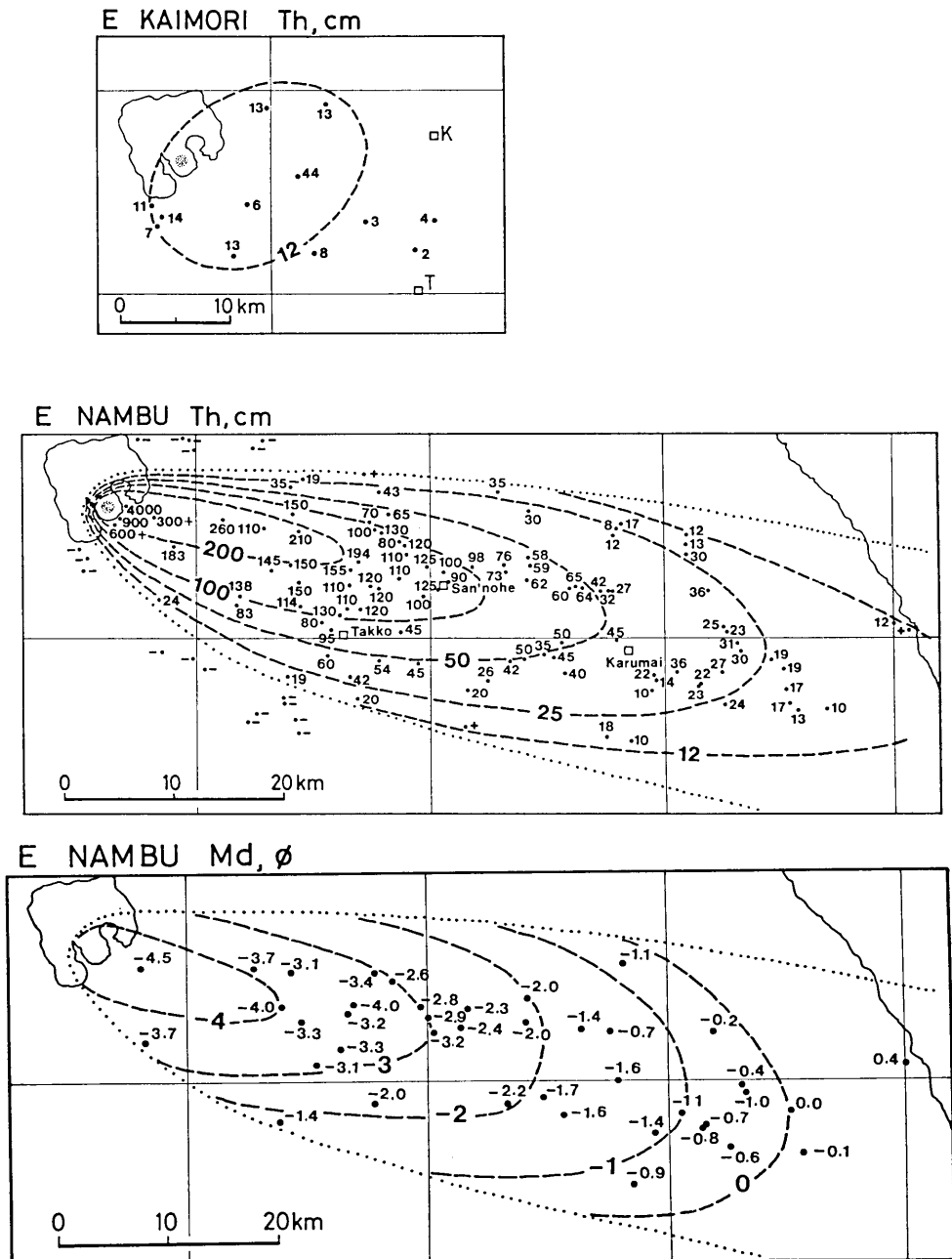


Fig. 19. Dispersal maps of E.

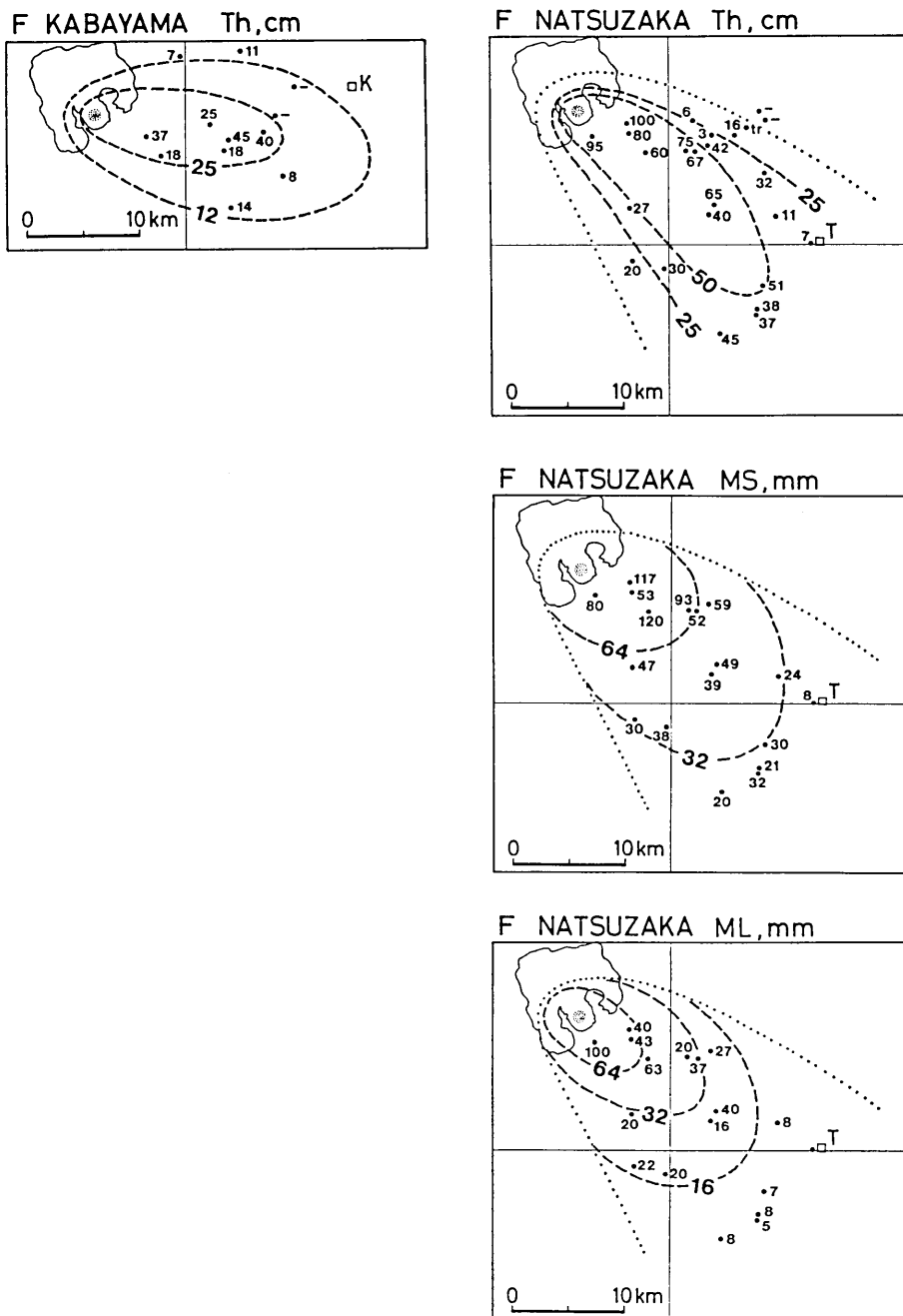


Fig. 20. Dispersal maps of F.

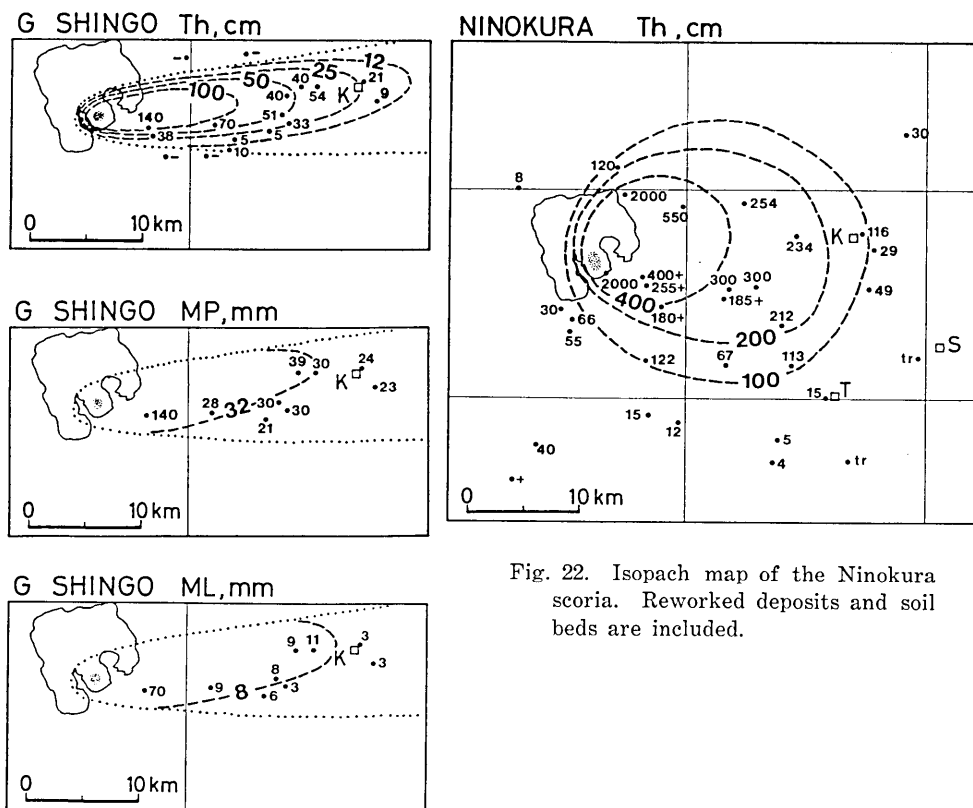


Fig. 21. Dispersal maps of G.

mainly of finely vesiculated yellow pumice fragments; MP is 3.0 cm and ML is 0.3 cm. Small scoria fragments derived from vent walls are abundant in particular horizons. The narrow dispersal fan extends eastward and the 12 cm isopach covers an area of 171 km² (Fig. 21). MP and ML on the northern side of the dispersal axis are larger than those on the south. This is probably due to a northerly wind at the low-altitude. The asymmetric dispersal pattern caused by the low elevation winds oblique to the high-altitude winds has been known for the Tarumai-b pumice (SUZUKI *et al.*, 1973) and Fuji 1707 deposit (MIYAJI, 1984). No fallout ash bed is found in G.

Ninokura (ca. 13,000–11,000 y B.P.)

Ninokura scoria is a collective name for the series of fallout deposits which are the products of successive eruptions from the Goshikiwa volcano during the period 13,000–11,000 years ago. Individual eruptive

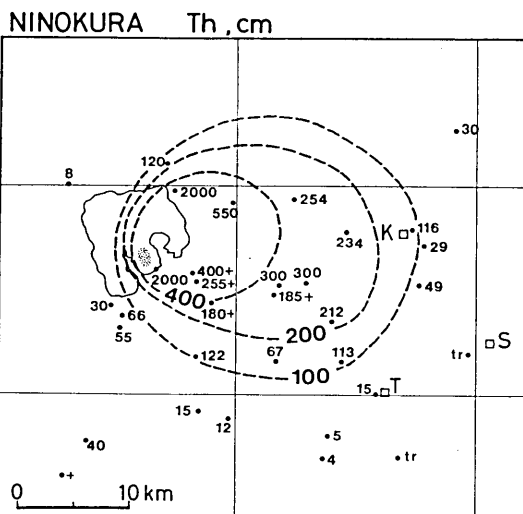


Fig. 22. Isopach map of the Ninokura scoria. Reworked deposits and soil beds are included.

episodes are poorly defined because, as is the case of a basaltic activity, the dormant interval between the eruptions was too short for sufficient development of a (humic) soil bed. The total thickness of the Ninokura scoria, including reworked deposits and soil beds, is shown in Fig. 22.

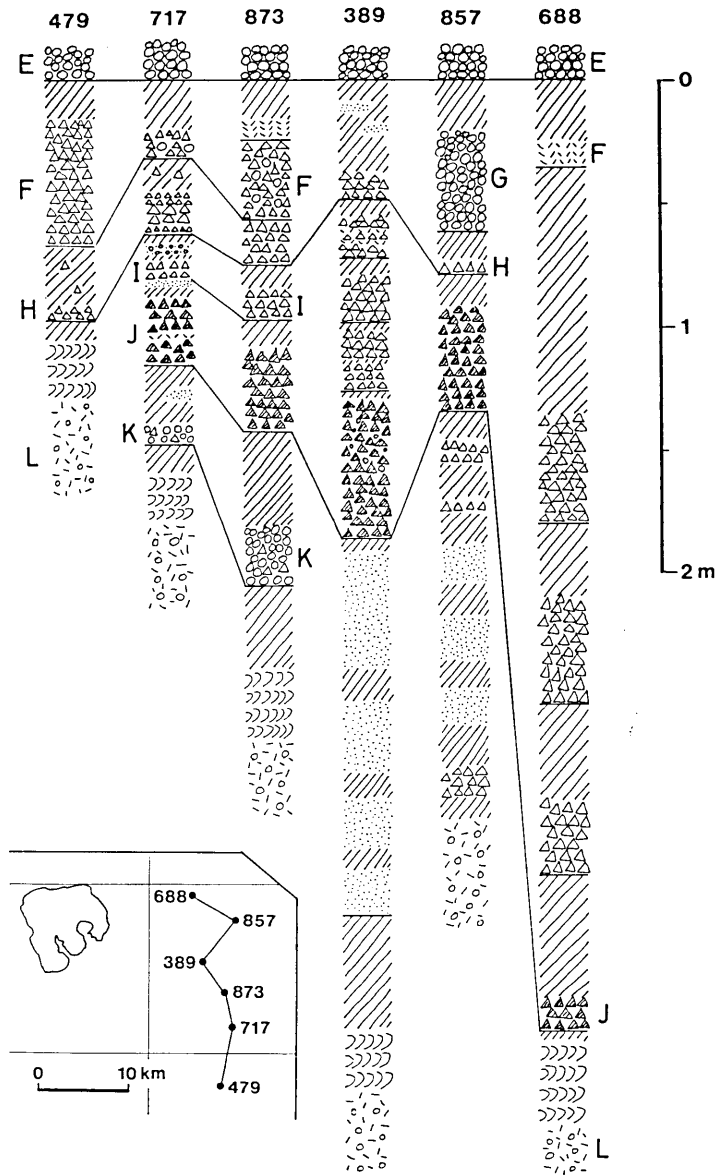


Fig. 23. Representative columnar sections of the Ninokura scoria. Symbols are as in Fig. 5.

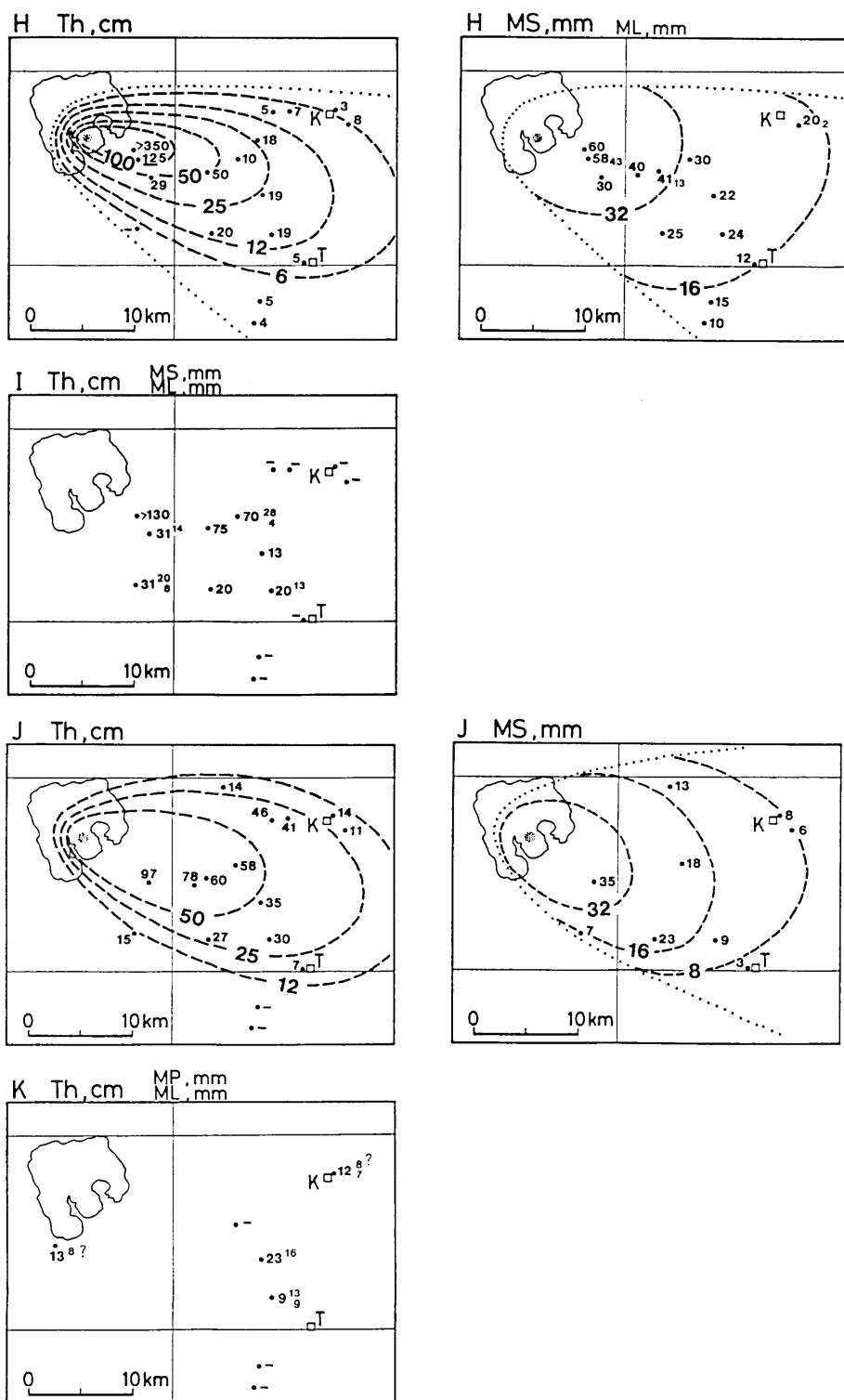


Fig. 24. Dispersal maps of H, I, J, and K.

Representative columnar sections are shown in Fig. 23; the lower part is characteristic for loose, bluish coarse ash, the middle part is for poorly vesiculated scoria, and upper part is for well vesiculated scoria. Four conspicuous deposits (H, I, J, and K; Fig. 24) are described below.

The youngest deposit of the Ninokura scoria, H, consists of spinose black scoria showing reverse grading. At a roadcut west of Towariyama (828:5.2 km, 112°) it is 125 cm thick and has MS=5.8 cm, ML=4.3 cm.

I is an accumulation from a series of weak explosions. The deposit is composed of an alternation of coarse scoria beds and fine ash beds. It is difficult to distinguish a primary fallout ash bed from a secondary reworked one. Measured thickness is so variable that no reliable isopach is drawn in Fig. 24. A good section of I, 70 cm thick, is exposed on a roadcut west of the Ninokura dam (389:14.6 km, 98°):

- 10 cm spinose, strong brown scoria (H)
- 7 cm brown fine ash

-
- I 17 cm mixture of light brown scoria and poorly vesiculated black scoria ; MS 1.8 cm
 - 7 cm blue fine sand ; bedded
 - 19 cm spinose brown scoria ; MS 2.8 cm
 - 3 cm brown fine ash with scattered scoria fragments
 - 12 cm spinose dark brown scoria ; MS 1.2 cm
 - 1 cm brown fine ash
 - 11 cm mixture of yellow and brown spinose scoria ; MS 1.6 cm
-

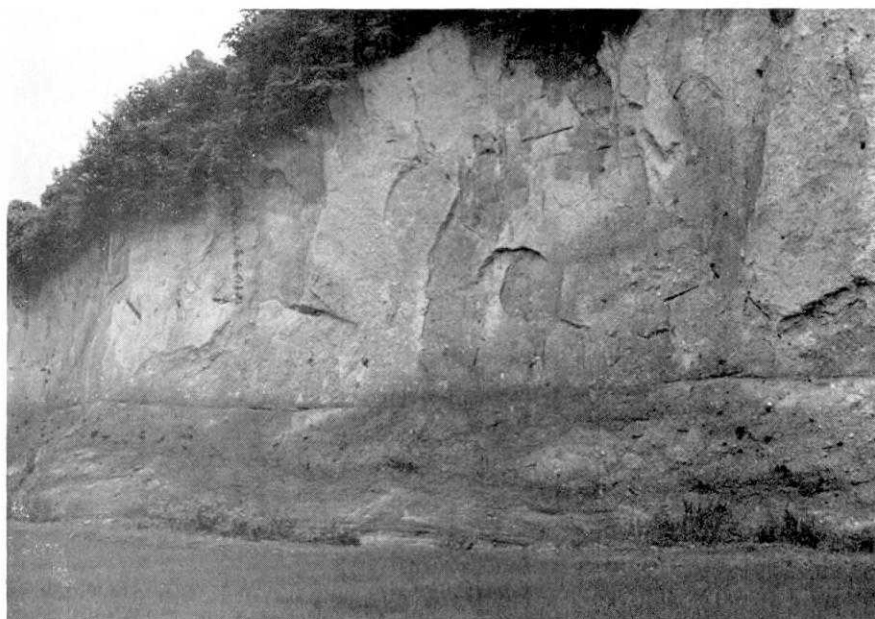
- 5 cm brown fine ash
- 58 cm poorly vesiculated scoria (J).

Scoria fragments of J are conspicuous for their glossy and smooth surfaces and for a poorly vesiculated interior. The size sorting is achieved extremely well and fines are completely removed. The type section is obtained from a roadcut west of the Ninokura dam (389:14.6 km, 98°) where the thickness is 58 cm and the maximum scoria size is 1.8 cm.

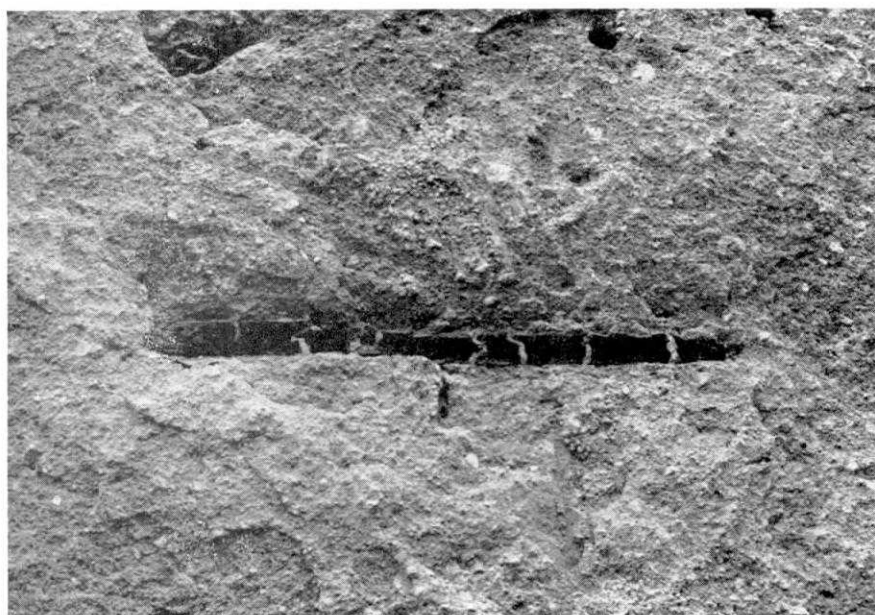
K is composed mainly of pumice fragments and of darker colored scoria fragments. It is rarely exposed and the outline of the distribution is not yet known. K is 23 cm thick at Sugisawa (873:17.7 km, 108°) and the maximum pumice size is 1.6 cm.

L (13,000 y B.P.)

This eruptive episode produced the voluminous Hachinohe ignimbrite and the underlying Hachinohe (fallout) ash. The eruptive activity created the present Towadako caldera at the source. The deposits are well exposed

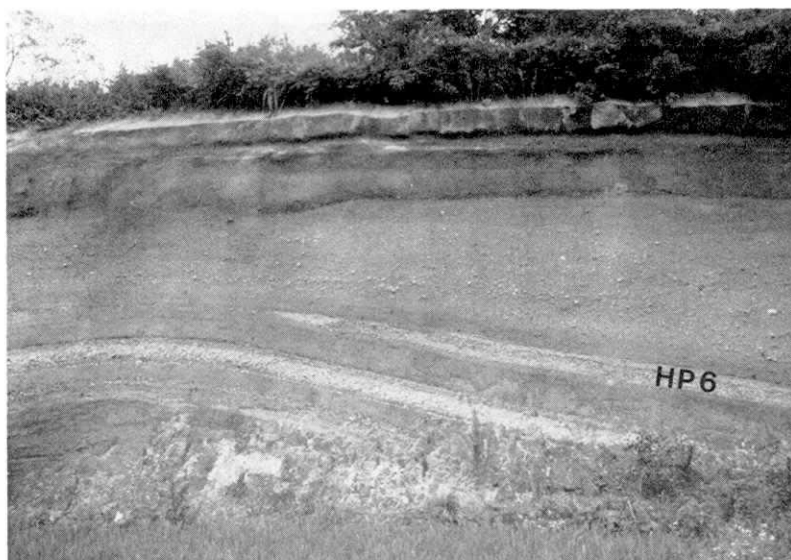


(a)



(b)

Fig. 25. Hachinohe ignimbrite. (a) At Yokozawa (132: 23.5 km, 95°). The lower 3.5 m thick part is rich in lithic fragments and depleted in fine ash. Underlying HP6 pumice bed is seen at the lowest level of the outcrop. (b) Close-up view of a carbonized log at the same locality as (a).



(c)



(d)

Fig. 25. Hachinohe ignimbrite. (c) At Maita (198: 29.4 km, 67°) showing the erosive power of the Hachinohe pyroclastic flow; a part of the underlying HP6 pumice bed (35 cm thick) has been removed. (d) A segregation pipe seen at Kakkotai (282: 26.9 km, 101°). Digger is 45 cm long.

at Yokozawa (132:23.5 km, 95°; Fig. 25a), where about 10 m thick Hachinohe ignimbrite overlies 163 cm thick Hachinohe ash.

The distribution of the Hachinohe ignimbrites is shown in Fig. 26 being combined with the Ofudo ignimbrite (N). Throughout the distribution the Hachinohe ignimbrite is totally non-welded and contains many carbonized logs as large as 50 cm across and 2 m long (Fig. 25a, b). They are lying subhorizontally and their orientations point to the vent position, as shown by FROGGATT *et al.* (1981) for the Taupo ignimbrite. From Fig. 25c it is evident that the Hachinohe pyroclastic flow possessed some erosive power. A part of the underlying pumice bed (HP6) has been removed. There are many segregation pipes in the ignimbrite (Fig. 25d), constituents of which are rich in heavies, *i.e.* lithics and crystals, and they are extremely depleted in fines. Ballistic lithic blocks up to 1 m

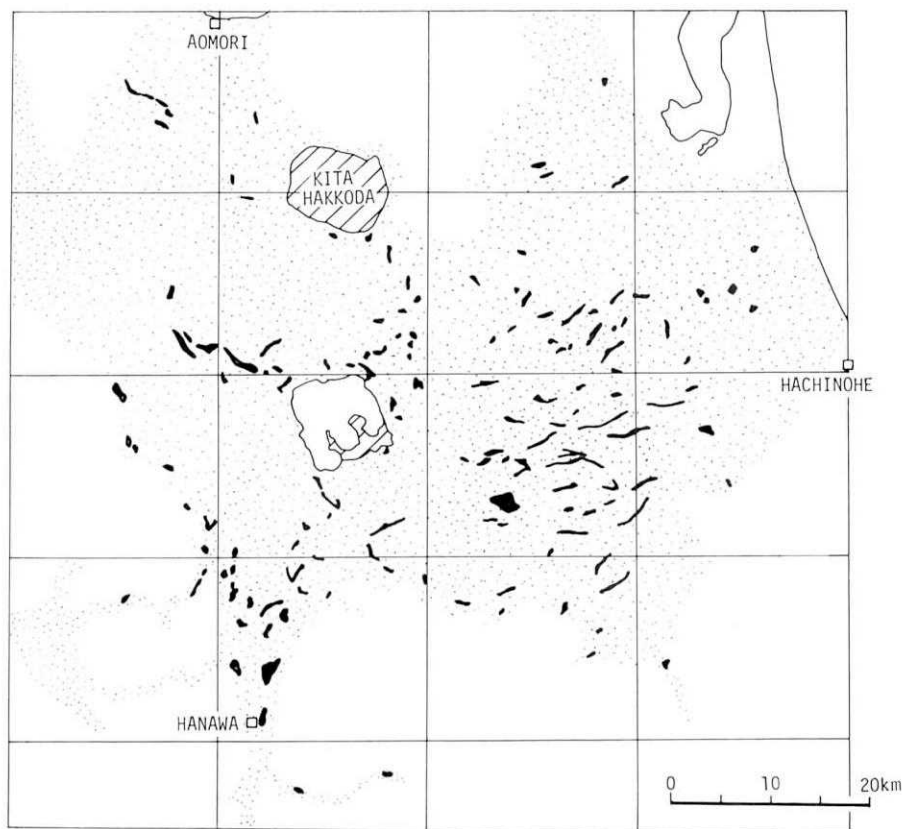


Fig. 26. Distribution map of the Hachinohe and Ofudo ignimbrites. Solid black part represents the outcrops. Stippled part is the area passed over by the pyroclastic flows. Volcanic edifices younger than the Hachinohe ignimbrite are obliquely ruled.

across are seen at many proximal exposures, *e.g.* at Sobegawa (174:9.4 km, 52°). Flood deposits generally overlie the ignimbrite with an erosive contact.

The isopach map of the Hachinohe ash is shown in Fig. 27. It has been described elsewhere (HAYAKAWA, 1983a) and is not further considered here.

M (ca. 17,000 y B.P.)

At Kobayashi (868:25.5 km, 69°), M crops out between L and N:

250 cm Hachinohe ash (L)

15 cm brown soil

M 27 cm yellow fine ash with scattered pumice lapilli; draping the original topography; MP 1.6 cm (Maita 2 ash)

8 cm Ash-coated yellow pumice; MP 4.0 cm, ML 1.2 cm (Maita 1 pumice)

24 cm brown soil

100 cm laminated sand beds (flood deposit)

>200 cm Ofudo ignimbrite (N).

The dispersal fan of the Maita 1 pumice is very narrow and elongated to N68°E (Fig. 28). The Maita 2 ash deposit is poorly sorted and contains a large amount of fine ash, suggesting a possibility of flow origin.

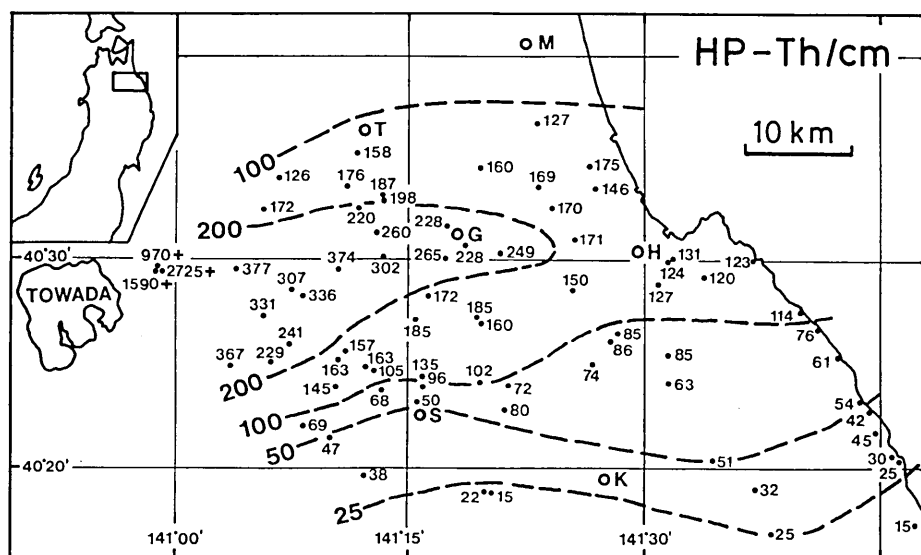


Fig. 27. Isopach map of the Hachinohe ash. M: Misawa, T: Towada, G: Gonohe, H: Hachinohe, S: San'nohe, K: Karumai.

Nevertheless, it is concluded that the ash deposit is of fall origin because it drapes the lower Maita 1 pumice without eroding and because no evidence is found that it passes into a thick valley-pond type "normal" ignimbrite.

N (25,000 y B.P.)

Products of the eruptive episode N are voluminous Ofudo ignimbrite and the underlying Kirida fallout deposits. The type section is a roadcut at Sobegawa (378:9.4 km, 51°):

(no flood deposit here)

800 cm Ofudo ignimbrite

43 cm white ash with scattered pumice lapilli in the lower half (Kirida 4 ash)

59 cm white plinian pumice; MP 2.5 cm, ML 1.5 cm (Kirida 3 pumice)

14 cm bluish gray ash (Kirida 2 ash)

3 cm blue lithic lapilli (Kirida 1 ash).

Isopach maps of the Kirida deposits are shown in Fig. 29. The lower two have a limited dispersal, whereas the upper two are widely dispersed having nearly circular isopachs.

The lithology of the Ofudo ignimbrite is very similar to that of the Hachinohe. It is difficult to distinguish between them where the underlying fallout deposits are not exposed. With the use of a hand lense, however, they are distinguishable by the presence of hornblende phenocrysts: the Hachinohe carries hornblende whereas the Ofudo does not. In many places the Ofudo is covered by flood deposits in the same way as the Hachinohe ignimbrite.

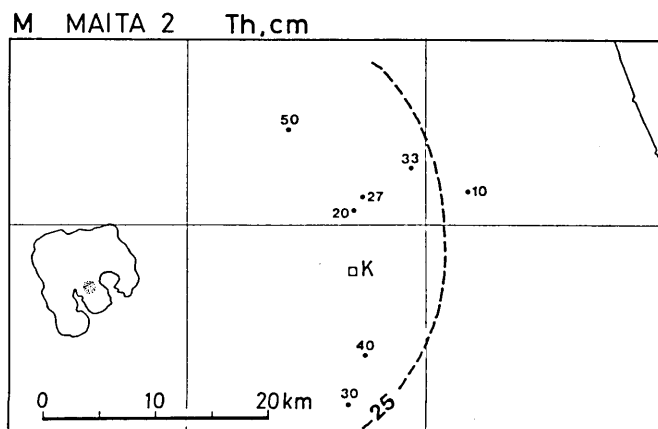


Fig. 28. Dispersal maps of M. K: Kanegasawa.

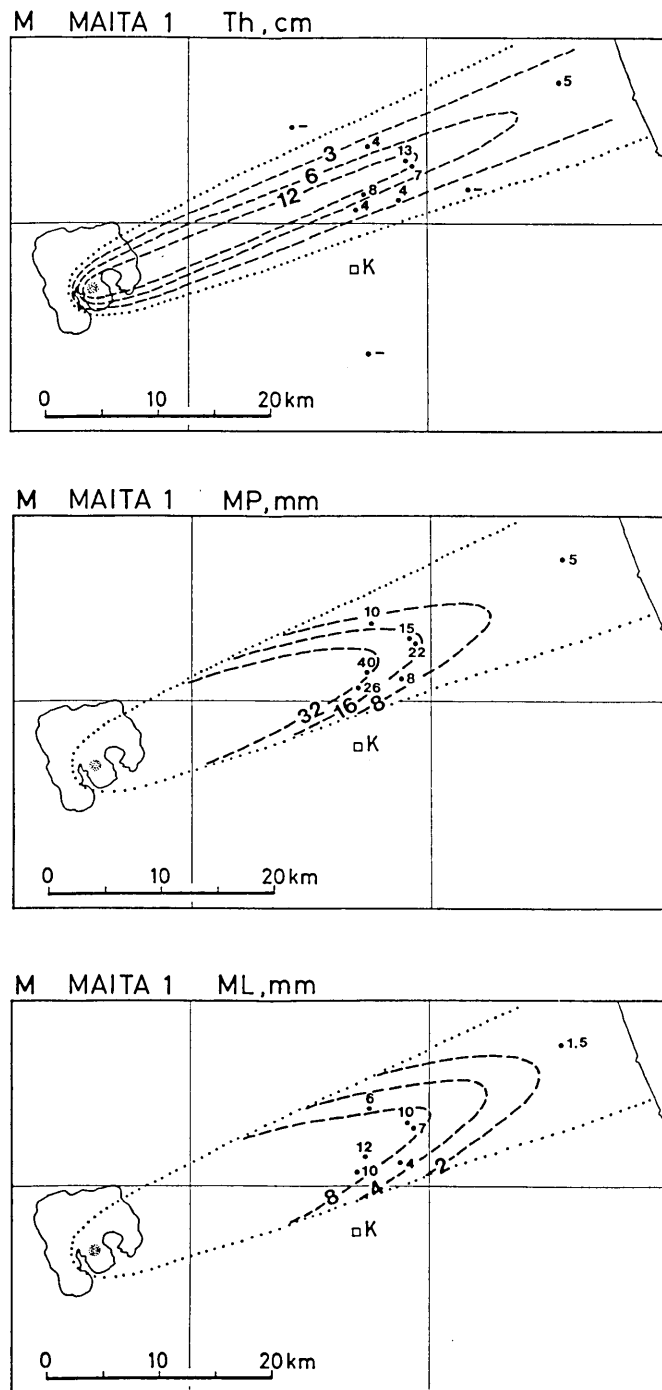


Fig. 28. (continued)

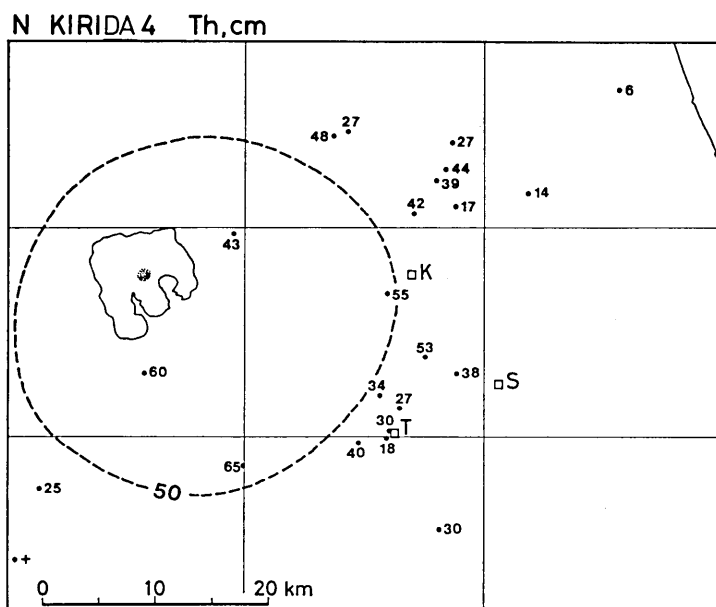


Fig. 29. Dispersal maps of N.

O (ca. 35,000 y B.P.)

O appears at Kawaramachi (871 : 34.4 km, 74°):

(N)

50 cm brown soil

-
- O 40 cm coarse pumice fragments and a comparable amount of coarse lithic fragments; MP 5.4 cm, ML 2.5 cm
- 16 cm pale brown fine ash with scattered pumice lapilli
- 11 cm coarse pumice fragments and a comparable amount of coarse lithic fragments; MP 2.2 cm, ML 1.0 cm
-

5 cm brown ash

(P).

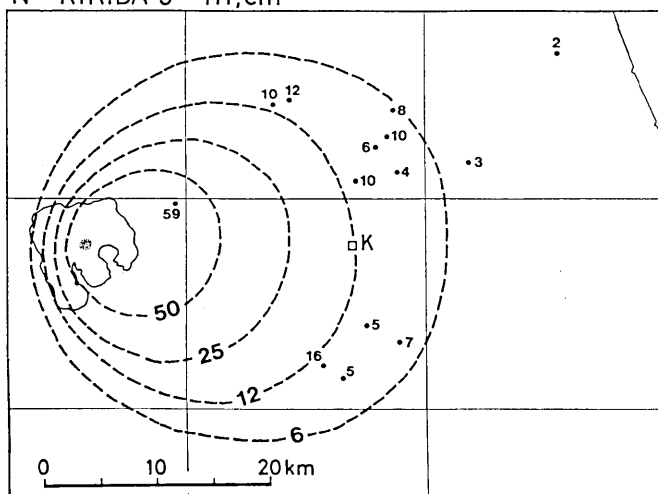
No map is drawn because of the scarcity of data.

P (ca. 45,000 y B.P.)

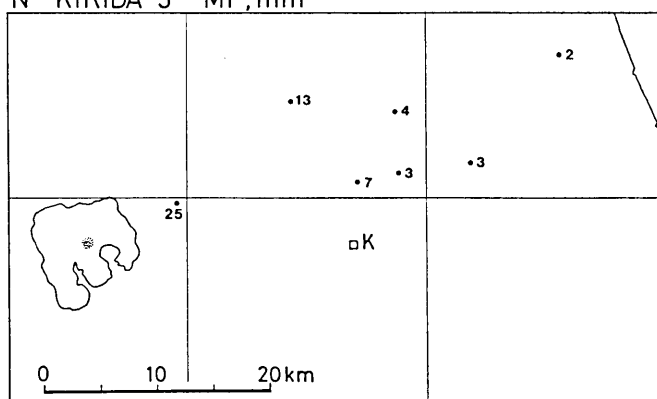
P appears at Okuse (709 : 23.0 km, 49°):

- 35 cm orange pumice
- 10 cm lithic concentration zone
- 72 cm orange pumice; MP 2.2 cm, ML 0.7 cm
- 1.5 cm dark blue fine ash with scattered lithic lapilli
- 0.5 cm brown fine ash

N KIRIDA 3 Th,cm



N KIRIDA 3 MP,mm



N KIRIDA 3 ML,mm

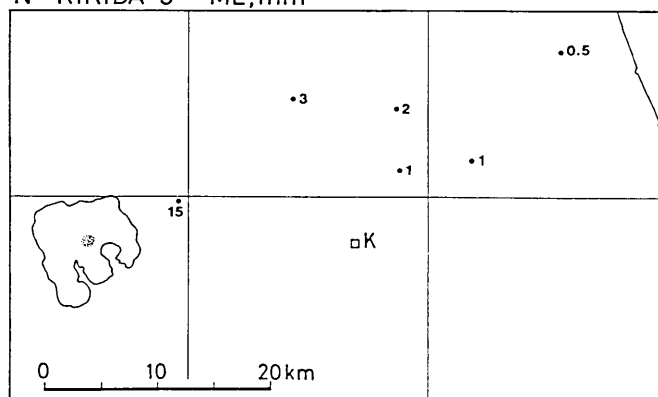


Fig. 29. (continued)

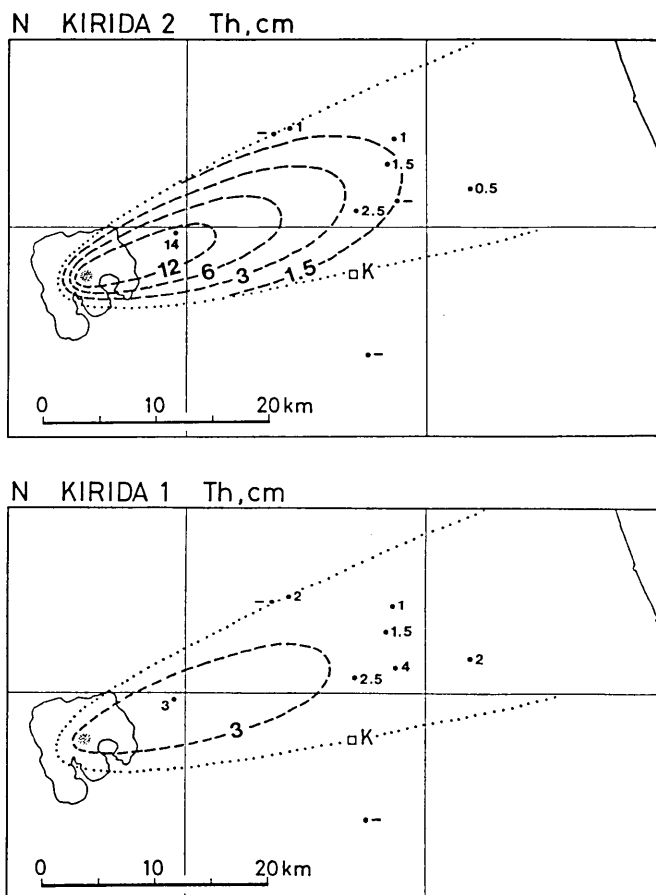


Fig. 29. (continued)

3 cm dark blue fine ash.

The upper 117 cm part is a plinian product; the pumice is extremely poor in crystals. The dispersal is shown in Fig. 30.

Q (ca. 55,000 y B.P.)

This is the oldest eruptive episode of the caldera-forming stage, which produced the Okuse ignimbrite and the underlying fallout deposits. They are exposed at Okuse (862:18.3 km, 46°; Fig. 31):

- 300 cm bedded silt containing pumice lapilli (flood deposit)
- 2000 cm Okuse ignimbrite
- 2 cm black ash; hard
- 1 cm brown ash
- 3 cm bluish gray scoria

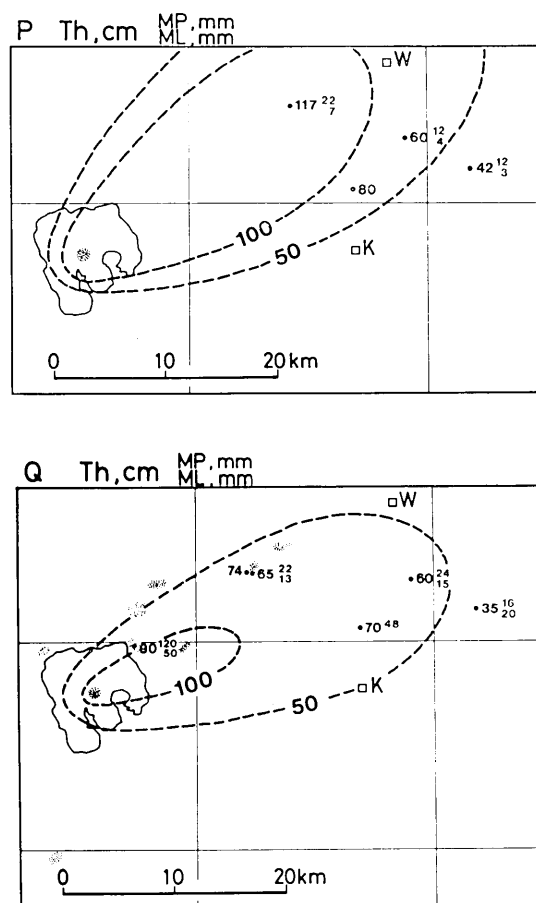


Fig. 30. Dispersal maps of P and Q. Stippled in Q is the Okuse ignimbrite. W: Towada.

- 8 cm bluish gray scoria with ash
- 8 cm white pumice with abundant obsidian
- 30 cm white pumice; MP 2.2 cm, ML 1.3 cm
- 9 cm ash-coated pumice; dark brown surface
- 6 cm fine-grained lithic lapilli.

The fallout deposits are distinctive for a color variation suggesting a vertical zoning of the chemical composition, more mafic toward the top. The isopach map is shown in Fig. 30. Juvenile fragments of the overlying Okuse ignimbrite is petrographically heterogeneous; white pumice, black scoria, and streaky fragments are embedded within a dark ash matrix. All the three types are well vesiculated. A lithic lag breccia (DRUITT and SPARKS, 1982), the maximum block size of which is 2 m across, is seen on the



Fig. 31. Fallout deposit of Q overlain by the Okuse ignimbrite at Okuse (862: 18.3 km, 46°). Spade is 80 cm long.

northeastern caldera wall at Aobunayama (728:6.8 km, 20°). The distribution of this ignimbrite is shown in Fig. 30. It also appears on the northwestern wall at Takinosawa (656:8.0 km, 316°), to the south of the caldera (Horiganai; 758:13.3 km, 199°), and to the northeast (Okuse; 710:21.7 km, 45°).

A columnar section of pyroclastic deposits older than Q is shown in Fig. 32. The dispersal of each deposit is hardly known because of limited exposures. Among them, V is distinctive, the thickness being 107 cm with MP=2.8 cm and ML=0.9 cm at Kirida (193:27.0 km, 60°; Fig. 33). W is a pinkish white fine ash from Toya Volcano, 240 km north of Towada, which erupted about 110,000 years ago (MACHIDA, 1983). The maximum thickness measured in the Towada area is 16 cm (Fig. 34). The dispersal map of X, plinian pumice deposit below W, is also shown in Fig. 34.

Areas enclosed by isopachs are plotted in Fig. 35 against the thickness for each fallout deposit. Same plots against MP and ML are shown in Fig. 36.

193 - 200 - 704

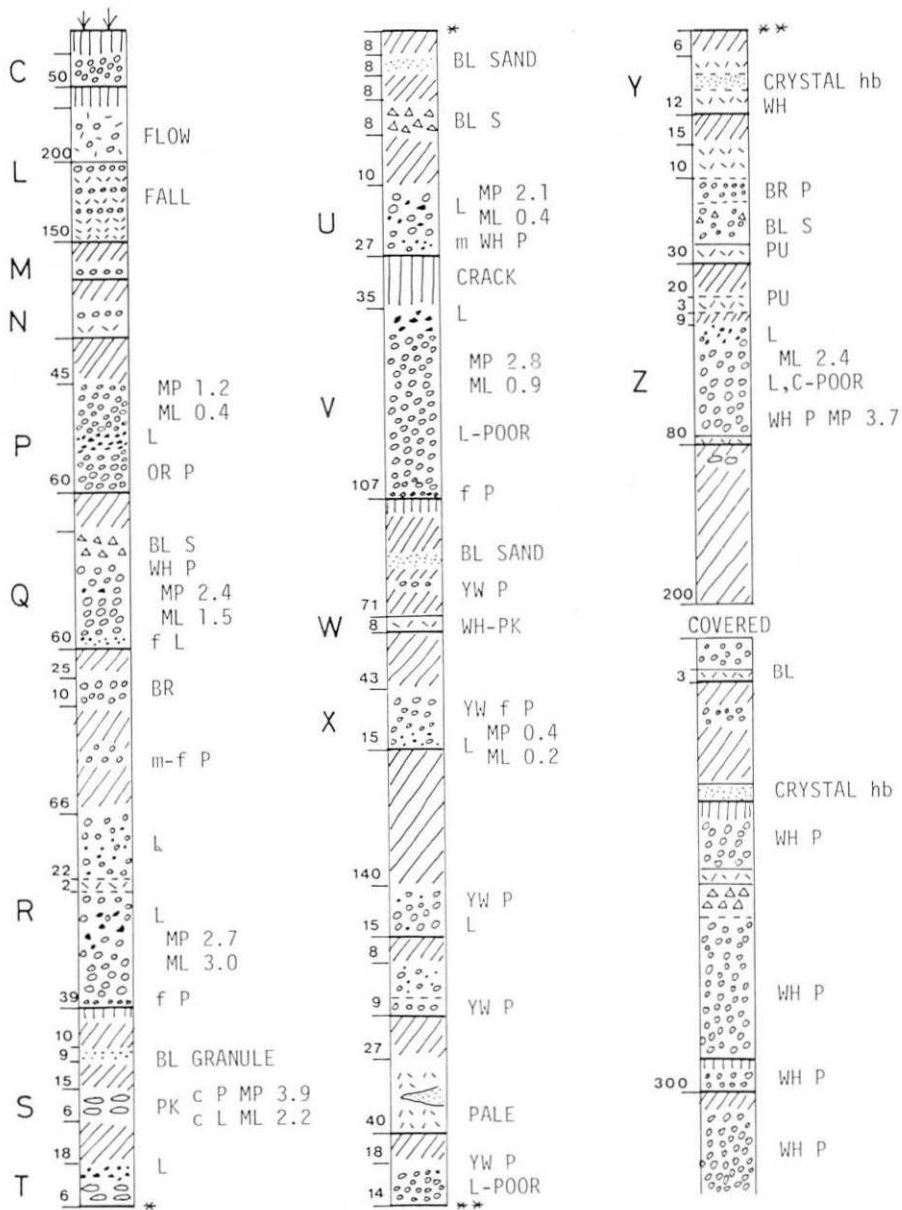


Fig. 32. Columnar section showing deposits older than Q, compiled from two sections at Kirida (193: 27.0 km, 60°; 704: 28.2 km, 63°) and one at Maita (200: 29.8 km, 66°). Symbols and abbreviations are as in Fig. 5 and Fig. 6, respectively. Thickness, MP, and ML values are all in cm.

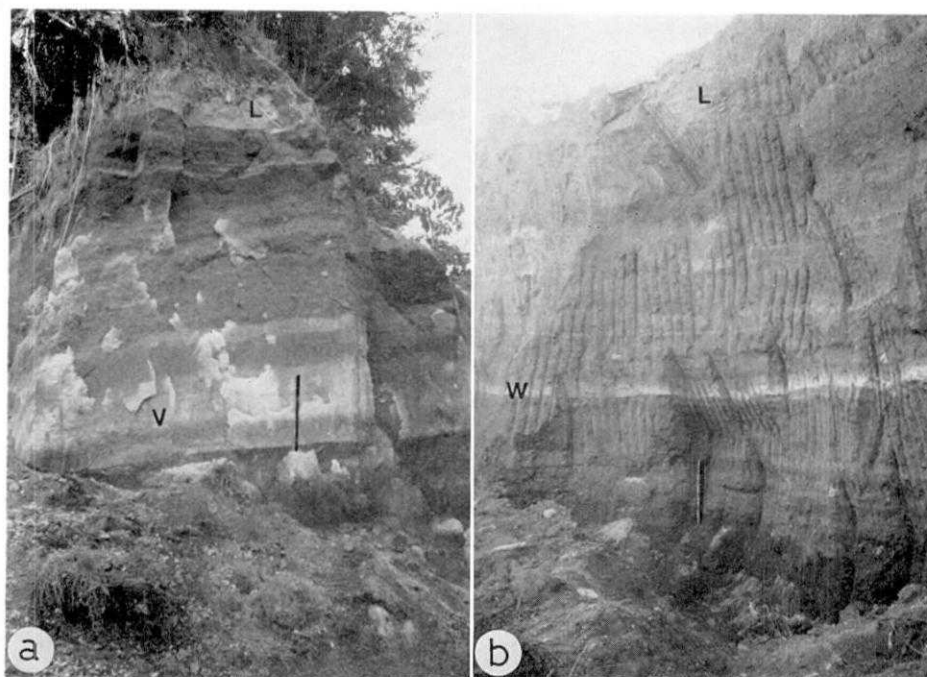


Fig. 33. Pyroclastic deposits older than L. (a) At Kirida (193: 27.0 km, 60°). Bar is 1 m long. (b) At Hachinohe (232: 53.6 km, 83°). Bar is 1 m long.

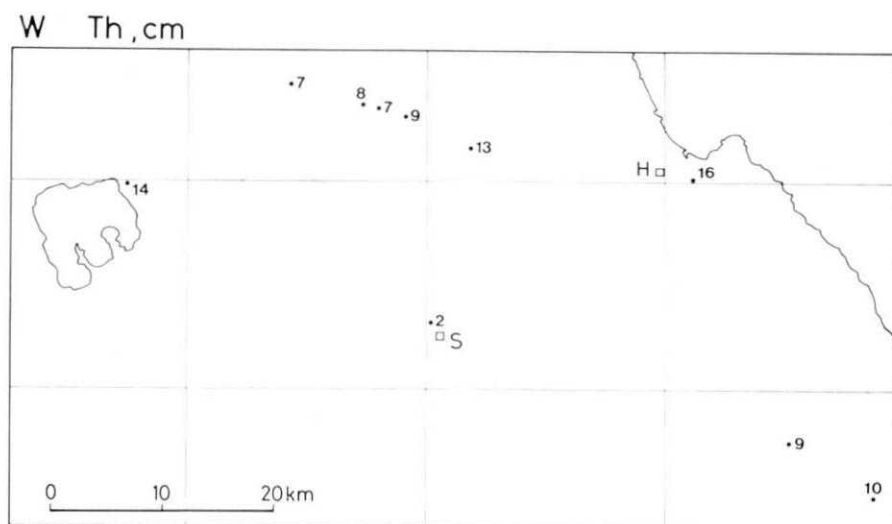


Fig. 34-1 Dispersal map of W.

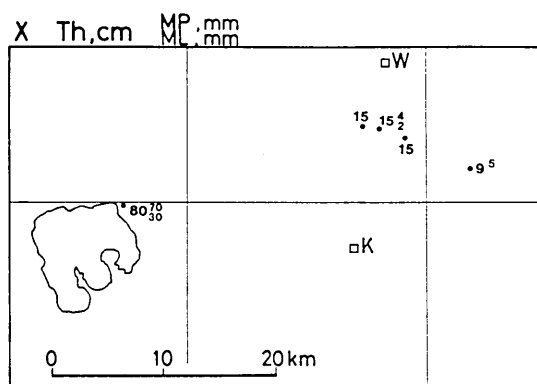


Fig. 34-2. Dispersal map of X.

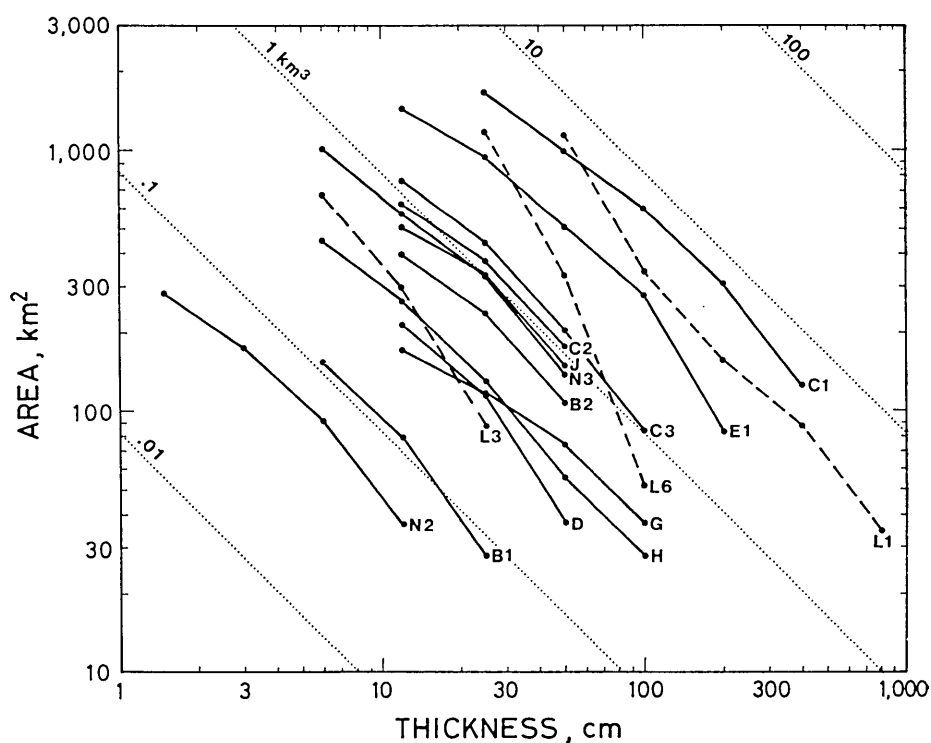


Fig. 35. Plots of the areas enclosed by isopachs against the thickness for the deposits for which more than three isopachs are available. B1: Mayogatai pumice, B2: Sobe ash, C1: Chuseri pumice, C2: Kanegasawa pumice, C3: Utarube ash, D: Oguni pumice, E1: Nambu pumice, G: Shingo pumice, L1: HP1 ash, L3: HP3 ash, L6: HP6 pumice, N2: Kirida 2 ash, N3: Kirida 3 pumice. The dotted lines give the volumes of deposits (Fig. 42).

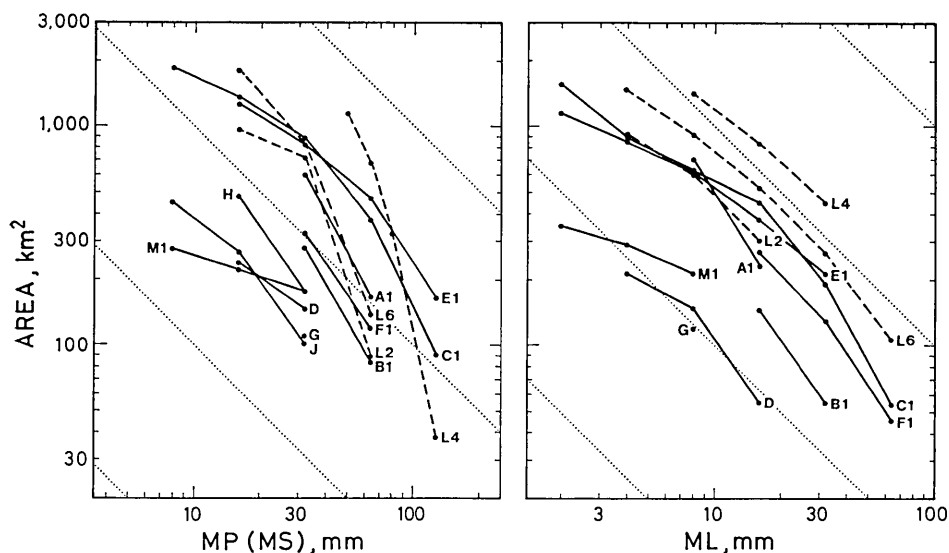


Fig. 36. Plots of the areas enclosed by isogrades of MP (MS) and ML. Codes are as in Fig. 35, with the addition of A1: Oyu 1 pumice, L2: HP2 pumice, L4: HP4 pumice, M1: Maita 1 pumice.

5. Volume and mass of fallout deposits

Estimating the total volume and mass of a fallout deposit is an important aspect of pyroclastic studies. A common method used for the estimation has been to measure the area enclosed by each isopach and then to plot the area against the thickness as shown in Fig. 34; integration of the resulting curve then yields the volume. However, there are two uncertainties in this method as stated by WALKER (1981c): how to extrapolate the curve at the low-thickness end, and which limiting thickness to take at this end.

Crystal method

A new method for determining the total mass of a deposit, which greatly reduces the uncertainties of extrapolation, is developed by WALKER (1980). It depends on the following facts: (1) liberated crystals fall closer to the source than the pumice fragments or shards of similar sizes and (2) the size range of crystals is generally limited in the range 2 to 1/16 mm (Fig. 37). If a sufficient land area is provided, most parts of the dispersal area of the crystals will be successfully mapped and then the total quantity of erupted crystals can be determined. The total mass erupted is then derived from dividing it by the crystal content of large

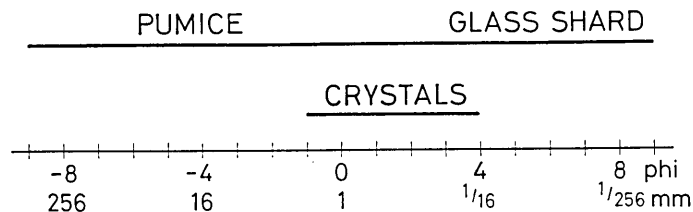


Fig. 37. Diagram showing general size range of pumice, glass shard, and crystals occurring in plinian deposits.

pumice clasts which is assumed to be the same as that in the erupted magma.

This crystal method has been applied only to three plinian deposits in New Zealand, *i. e.* Taupo (WALKER, 1980), Waimihia and Hatepe (WALKER, 1981a), because the method demands sievings and component analyses for a large number of samples collected from widely scattered localities. The present author applied it here to the Chuseri and Nambu plinian deposits of Towada Volcano. The method was partly modified as follows: crystal content was measured for each size class instead of measuring only the total content of crystals as was done by WALKER (1980, 1981a). In this way, duplicate or triplicate results may be obtained for a single deposit so that the accuracy of the method can be tested.

Large pieces of pumice fragments were taken from both pumice deposits. They were weighed, carefully crushed, and sieved. Then, crystals in each size class were separated by panning in water. This procedure yields the weight percentage of crystals in the pumice fragments (Table 8). The Chuseri and Nambu deposits are highly porphyritic and contain crystals as much as 14.5 wt. % and 23.3 wt. %, respectively.

These figures are far larger than 3-3.3 wt. % for the above-mentioned three deposits in New Zealand (WALKER, 1980, 1981a). Therefore, the Chuseri and Nambu deposits have an advantage in that the total mass can be more precisely calculated by the total quantity of crystals than the New Zealand examples.

From the isopach maps (Figs. 16 and 19) and bulk density diagram of the deposits (Fig. 38), isograde maps have first been constructed (Fig. 39, m) showing the mass of each deposit (g) overlying a unit horizontal area (cm^2) of the underlying surface. From the sieve analyses isograde maps for each size class have been derived (Fig. 40) showing the mass per unit area (g/cm^2) of each size. By panning in water, the content of heavies (*i. e.* crystals+lithics) has been determined in sieved samples and then isograde maps (Figs. 39, $0\phi\text{H}$, $1\phi\text{H}$, $2\phi\text{H}$) of the heavies' mass per

Table 8. Weight percentage of crystals in large pumice fragments.
Chuseri pumice

Sample	wt. (g)	2-1 mm	1-1/2	1/2-1/4	1/4-1/8 mm	Total
263	21.97	0.2	3.1	6.6	n. d.	n. d.
263	18.57	0.3	3.8	7.3	n. d.	n. d.
263	12.70	0.3	3.4	6.9	n. d.	n. d.
263	8.41	0.1	2.5	6.7	n. d.	n. d.
263	9.82	0.3	4.6	9.4	n. d.	n. d.
263-10	8.88	0.5	2.4	6.0	4.1	12.8
261	16.09	0.2	1.4	6.0	6.2	13.8
436-1	1.86	1.1	5.9	5.9	3.8	16.7
436-2	10.25	0.8	3.1	5.0	4.0	12.9
436-3	13.71	0.3	2.8	6.8	3.4	13.3
436-4	10.43	0.8	3.7	6.5	3.2	14.2
436-5	11.11	1.5	5.5	7.9	2.2	17.1
Average	143.80	0.45	3.3	6.8	4.0	14.5
	(1 σ)	0.41	1.2	1.1	1.1	1.6

n. d.: not determined.

Nambu pumice

Sample	wt. (g)	2-1 mm	1-1/2	1/2-1/4	1/4-1/8 mm	Total
385	12.44	1.6	6.6	7.9	3.1	19.2
389-2	6.64	2.4	8.3	8.7	2.3	21.7
389-2	8.49	1.3	6.2	7.1	3.5	18.1
291-2	17.62	3.2	9.9	8.6	2.8	24.5
273-1	20.23	1.7	6.5	7.5	3.0	18.6
697-1	2.63	1.1	4.9	4.9	2.3	13.3
697-2	20.65	2.0	6.5	8.2	4.6	21.3
697-3	17.34	3.4	7.5	7.8	4.6	23.3
697-4	11.28	2.8	7.1	9.8	5.7	25.4
697-5	10.01	5.0	8.7	9.5	5.3	28.5
697-6	9.47	5.3	8.2	9.1	4.7	27.2
697-7	17.35	5.4	9.4	7.6	2.6	25.0
697-8	15.09	8.0	9.5	6.8	3.4	27.8
697-9	17.20	7.9	9.3	6.2	3.6	27.1
697-10	1.22	6.6	8.2	7.4	4.1	26.2
Average	177.66	3.7	7.9	8.0	3.7	23.3
	(1 σ)	2.2	1.4	1.2	1.0	4.2

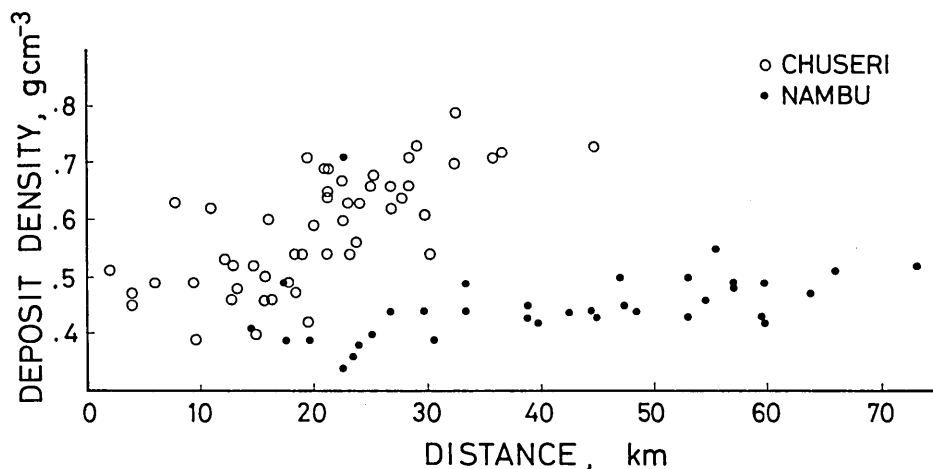


Fig. 38. Plots of the bulk density of the Chuseri deposit and the Nambu deposit against the distance from the source.

Table 9. Mass calculations for the Chuseri and Nambu pumice deposits.
The values for mass are all in units of 10^{15} g.

size class (mm)	Chuseri			Nambu		
	2	1	1/2	2	1	1/2
<i>a</i> crystal % in pumice	0.45	3.3	6.8	3.7	7.9	
<i>H</i> mass of heavies	0.021	0.146	0.183	0.022	0.064	
<i>b</i> crystal % in heavies	70	98	99	95	99	
<i>C</i> mass of crystals	0.0147	0.143	0.181	0.0209	0.0634	
<i>M'</i> mass necessitated by <i>C</i>	3.25	4.33	2.67	0.57	0.80	
<i>M''</i> total mass >2 mm	0.59	0.59	0.59	0.28	0.28	
<i>M</i> total mass erupted	3.84	4.92	3.26	0.85	1.08	

$$C = bH/100, M' = 100 C/a, M = M' + M''.$$

unit area of each size have been derived. The following and Table 9 summarize the mass calculation procedure.

Cumulative mass within each isograde in Fig. 39 is plotted against the mass above a unit horizontal area (g/cm^2) on Fig. 41. This plot clearly demonstrates an exponential increase of cumulative mass with decrease of the mass above a unit area, and extrapolation to $0 \text{ g}/\text{cm}^2$ gives the total mass of heavies, *H*. The total quantity of crystals, *C*, is determined using crystal contents in the heavies; crystals account for 70 to 99 wt. % of the heavies in each size class. The mass of magma necessitated by *C*, *M'*, is then calculated: $M' = 100 C/a$, where *a* is crystal % in large pumice fragments. Some of the crystals were not liberated during the eruption and are kept enclosed in large pumice fragments so that the

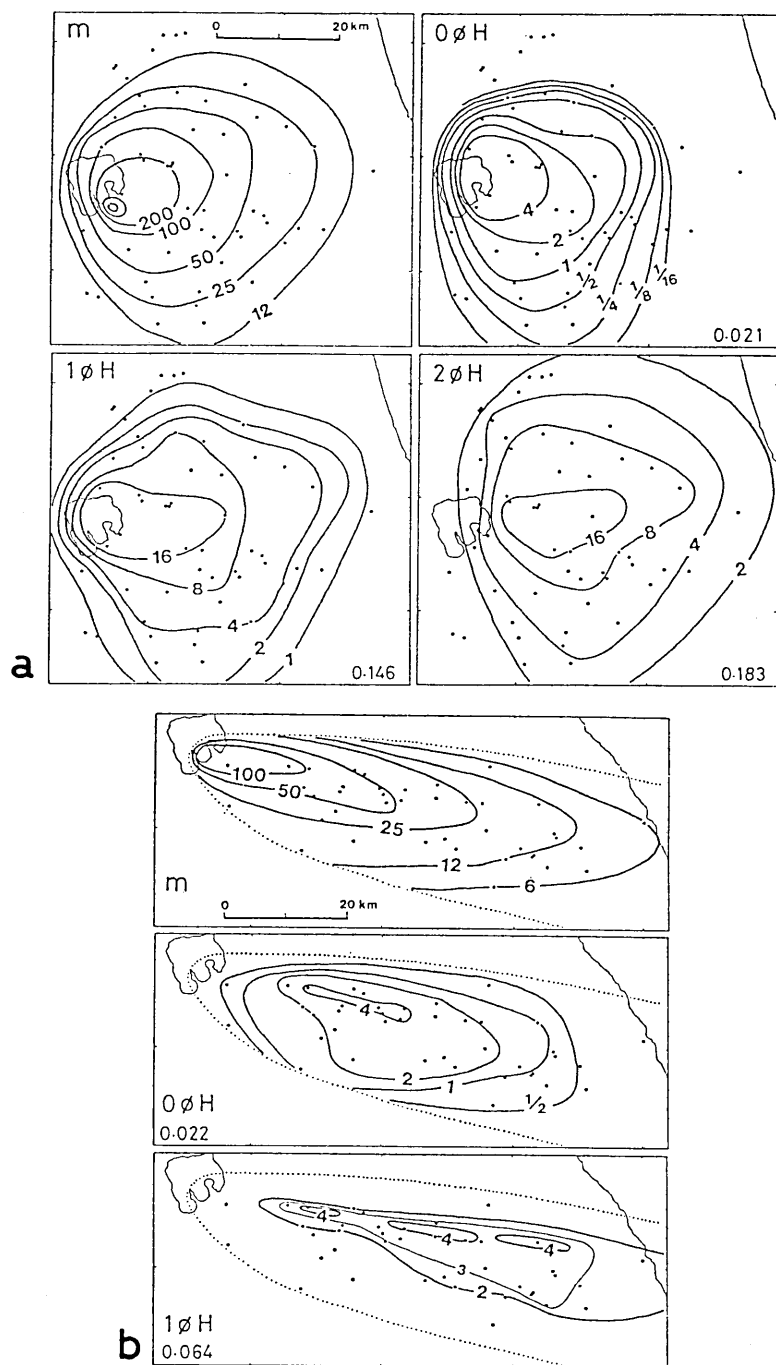


Fig. 39. Isograde maps showing mass per unit area (g/cm^2) for (a) the Chuseri deposit and (b) the Nambu deposit. m: mass of the deposit. 0øH: mass of 2-1 mm size heavies (*i. e.* crystals+lithics). 1øH: mass of 1-1/2 mm size heavies. 2øH: mass of 1/2-1/4 mm size heavies. The figure in the bottom corner of each gives the total mass (in units of 10^{15} g) of heavies of the size class calculated from a cumulative mass plot in Fig. 41.

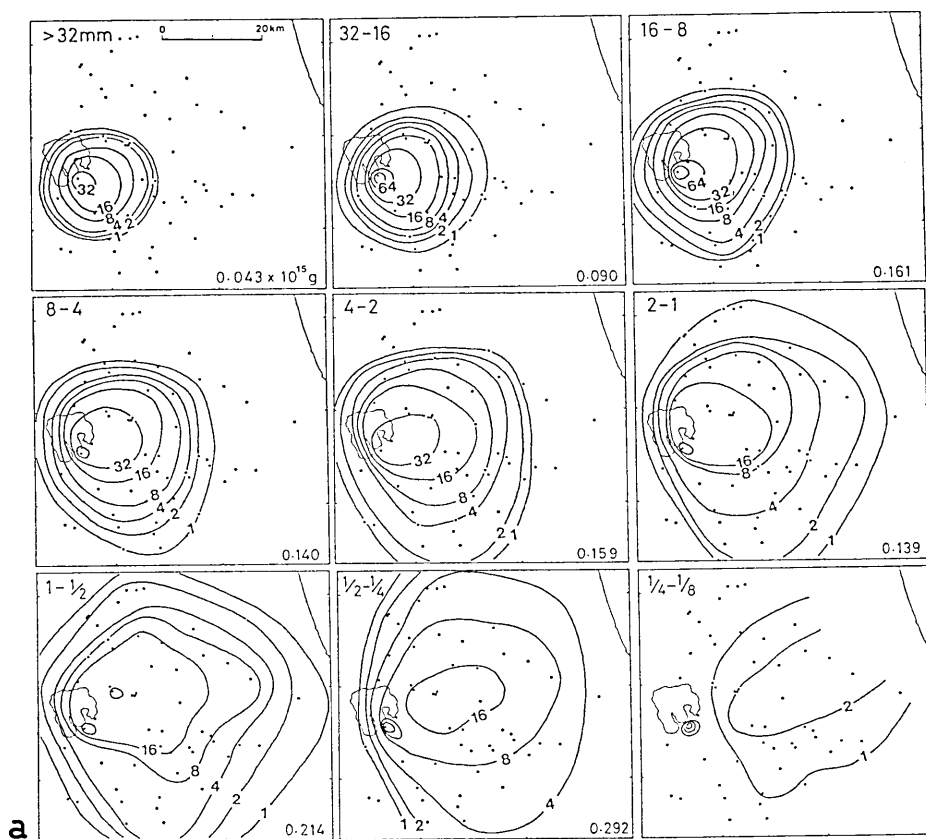


Fig. 40. Isograde maps showing mass per unit area (g/cm^2) of each size class for (a) the Chuseri deposit and (b) the Nambu deposit. The figure in the bottom corner of each gives the total mass (in units of 10^{15} g) of the size class calculated from a cumulative mass plot in Fig. 41.

mass of the large pumice fragments should be added to M' . It is assumed that pumice fragments larger than 2 mm enclose crystals in the same proportion as the magma erupted and those smaller than 2 mm contain no crystals. The total mass larger than 2 mm is obtained by the integration of isograde maps for each size class (Fig. 40): 0.59×10^{15} g for the Chuseri deposit and 0.28×10^{15} g for the Nambu deposit. Added to M' , each yield the total erupted mass, M . The duplicate or triplicate results for a single deposit agree reasonably (Table 9) and the average values are 4.01×10^{15} g for the Chuseri deposit and 0.97×10^{15} g for the Nambu deposit. The maximum deviations from the average values are 23% for the Chuseri deposit and 12% for the Nambu deposit. In this calculation lithic fragments finer than 2 mm are not included. However, the amounts are

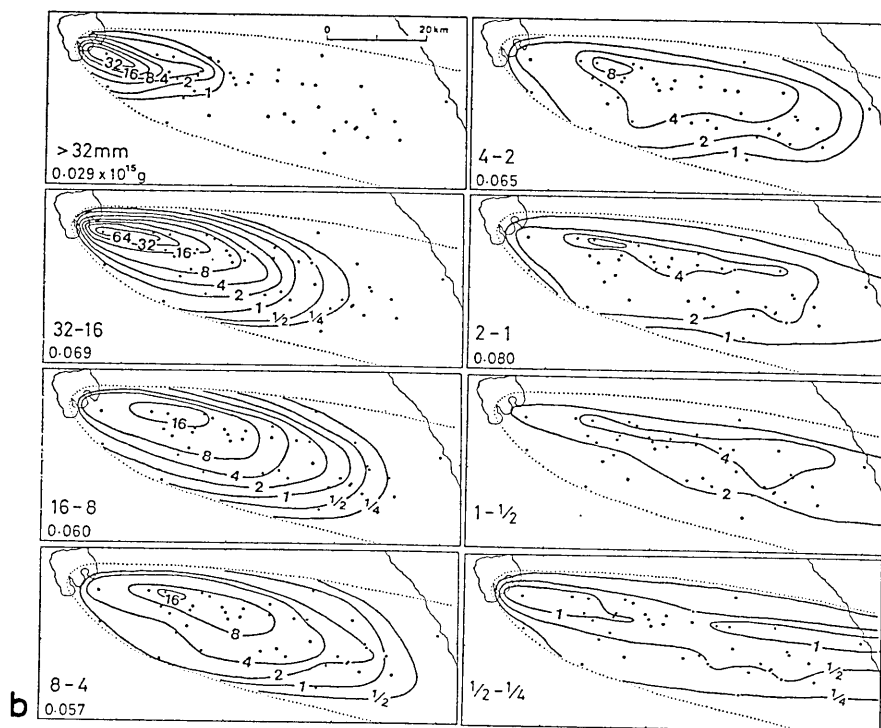


Fig. 40. (continued)

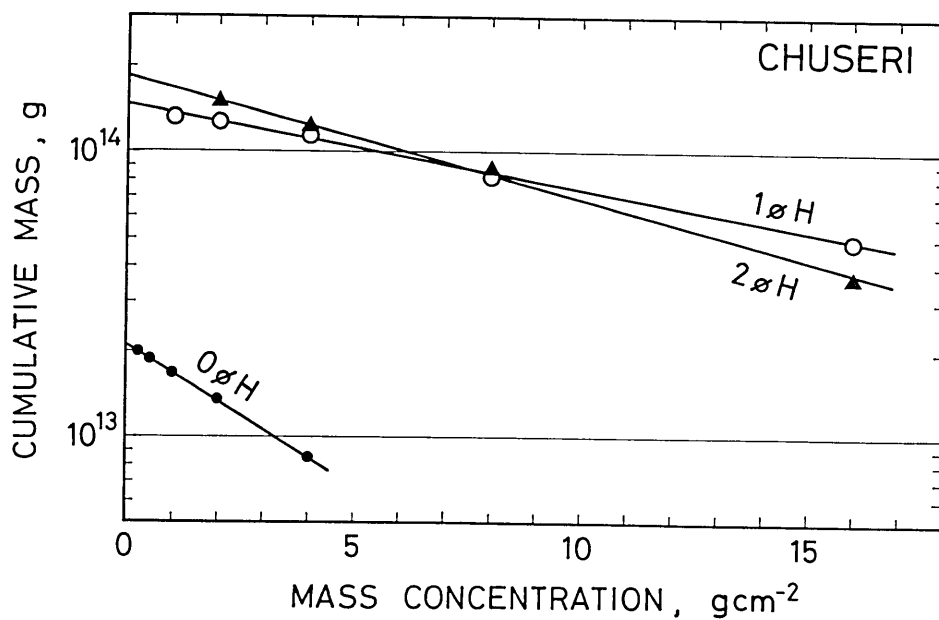


Fig. 41. Cumulative mass plots against mass concentration (g/cm^2). The total mass is obtained at $0 \text{ g}/\text{cm}^2$. Examples are shown for the heavies of the Chuseri deposit (Fig. 39a).

smaller than analytical errors. For the Chuseri deposit it is less than 2% of the total mass (Fig. 17).

Empirical formula for volume estimation of a fallout deposit

The crystal method needs a large number of sievings and component analyses. Therefore, it is useful for practical use to establish a formula which determines the volume of a deposit using only the isopach map.

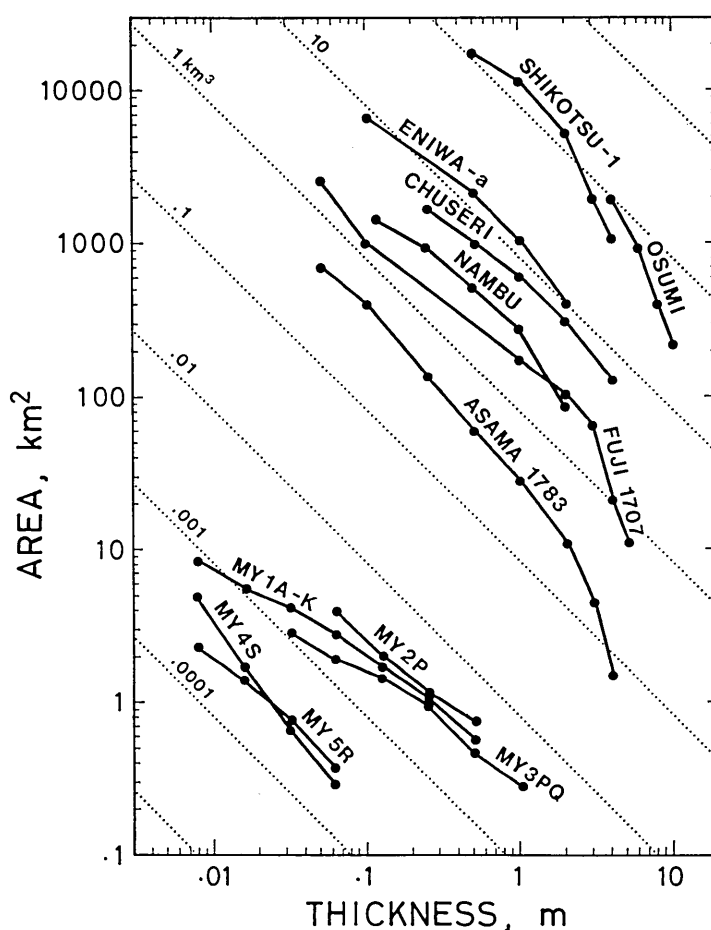


Fig. 42. Relation between the areas enclosed by isopachs, S , and the thickness, T , for the Miyakejima 1983 deposit (MY; HAYAKAWA *et al.*, 1984) and for some plinian deposits (references are given in Table 12). The product TS is almost constant for each deposit excepting the Osumi deposit and some of the Miyakejima deposit. The dotted lines are iso-volume lines assuming $V=12.2 TS$.

Plots of the area enclosed by an isopach, S , against the thickness, T , (Figs. 35 and 42) suggest that the product, TS , is almost constant for each deposit. It is evident from Table 10 that the volume, V , is nearly proportional to TS : the ratio of V to TS is almost constant for the five deposits for which the mass (and volume) has been determined by the crystal method, giving the average value of 12.2. Thus, a volume estimation formula is proposed:

$$V = 12.2TS. \quad (1)$$

This formula has an advantage over the crystal method in that the volume of a deposit may be determined using only one isopach. When more than one isopach are available for a deposit, the isopach which is best constrained by the data points may as well be taken.

Assuming that the bulk density of deposit equals 0.7 g/cm^3 , the total erupted mass, M , is calculated as:

$$M = 8.5 \times 10^{10} TS \quad (2)$$

where M is given in g, T in cm, and S in km.

More than 90% of the total energy released by a volcanic eruption producing juvenile materials is occupied by the thermal energy carried out by eruptive products. An approximate amount of the total energy, E , is therefore expressed as a function of M :

$$E = 1.5 \times 10^{10} M \quad (3)$$

where E is given in erg and M in g (NAKAMURA, 1965, 1974). Then, substituting equation (2) for equation (3) yields

Table 10. Ratio of V to TS for the deposits for which the mass (and volume) has been determined by the crystal method.

	$M (\times 10^{15} \text{ g})$	$V (\text{km}^3)$	$T (\text{cm})$	$TS (\text{km}^3)$	V/TS
Taupo*	13.74	24	50	1.53	15.7
			25	2.27	10.6
Waimihia*	17.77	29.08	50	2.26	12.9
			25	1.90	15.3
Hatepe*	3.70	6.00	50	0.530	11.3
			25	0.455	13.2
Chuseri	4.01	6.68	100	0.593	11.3
			50	0.495	13.5
Nambu	0.97	2.16	50	0.253	8.5
			25	0.232	9.3
(Average)					12.2

* WALKER, 1980, 1981a.

$$E = 1.2 \times 10^{21} TS.$$

For the fallout deposits of Towada Volcano the volume is calculated using equation (1), and then the mass is calculated from the estimated deposit densities (Table 11). The masses are summed and plotted against time, together with the roughly estimated mass of the ignimbrites and lavas, to give the long-term rate of magma discharge of Towada Volcano (Fig. 43). During the past 55,000 years the total magma erupted amounts to 1.5×10^{17} g. This corresponds to the discharge rate of 1.1 km^3 per thousand years of dense rock equivalent. The rate can be more precisely determined for the post-caldera volcanism during the past 13,000 years; the total magma erupted amounts to 2.9×10^{16} g and the discharge rate is $0.9 \text{ km}^3/\text{ky}$ of dense rock equivalent.

Table 12 lists volumes calculated by equation (1) for 42 plinian deposits in Japan other than Towada. The frequency histogram for 57 plinian deposits, including 15 deposits of Towada, is shown in Fig. 44. The maximum is 125 km^3 for the Shikotsu 1 deposit and the minimum is 0.11 km^3 for the Maita 1 deposit of Towada. There is a great variation of more than three orders of magnitude. The median volume is 2.7 km^3 , however, this may be somewhat too large because of a sampling bias in favor of the larger plinian deposits.

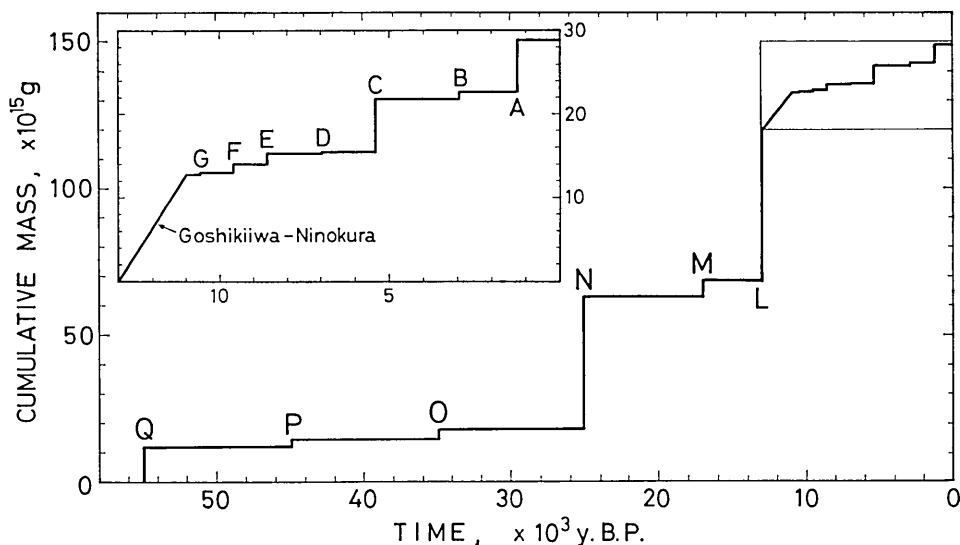


Fig. 43. Cumulative mass plotted against time for all erupted materials from Towada Volcano.

Table 11. Volume and mass of the eruptive products from Towada Volcano.
Deposit densities in parentheses are inferred values from direct measurements of others.

	Isopach used (cm)	Volume (km ³)	Deposit density (g/cm ³)	Mass ($\times 10^{15}$ g)
A Ogurayama	—	0.225	2.1	0.47
Kemanai	—	ca. 5.	0.9	ca. 4.5
Oyu 3	3	0.14	0.75	0.11
Oyu 2	12	0.67	(0.8)	0.54
Oyu 1	12	0.70	0.75	0.53
B Sobe	25	0.72	(1.1)	0.79
Mayogatai	12	0.12	(0.75)	0.09
C Utarube	25	1.35	(1.1)	1.49
Kanegasawa	25	1.15	(0.7)	0.81
Chuseri	100	6.68	0.6	4.01
D'	—	ca. 0.1	(1.1)	ca. 0.1
D Oguni	25	0.34	(0.6)	0.20
E Kaimori	12	0.35	(1.1)	0.39
Nambu	50	2.16	0.45	0.97
F Kabayama	25	0.31	(1.1)	0.34
Natsuzaka	50	0.95	(0.6)	0.57
G Shingo	50	0.45	(0.55)	0.25
Goshikiwa	—	2.50	(2.6)	6.5
Ninokura	200	7.9	(0.8)	6.3
L Hachinohe i	—	ca. 40.	(1.0)	ca. 40.
Hachinohe 6	25	3.6	(0.45)	1.62
Hachinohe 5	50	2.9	(0.8)	2.32
Hachinohe 4	40	1.9	(0.45)	0.86
Hachinohe 3	6	0.50	(0.8)	0.40
Hachinohe 2	4	0.47	(0.45)	0.21
Hachinohe 1	50	6.8	0.8	5.44
M Maita 2	25	ca. 7.	(0.8)	ca. 5.6
Maita 1	6	0.11	(0.5)	0.055
N Ofudo	—	ca. 40.	(1.0)	ca. 40.
Kirida 4	50	5.2	(0.8)	4.2
Kirida 3	12	0.83	(0.5)	0.42
Kirida 2	1.5	0.052	(1.0)	0.052
Kirida 1	3	0.047	(1.0)	0.047
O	—	ca. 5.	(0.7)	ca. 3.5
P	100	4.3	(0.7)	3.0
Q Okuse	—	ca. 10.	(1.0)	ca. 10.
(fall)	50	2.7	(0.7)	1.9

Table 12. Volume, V , and azimuth of the dispersal axis, A , of 42 Japanese plinian deposits. Volumes are calculated using a equation, $V=12.2 TS$, where T is the thickness of the best constrained isopach and S is the area enclosed by the isopach.

Volcano	Deposit	V (km ³)	T (cm)	A (°)	Reference
1 Shikotsu	1	125	200	110	KATSUI, 1959
2 —	2	22	30	89	—
3 Eniwa	a	13	50	88	KASUGAI <i>et al.</i> , 1968
4 Tarumai	a	2.2	100	61	SOYA, 1972
5 —	b	3.5	100	95	—
6 Usu	b	3.7	25	97	Oba & Kondo, 1964
7 Nantai	Shichihon-zakura	2.5	25	107	KANTO LOAM RE- SEARCH GROUP, 1965
8 —	Imaichi	3.8	50	110	—
9 Akagi	Kanuma	25	100	94	—
10 —	Yunokuchi	1.2	25	110	—
11 Haruna	Futatsudake	1.2	50	43	—
12 —	Hassaki	2.2	25	95	—
13 Asama	1783	0.41	25	107	MINAKAMI, 1942
14 —	Tsumagoi	3.1	50	32	HAYAKAWA, 1983c
15 Yatsugatake	YPm-4	0.77	30	90	KAWACHI <i>et al.</i> , 1978
16 —	GoP ₁	11	30	110	MACHIDA <i>et al.</i> , 1974
17 Fuji	1707	2.1	100	88	TSUYA, 1955
18 —	Zunazawa	1.3	100	133	MACHIDA, 1964
19 —	Osawa	1.1	50	234	—
20 —	Omuro	0.65	50	83	—
21 Hakone	CCP-1	1.7	20	87	MACHIDA, 1971
22 —	Sanshokuki	1.7	20	94	—
23 —	Tokyo	7.4	50	71	—
24 —	Obaradai	6.7	60	79	—
25 —	KmP-7	5.0	50	69	—
26 —	K1P-13	3.6	100	64	—
27 —	TAm-5	14	100	68	MACHIDA <i>et al.</i> , 1974
28 —	TAm-1	9.8	100	70	—
29 —	TB-1	5.5	50	72	—
30 —	TCu-1	7.0	100	72	—
31 Higashi Izu	Kawagodaira	0.66	40	282	SHIRAO, 1981
32 Ontake	1	26	60	98	KOBAYASHI <i>et al.</i> , 1967
33 Daisen	Kurayoshi	56	50	71	MACHIDA & ARAI, 1979
34 —	Matsue	7.5	100	272	—
35 Aso	A	7.9	200	57	ONO <i>et al.</i> , 1977
36 —	D	3.4	100	68	—
37 Sakurajima	1914	0.45	50	100	KOBAYASHI, unpubl.
38 —	1779	0.29	50	103	—
39 —	1471	1.2	50	67	—
40 Aira	Osumi	94	400	120	KOBAYASHI <i>et al.</i> , 1983
41 Ikeda	Ikeda	2.8	50	87	NARUO & KOBAYASHI, unpubl.
42 Kikai	Koya	18	50	68	HAYAKAWA, unpubl.

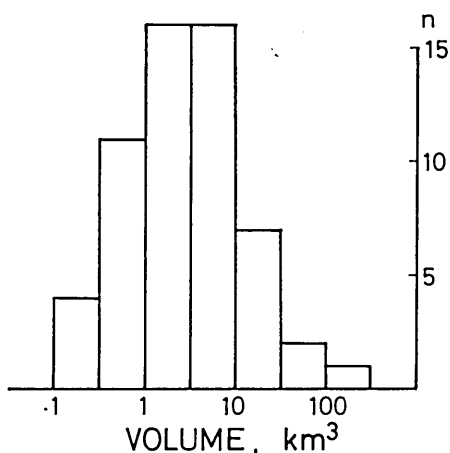


Fig. 44. Volume frequency histograms for 57 Japanese plinian deposits. Data from Tables 11 and 12.

Holocene Japanese plinian deposits are listed in Table 13. For 21 deposits out of 34, the isopach maps are available and the volumes are calculated. The median value is 1.2 km^3 . The maximum is 18 km^3 for the Koya deposit of Kikai. The 14 youngest eruptions are historic. Besides the deposits listed in Table 13, there are some more candidates such as those in Mashu, Asama, Fuji, and Sakurajima volcanoes. However, the reliable identification and age determination for them are not yet available.

6. Factors governing the dispersal of fallout deposits

The dispersal of fallout deposits depends on three factors: (1) the height reached by the pyroclasts, (2) the wind velocity and direction, and their height variation, and (3) the grain size population within the eruption column.

Height reached by the pyroclasts

Sorting of pyroclasts by size and density occurs in the eruption column; smaller and less dense pyroclasts are carried to greater heights being released at greater distances from the vent and attain greater ranges than larger and denser pyroclasts (WILSON, 1976). It is clear, however, that pyroclasts are laterally displaced by the wind at the time of the eruption as they fall from the column. The maximum range which pyroclasts would have attained in the absence of wind can be derived, following WILSON (1976) and WALKER *et al.* (1984), by measuring the cross-wind range R_c , which is the greatest distance from the dispersal axis measured along a line at right angle to it, on a MP or ML isograde of a given size (Fig. 45). The ML isogrades can be a more valid basis than the MP isogrades for this purpose because the latter depends partly on the pumice density and is influenced also by pumice breakage

Table 13. Holocene Japanese plinian deposits. Data sources are listed in Table 12 with addition of KATSUI *et al.*, 1975; SASAKI *et al.*, 1970; ARAMAKI, 1963; and ARAI and MACHIDA, 1980.

Age	Volcano	Volume (km ³)
1929 AD	Komagatake (a)	?
1914	Sakurajima	0.45
1856	Komagatake (c ₁)	?
1783	Asama	0.41
1779	Sakurajima	0.29
1739	Tarumai (a)	2.2
1707	Fuji	2.1
1694	Komagatake (c ₂)	?
1667	Tarumai (b)	3.5
1663	Usu	3.7
1640	Komagatake (d)	?
1471	Sakurajima	1.2
1108	Asama	?
915	Towada (A)	0.84
ca. 600	Haruna	1.2
2500 yBP	Fuji (Zunazawa)	1.3
2700	Fuji (Osawa)	1.1
2900	Kawagodaira	0.66
3000	Towada (B)	0.12
3000	Fuji (Omuro)	0.65
3000	Kirishima (Miike)	?
3500	Komagatake (f)	?
5000	Komagatake (g)	?
5000	Numazawanuma	?
5400	Towada (C)	6.7
5750	Ikeda	2.8
6000	Komagatake (h)	?
6300	Kikai	18.
7000	Mashu	?
7000	Towada (D)	0.34
8600	Towada (E)	2.2
8940	Tarumai (d)	?
9600	Towada (F)	0.95
10000	Hijiori	?

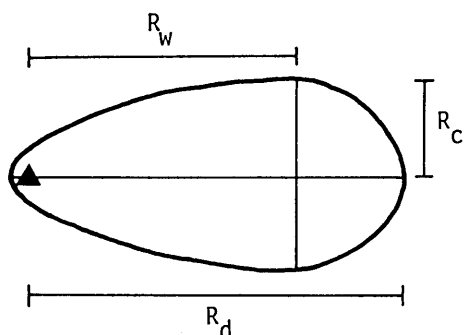


Fig. 45. Graphic explanation of downwind range, R_d , cross-wind range, R_c , and net displacement by the wind, R_w (after WALKER *et al.*, 1984). Triangle is the source and solid curve is a MP or ML isograde.

as stated by WALKER (1981c).

The R_c values of five ML isogrades for the Nambu pumice deposit are listed in Table 14. They become progressively larger for smaller lithic fragments as is expected. The R_c value for 8 mm size lithic fragments may be taken for comparison between various deposits, for the ML isograde of the size is the most readily available. In Table 15 the R_c values for 11 plinian deposits of Towada Volcano are listed with those for the deposits of Taupo (WALKER, 1980), Waimihia and Hatepe (WALKER, 1981a), Osumi (KOBAYASHI *et al.*, 1983), and Miyakejima 1983-2P (HAYAKAWA, unpublished data). The Miyakejima deposit is composed mainly of poorly vesiculated scoria fragments due to water-chilling and hence it is not strictly a plinian deposit. However, the characteristic feature of the eruption column was similar to those of the plinian type; it was sustained for 136 min with a height of 8 km (HAYAKAWA *et al.*, 1984). Fig. 46 shows that the R_c of plinian deposits increases with an increase in the mass of the deposit. This implies that eruption columns with a larger mass output reach higher elevations than smaller ones. Absolute column heights cannot be designated by the R_c value alone and other independent factors are needed, such as wind velocities or diffusion coefficients of pyroclasts in the eruption column.

Table 14. Downwind range, R_d , cross-wind range, R_c , and net displacement by the wind, R_w , during fall for five lithic sizes of the Nambu deposit.

ML (mm)	R_d (km)	R_c (km)	R_w (km)
32	20.8	5.8	15.0
16	29.0	8.3	20.7
8	38.2	10.4	27.8
4	47.9	11.4	36.5
2	59.5	12.4	47.1

Table 15. Mass (M), cross-wind range (R_c), and net displacement by the wind (R_w). R_c and R_w are values for 8 mm size lithic fragments.

	M (10^{15} g)	R_c (km)	R_w (km)	References
Oyu 1	0.53	14.1	17.2	
Mayogatai	0.09	6.6	16.2	
Chuseri	4.01	13.4	8.2	
Oguni	0.20	4.7	14.7	
Nambu	0.97	10.4	27.8	
Natsuzaka	0.57	9.5	14.8	
Shingo	0.25	2.9	19.1	
Hachinohe 6	1.62	17.5	24.2	
Hachinohe 4	0.86	22.5	33.6	
Hachinohe 2	0.21	7.6	47.0	
Maita 1	0.05	3.1	29.3	
Taupo	13.74	50.6	31.7	WALKER, 1980
Waimihia	17.77	40.4	54.8	WALKER, 1981a
Hatepe	3.70	22.6	11.4	WALKER, 1981a
Osumi	66.	37.3	17.1	KOBAYASHI <i>et al.</i> , 1983
Miyakejima 1983-2P	0.0036	1.05	9. (?)	HAYAKAWA, unpubl.

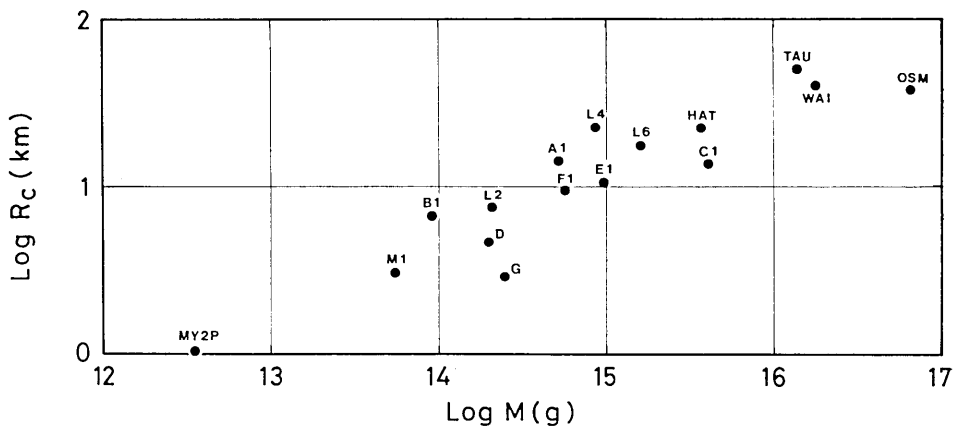


Fig. 46. Plots of the cross-wind range, R_c , for 8 mm size lithic fragments against the mass, M . Codes are as in Figs. 35 and 36, with the addition of TAU: Taupo, WAI: Waimihia, HAT: Hatepe, MY2P: Miyakejima 1983-2P. Data sources are listed in Table 15.

Wind velocity and direction

Fig. 47 is the 20-year data set of meteorological measurements collected over Akita ($39^{\circ}43'N$, $140^{\circ}06'E$), 100 km southwest of Towada. The most frequent wind direction above 2 km elevation is nearly constant throughout the year with an azimuth of 264° , *i.e.* westerlies. In summer (June-August), however, a significant change of wind azimuth occurs above 20 km, when the dominant direction is from the ENE. The velocity of wind varies both as a function of altitude and season. Each seasonal wind profile has the maximum near 11 km and the velocity is the highest (max. 45 m/s) in winter and the lowest (max. 27 m/s) in summer.

The dispersal axes of 53 Japanese plinian deposits are shown as a frequency diagram in Fig. 48. Most (77%) of them are plotted between 60° and 110° corresponding to the westerlies near 11 km elevation, however, 8% of the Japanese plinian deposits are dispersed westward having dispersal axes between 180° and 360° . The Oyu 1 and 3 deposits are examples. The eruption in summer may be responsible for the distribution, when easterlies prevail above 20 km and relatively low velocity winds are dominant below 20 km. The probable date of August 17 for the Oyu plinian eruption described by an old document is conformable to this model. There is a possibility that, for plinian deposits dispersed westward, unusual decreasing rates of thickness and grain size away from the source may be found reflecting a possible strong variation of wind direction with height.

Many of the fallout ashes of Towada Volcano have nearly circular isopachs. This is probably due to unstable low velocity winds blowing below the height of a few km throughout all seasons, and also due to a relatively long eruption duration, during which the wind direction can change.

The displacement of pyroclasts by wind, R_w , is estimated by the difference between R_d and R_c , where R_d is the maximum distance of an isopleth along the dispersal axis (down-wind range; Fig. 45). If a pyroclast is displaced a horizontal distance R_w by an average wind velocity v , the time required, $t = R_w/v$, equals the fall time of the pyroclast from its release height (WALKER *et al.*, 1984). Assuming wind velocities of 20, 30, and 40 m/s, the maximum release height is deduced for each of the ML sizes of the Nambu deposit using the fall time taken from WILSON (1972). Results are given in Table 16, where the release height for 4 and 2 mm size lithic fragments are apparently lower than that for larger

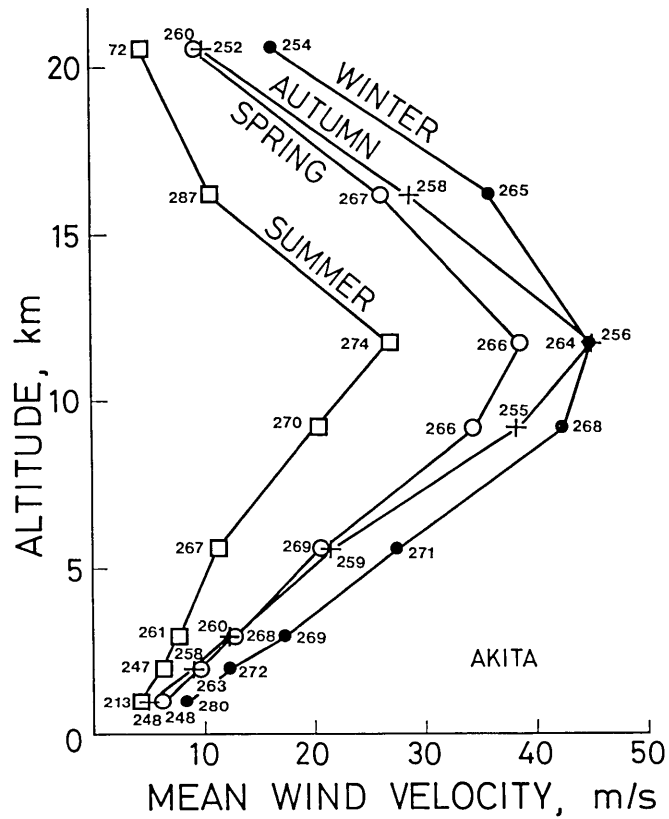


Fig. 47. Seasonal vertical variations in mean wind velocity recorded at Akita ($39^{\circ}43'N$, $140^{\circ}06'E$) for 1961–1980. The direction is expressed by numerals. Data from TOKYO ASTRONOMICAL OBSERVATORY (1984).

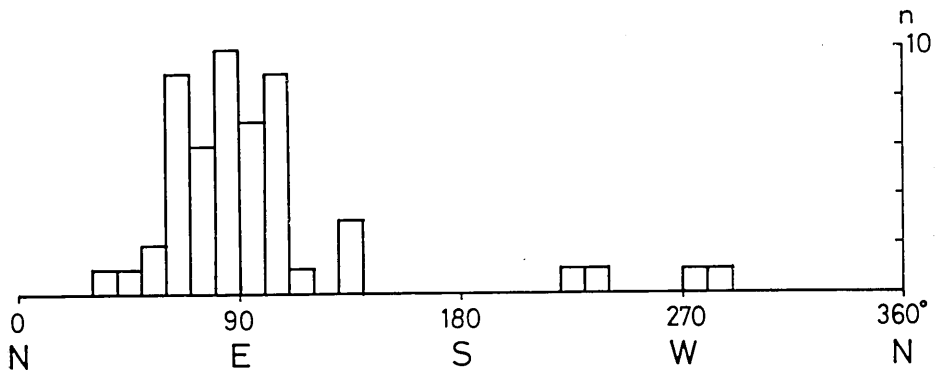


Fig. 48. Frequency of azimuth of the dispersal axis of 53 Japanese plinian deposits. Data from Table 12, and 11 deposits of Towada Volcano.

Table 16. Fall time (t) and release height (z) for the five lithic sizes of Table 14 implied by a few assumed wind velocities (v).

ML (mm)	$v=20$ m/s		$v=30$ m/s		$v=40$ m/s	
	t (s)	z (km)	t (s)	z (km)	t (s)	z (km)
32	750	40	500	14	375	9
16	1035	55	690	17	518	10
8	1391	55	927	19	695	11
4	1826	50	1217	16	913	10
2	2355	28	1570	12	1178	8

lithic fragments in all cases. It is interpreted that 4 and 2 mm size lithic fragments were displaced by average wind velocities lower than those working on larger lithic fragments. They probably reached near 20 km or more in the eruption column where the wind velocity is relatively low (Fig. 47). A plausible solution of the eruption condition for the Nambu deposit is that 32–4 mm size lithic fragments reached the maximum height of 10–15 km in the eruption column and were displaced by winds having an average velocity of 30–40 m/s, and 4–2 mm size lithic fragments reached 15–20 km in height and displaced by winds of 20–30 m/s. For 4 mm size lithic fragments, it must have taken about 20 min between the detachment from the eruption column and the landing on the ground 48 km east of the source.

Grain size population of the eruption column

The dispersal of fallout deposits is also influenced by the grain size population of the eruption column (WALKER, 1980); columns composed of finer populations disperse the deposits more widely than those of coarser populations. The population is also an important factor in the convective eruptive columns since it determines the rate of energy transfer from magma particles to in-drawn air (WILSON *et al.*, 1978).

The population can be determined by estimating the grain size distribution of the whole deposit. It has been estimated for the five plinian deposits (Tarumai b, SUZUKI *et al.*, 1973; Taupo, Waimihia, and Hatepe, WALKER, 1980, 1981a; Askja 1875, SPARKS *et al.*, 1981) and for the two phreatoplinian deposits (Hatepe and Rotongaio ashes, WALKER, 1981b). An attempt has now been made to estimate the populations for the Chuseri and Nambu deposits. The total mass of each size class is calculated by integration of the mass per unit area maps (Fig. 40). Then, each of them is divided by the total erupted mass determined by the crystal method.

Table 17 lists the results. Below 1/4 mm for the Chuseri deposit and below 1 mm for the Nambu deposit most of the dispersal areas lie at sea so that only the total masses are known from the crystal method. Grain size populations for three ash beds (HP1, HP3, and HP5) of the Hachinohe phreatomagmatic deposit at Ishizawa (230:33.6 km, 80°) are also listed in Table 17. They can be regarded as the whole-deposit grain size populations because of the negligible amount of grain size fractionation away from the source (HAYAKAWA, 1983a).

The populations of the Towada and New Zealand examples are plotted on a probability graph paper in Fig. 49. The Chuseri population is similar to the New Zealand plinian populations, however, the Nambu population is distinctly coarser than the others. This implies that the Nambu deposit was less widely dispersed than the Chuseri deposit if the same wind condition was provided. The reason is not known why the low degree of fragmentation occurred in the Nambu eruption column.

The Hachinohe populations are similar to the New Zealand phreato-plinian ones. A convergence occurs in the finer parts between phreato-plinian deposits and all plinian deposits except the Nambu. The plinian deposits differ from the phreato-plinian only in their having a larger tail of coarse pumice. The great difference in field appearance between coarse

Table 17. Whole-deposit grain size populations. Chuseri and Nambu deposits are determined by the crystal method. HP1, HP3, and HP5 ash deposits are results of the grain size analyses of the deposits at Ishizawa (230:33.6 km, 80°).

Class	Chuseri	Nambu	HP1	HP3	HP5
-5 phi 32 mm	1.1	3.0	—	—	—
-4 16	3.3	10.1	—	—	—
-3 8	7.3	16.3	—	1.1	1.0
-2 4	10.8	22.2	1.4	2.8	3.2
-1 2	14.8	28.9	4.7	4.8	5.7
0 1	18.3	37.1	8.2	8.4	8.7
1 500 μ m	23.6		12.4	13.5	13.3
2 250	30.9		16.4	20.5	21.1
3 125			24.0	31.5	33.9
4 63			40.4	44.7	49.1
5 31			58.3	55.2	62.9
6 16			73.2	70.4	76.8
7 8			92.4	91.9	93.6
8 4			98.1	97.8	98.1
9 2			99.8	99.7	99.8

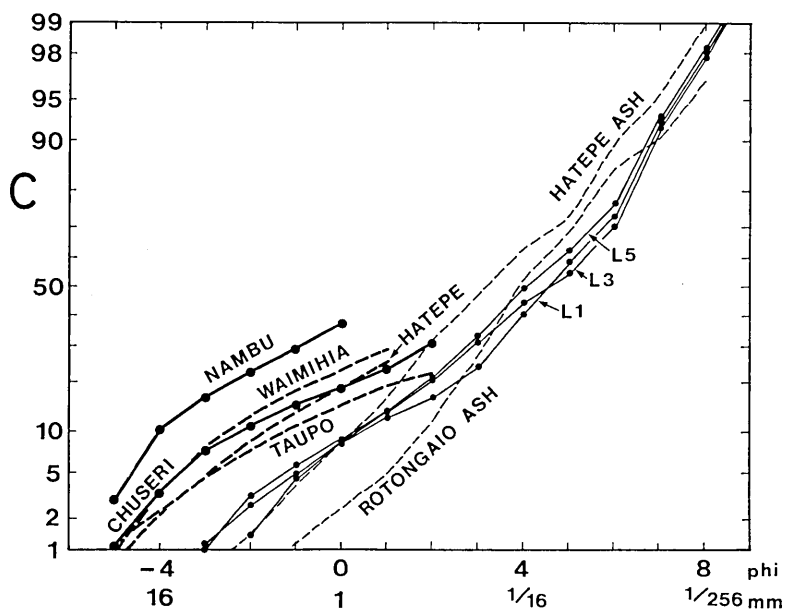


Fig. 49. Whole-deposit grain size populations, plotted on probability graph paper, for deposits of plinian (thick curves) and phreatomagmatic (thin curves) eruptions. C: weight percentage coarser than given grain size. L1: HP1 ash, L3: HP3 ash, L5: HP5 ash. Taupo, Waimihia, Hatepe, Hatepe ash, and Rotongaio ash after WALKER 1980, 1981a, and 1981b.

plinian pumice deposits and fine phreatoplinian deposits may well reflect merely a different depositional mechanism as has been considered by WALKER (1981c); phreatoplinian eruption clouds are prone to be scavenged near the source by water because their eruptions occur under aqueous conditions, but the "dry" cloud of plinian eruptions keeps possessing fine ash for a hundred or more km from the source and substantially no deposition of fine ash occurs near the source area because the terminal velocity of the particles is too low.

7. Conclusions

This study of the pyroclastic deposits enabled the writer to document the eruptive styles and scales of Towada Volcano and reveal the volcano's eruptive history. It has been shown that eruptive episodes have taken place at the rate of once every 1,000 to 2,000 years over the past 10,000 years, and that the latest occurred about 1,070 years ago. Although there is no sign of current volcanic activity in the area of Towada Volcano, the volcano must be regarded no less active today than it has been in the

past. This study therefore provides a basis for the general, long-term prediction of future volcanic activity.

Acknowledgments I wish to thank Shigeo Aramaki for his encouragement and constructive criticism during this study. I am grateful to Kiyotaka Chinzei, Toshitsugu Fujii, Ikuo Kushiro, Tetsuo Kobayashi, Kazuaki Nakamura, Yasuo Nakamura, and Takeo Suzuki for valuable discussions.

References

- ARAI, F. and MACHIDA, H., 1980, Catalogue of the Japanese tephra I, *Karuishi Gaku Zasshi*, no. 6, 65-76. (in Japanese)
- ARAMAKI, S., 1963, Geology of Asama Volcano, *Jour. Fac. Sci., Univ. Tokyo sec. 2*, 14, 229-443.
- BOOTH, B., CROASDALE, R. and WALKER, G.P.L., 1978, A quantitative study of five thousand years of volcanism on Sao Miguel, Azores, *Phil. Trans. Royal Soc. London, ser. A*, 288, 271-319.
- CHIBA, M., 1966, Genesis of magmas producing pumice flow and fall deposits of Towada Caldera, Japan, *Bull. Volcanologique, ser. 2*, 29, 545-558.
- DRUITT, T.H. and SPARKS, R.S.J., 1982, A proximal ignimbrite breccia facies on Santorini, Greece, *Jour. Volcanol. Geotherm. Res.*, 13, 147-171.
- FROGGATT, P.C., WILSON, C.J.N. and WALKER, G.P.L., 1981, Orientation of logs in the Toupo ignimbrite as an indicator of flow direction and vent position, *Geology*, 9, 109-111.
- HAYAKAWA, Y., 1983a, The Hachinohe ash: An example of an accretionary lapilli-fall deposit from Towada Volcano, Japan, *Bull. Volcanol. Soc. Japan, ser. 2 (KAZAN)*, 28, 25-40. (in Japanese with English abstract)
- HAYAKAWA, Y., 1983b, Chuseri tephra formation from Towada Volcano, Japan, *Bull. Volcanol. Soc. Japan, ser. 2 (KAZAN)*, 28, 263-273. (in Japanese with English abstract)
- HAYAKAWA, Y., 1983c, Geology of Kusatsu-Shirane volcano, *Jour. Geol. Soc. Japan*, 89, 511-525. (in Japanese with English abstract)
- HAYAKAWA, Y., ARAMAKI, S., SHIRAO, M., KOBAYASHI, T., TOKUDA, Y., TSUKUI, M., KATO, T., TAKADA, A., KOYAGUCHI, T., KOYAMA, M., FUJII, T., OSHIMA, O., SOYA, T. and UTO, K., 1984, Pyroclastic fall deposits of the October 3-4, 1983, eruption of Miyakejima Volcano, *Bull. Volcanol. Soc. Japan, ser. 2 (KAZAN)*, 29, S208-S220. (in Japanese with English abstract)
- HIRAYAMA, J. and ICHIKAWA, K., 1966, Shirasu flood of 1,000 years ago, *Monthly Rev. Geology (CHISHITSU NEWS)*, no. 140, 10-28. (in Japanese)
- ISSHIKI, N., ONO, K., HIRAYAMA, J. and OTA, R., 1965, Age determinations by radio-carbon ^{14}C , *Monthly Rev. Geology (CHISHITSU NEWS)*, no. 133, 20-27. (in Japanese)
- KANTO LOAM RESEARCH GROUP, 1965, *Kanto Loam—its origin and nature*, Tsukiji Shokan, Tokyo, 378p. (in Japanese)
- KASUGAI, A., KIMURA, H., KOSAKA, T., MATSUZAWA, I. and NOGAWA, K., 1968, On the Obihiro volcanic sand in the Tokachi Plain, East Hokkaido, *Earth Science (Jour. Assoc. Geol. Collab. Japan; CHIKYU KAGAKU)*, 22, 137-146. (in Japanese with English abstract)
- KATSUI, Y., 1959, On the Shikotsu pumice-fall deposit—special reference to the activity

- just before the depression of the Shikotsu caldera, *Bull. Volcanol. Soc. Japan, ser. 2*, 4, 33-48. (in Japanese with English abstract)
- KATSUI, Y., ANDO, S. and INABA, K., 1975, Formation and magmatic evolution of Mashu Volcano, East Hokkaido, Japan, *Jour. Fac. Sci., Hokkaido Univ., ser. IV.*, 16, 533-552.
- KAWACHI, S., NAKAYA, S. and MURAKI, K., 1978, YPm-IV pumice bed in Northern Yatsugatake, Yatsugatake Volcanic Chain, central Japan —Studies on Yatsugatake tephra Part I—, *Bull. Geol. Survey Japan*, 29, 793-805.
- KAWANO, Y., 1939, Chemical study on the ejecta of the Towada Volcano, *Jour. Jap. Assoc. Mineral. Petrol. Economic Geologists (GANKO)*, 22, 259-275. (in Japanese)
- KOBAYASHI, K., SHIMIZU, H., KITAZAWA, K. and KOBAYASHI, T., 1967, The Pumice-fall deposit "Pm-I" supplied from Ontake Volcano, *Jour. Geol. Soc. Japan*, 73, 291-308. (in Japanese with English abstract)
- KOBAYASHI, T., HAYAKAWA, Y. and ARAMAKI, S., 1983, Thickness and grain size distribution of the Osumi pumice fall deposit from the Aira caldera, *Bull. Volcanol. Soc. Japan, ser. 2 (KAZAN)*, 28, 129-140.
- KUNO, H., ISHIKAWA, T., KATSUI, Y., YAGI, K., YAMASAKI, M. and TANEDA, S., 1964, Sorting of pumice and lithic fragments as a key to eruptive and emplacement mechanism, *Japan. Jour. Geol. Geogr.*, 35, 223-238
- MACHIDA, H., 1964, Tephrochronological study of volcano Fuji and adjacent areas, *Jour. Geography (CHIGAKU ZASSHI)*, 73, 293-308. (in Japanese with English abstract)
- MACHIDA, H., 1971, Tephrochronological study in South Kanto Part I Stratigraphy of tephra and its relation to the history of volcano, *The Quaternary Research (DAIYONKI KENKYU)*, 10, 1-20. (in Japanese with English abstract)
- MACHIDA, H., 1983, Tephra studies: short review, *Jour. Geography (CHIGAKU ZASSHI)*, 92, 441-447. (in Japanese with English title)
- MACHIDA, H., ARAI, F., MURATA, A. and HAKAMATA, K., 1974, Correlation and chronology of the middle Pleistocene tephra layers in South Kanto, *Jour. Geography (CHIGAKU ZASSHI)*, 83, 302-338. (in Japanese with English abstract)
- MACHIDA, H. and ARAI, F., 1979, Daisen Kurayoshi pumice: Stratigraphy, chronology, distribution and implication to Late Pleistocene events in central Japan, *Jour. Geography*, 88, 313-330. (in Japanese with English abstract)
- MACHIDA, H., ARAI, F. and MORIWAKI, H., 1981, Two Korean tephra, Holocene markers in the Sea of Japan and the Japan Islands, *Kagaku*, 51, 562-569.
- MINAKAMI, T., 1942, On the distribution of volcanic ejecta (part I): The distributions of volcanic bombs ejected by the recent explosions of Asama, *Bull. Earthq. Res. Inst., Univ. Tokyo*, 20, 65-92.
- MIYAJI, N., 1984, Wind effect on the dispersion of the Fuji 1707 tephra, *Bull. Volcanol. Soc. Japan, ser. 2 (KAZAN)*, 29, 17-30. (in Japanese with English abstract)
- MOORE, J. G., NAKAMURA, K. and ALCARAZ, A., 1966, The 1965 eruption on Taal volcano, *Science*, 151, 955-960.
- MURAOKA, H. and HASE, H., 1981, Okiura caldera, discovery of a Valles-type caldera in the northern Honshu, Japan, 1981 IAVCEI Symposium, *Arc Volcanism, Abstracts.*, 242-243.
- NAKAMURA, K., 1965, Energies dissipated with volcanic activities—classification and evaluation, *Bull. Volcanol. Soc. Japan, ser. 2 (KAZAN)*, 10, 81-90. (in Japanese with English abstract)
- NAKAMURA, K., 1974, Preliminary estimate of global volcanic production rate, *Proceedings of a United States-Japan Cooperative Science Seminar*, 680 p., 273-285.
- OBA, Y. and KONDO, Y., 1964, Pumice-fall deposits of Usu Volcano, Hokkaido, *Bull. Volcanol. Soc. Japan, ser. 2*, 9, 75-86. (in Japanese with English abstract)
- OIKE, S., 1964, Absolute age of the Hachinohe pumice deposit, *Earth Science (Jour.*

- Assoc. Geol. Collab. Japan; *CHIKYU KAGAKU*), 18, 34-39. (in Japanese)
- OIKE, S., 1970, C-14 age of the Nambu pumice, *Earth Science (Jour. Assoc. Geol. Collab. Japan; CHIKYU KAGAKU)*, 24, 232-233. (in Japanese)
- OIKE, S., 1972, Holocene tephrochronology in the eastern foot-hills of the Towada volcano, northeastern Honshu, Japan, *The Quaternary Research (DAIYONKI KENKYU)*, 11, 228-235. (in Japanese with English abstract)
- OIKE, S., 1978, C-14 ages of the Ofudo pumice flow tuff to the south of the city of Towada, *Earth Science (Jour. Assoc. Geol. Collab. Japan; CHIKYU KAGAKU)*, 32, 109-110. (in Japanese)
- OIKE, S., MATSUYAMA, C. and TAKEUCHI, S., 1977, C-14 age of the fossil forest beneath the Hachinohe pumice deposit, *Earth Science (Jour. Assoc. Geol. Collab. Japan; CHIKYU KAGAKU)*, 31, 136-137. (in Japanese)
- OIKE, S. and NAKAGAWA, H., 1979, *Basic research for the regional agricultural development in Sannohe area*, Tohoku Noseikyoku Keikakubu, 1-103. (in Japanese)
- OIKE, S. and SHOJI, S., 1977, C-14 age of the buried soil just under the Hachinohe pumice deposit, *Earth Science (Jour. Assoc. Geol. Collab. Japan; CHIKYU KAGAKU)*, 31, 42. (in Japanese)
- ONO, K., MATSUMOTO, Y., MIYAHISA, M., TERAOKA, Y. and KAMBE, N., 1977, Geology of the Taketa district, *Quadrangle series, scale 1:50000*, Kagoshima (15) No. 23, Geological Survey of Japan. (in Japanese with English abstract)
- RITTMAN, A., 1962, *Volcanoes and their activity*, Wiley-Intersciences Publishers, New York, 305p.
- SASAKI, T., KATAYAMA, M. *et al.*, 1970, On the ash deposits in Oshima Peninsula, *HOKKAIDO NOGYO SHIKENJO DOSEI CYOSA HOKOKU*, 20, 255-286. (in Japanese)
- SATOH, H., 1966, Pumice flow deposits of the Towada caldera at the vicinity of Kosaka Town, Akita prefecture, Japan, *Jour. Geol. Soc. Japan*, 72, 405-411.
- SATOH, H., 1969, C-14 age of the Asamizu pumice flow deposit to the east of the Towada caldera, *Earth Science (Jour. Assoc. Geol. Collab. Japan; CHIKYU KAGAKU)*, 23, 131-132. (in Japanese)
- SHIRAO, M., 1981, Geology of Daruma volcano and adjacent areas, Izu peninsula, Japan, *Jour. Geol. Soc. Japan*, 87, 641-655. (in Japanese with English abstract)
- SOYA, T., 1972, Formation of the Tarumae Volcano with special reference to the activities in Ta-a and Ta-b stages, *Bull. Volcanol. Soc. Japan, ser. 2*, 16, 15-27. (in Japanese with English abstract)
- SPARKS, R.S.J. and WRIGHT, J.V., 1979, Welded air-fall tuffs, *C.E. Chapin and W.E. Elston, ed., Ash-Flow Tuffs, Geol. Soc. Amer. Spec. Paper 180*, 155-166.
- SPARKS, R.S.J., WILSON, L. and SIGURDSSON, H., 1981, The pyroclastic deposits of the 1875 eruption of Askja, Iceland, *Phil. Trans. Royal Soc. London*, 299, 241-273.
- SUZUKI, T., KATSUI, Y. and NAKAMURA, T., 1973, Size distribution of the Tarumai Ta-b pumice-fall deposit, *Bull. Volcanol. Soc. Japan, ser. 2*, 18, 47-63. (in Japanese with English abstract)
- TANIGUCHI, H., 1972, Petrological study on Towada Volcano, *Jour. Jap. Assoc. Mineral. Petrol. Economic Geologists (GANKO)*, 67, 128-138. (in Japanese with English abstract)
- TOKYO ASTRONOMICAL OBSERVATORY (ed.), 1984, *Rika nenpyo (Chronological Scientific Tables)*, Maruzen, Tokyo, 370-371.
- TSUYA, H., 1955, Geological and petrological studies of volcano Fuji, V. On the 1707 eruption of volcano Fuji, *Bull. Earthq. Res. Inst., Tokyo Imp. Univ.*, 33, 341-383.
- WALKER, G.P.L., 1980, The Taupo pumice: product of the most powerful known (ultraplinian) eruption? *Jour. Volcanol. Geotherm. Res.*, 8, 69-94.
- WALKER, G.P.L., 1981a, The Waimihia and Hatepe plinian deposits from the rhyolitic

- Taupo Volcanic Centre, *New Zealand Jour. Geol. Geophys.*, 24, 305-324.
- WALKER, G.P.L., 1981b, Characteristics of two phreatoplinian ashes, and their water-flushed origin, *Jour. Volcanol. Geotherm. Res.*, 9, 395-407.
- WALKER, G.P.L., 1981c, Plinian eruptions and their products, *Bull. Volcanologique, ser. 2*, 44, 223-240.
- WALKER, G.P.L. and CROASDALE, R., 1971, Two plinian-type eruptions in the Azores, *Jour. Geol. Soc. London*, 127, 17-55.
- WALKER, G.P.L., WRIGHT, J.V., CLOUGH, B.J. and BOOTH, B., 1981a, Pyroclastic geology of the rhyolitic volcano of La Primavera, Mexico, *Geol. Rundschau.*, 70, 1100-1118.
- WALKER, G.P.L., WILSON, C.J.N. and FROGGATT, P.C., 1981b, An ignimbrite veneer deposit: the trail-marker of a pyroclastic flow, *Jour. Volcanol. Geotherm. Res.*, 9, 409-421.
- WALKER, G.P.L., SELF, S. and WILSON, L., 1984, Tarawera 1886, New Zealand—a basaltic plinian fissure eruption, *Jour. Volcanol. Geotherm. Res.*, 21, 61-78.
- WILSON, L., 1972, Explosive volcanic eruptions—II The atmospheric trajectories of pyroclasts, *Geophys. Jour. Roy. Astr. Soc.*, 30, 381-392.
- WILSON, L., 1976, Explosive volcanic eruptions—III Plinian eruption columns, *Geophys. Jour. Roy. Astr. Soc.*, 45, 543-556.
- WILSON, L., SPARKS, R.S.J., HUANG, T.C. and WATKINS, N.D., 1978, The control of volcanic column heights by eruption energetics and dynamics, *Jour. Geophys. Res.* 83, 1829-1836.

十和田火山の火砕地質

東京大学地震研究所 早川由紀夫

十和田火山の周囲には火砕堆積物がよく露出し、テフラ層序学的手法を用いて過去の噴火を定量的に研究できる。多数の火砕堆積物層が累重した地層断面には、火山活動の休止期間に形成された土壌層が何層かはさまれており、それにより1回の噴火エピソードが定義される。すなわち1回の噴火エピソードによって生じた火砕堆積物は内部に土壌層をはさまない一連の地層として認識される。約20回の噴火エピソードによる火砕堆積物の層序・分布が詳しく記載された。分布は等層厚線図および等粒径線図(軽石の最大粒径、石質岩片の最大粒径、堆積物の中央粒径)を作成することによって示された。

約100万年前、現在の十和田火山の地域には子ノ口層を堆積させていた湖の周囲に、南八甲田火山、十和田山火山、爺倉岬火山など数座の中小火山が点在し、奥入瀬水底スコリア丘によって示されるような玄武岩質マグマの噴火活動と、白色降下軽石・火山灰によって示されるようなデイサイト～流紋岩質マグマの噴火活動がおこなわれていた。数10万年前、現在の田代平カルデラの位置から大規模火砕流を含む数回の噴火エピソードが起こり、石ヶ戸凝灰岩が堆積し、ところによっては100 m に達する厚さで湖が埋めつくされた。

約20万年前、十和田火山の噴火活動が始まり、比較的小規模な成層火山である青樫火山と発荷火山がまず形成された。青樫火山は大部分火砕物からなり、2枚の玄武岩質安山岩溶岩流をはさむ。発荷火山は大部分玄武岩質安山岩溶岩からなり、一部にスコリア流堆積物を露出する。

約5.5万年前からカルデラ形成期にはいり、山体の破壊が始まった。1.3万年前までの約4万年間に3回の大規模火砕流の噴出を含む6回以上の噴火エピソードによって現在の十和田湖カルデラが形成された。カルデラ完成後ほとんど時を置かずに後カルデラ噴火活動が始まり、短期間内に五色岩火山がカルデラ中心よりやや南寄りに生じた。その後数回のプリニー式噴火によりその火口は徐々に拡大され、5,400年前の噴火エピソード中の金ヶ沢軽石噴火の際にその火口は外湖と連結され、湖水が流入しほぼ現在の中湖火口となった。その時火口内に流入する湖水と噴出するマグマとの相互作用でマグマ水蒸気爆発が生じ、宇樽部火山灰が堆積した。

中湖火口壁には五色岩火山の内部構造がよく露出する。湖水面直上には水中堆積の火砕岩が見られ、その上に陸上堆積の火砕岩と溶岩が重なる。それらを日暮岩・烏帽子岩・猿子崎などの放射状岩脈群が貫ぬいている。瞰湖台に露出する溶結した降下火砕堆積物は、8,500年前の南部軽石であり、十和田火山から73 km 離れた三陸海岸種市町まで追跡される。

十和田火山最新の噴火は平安時代(おそらく西暦915年)に起こった大湯降下火砕堆積物、毛馬内火砕流堆積物、および御倉山溶岩円頂丘を噴出した噴火エピソードである。最近1万年間の噴火エピソードは7回を数え、十和田火山は現在も活動状態にあると言える。

十和田火山の岩石は玄武岩質安山岩から流紋岩質デイサイト(SiO_2 51~70%)まで変化に富む。斜長石・普通輝石・シソ輝石・磁鉄鉱の斑晶が常に含まれ、カンラン石がしばしば見られる。普通角閃石は1.3万年前の八戸火砕堆積物中に特徴的に見られる。

後カルデラ噴出物のうち中振軽石と南部軽石について結晶法(WALKER, 1980)により総重量を測定した。得られた値は、前者が 4.01×10^{15} g、後者が 0.97×10^{15} gである。降下火砕堆積物の総重量(あるいは総体積)を求める方法として結晶法は優れているが、大量の粒度分析と構成物組成分析を必要とするため、適用には多くの困難が伴う。多くの降下火砕堆積物は、層厚 T と、それが囲む面積 S の積 TS が T によらずほぼ一定であるという性質を持つ。そこで、1本の等層厚線が得られれば総体積 V を計算することができる経験式

$$V=12.2 TS$$

を提案する。定数は結晶法によって総体積が知られている5つのプリニー式堆積物の平均値を採用した。この経験式を用いて計算すると、日本のプリニー式降下火砕堆積物の最大は 125 km^3 、最小は 0.11 km^3 であり、両者の間には1,000倍のバリエーションが存在する。十和田火山の過去5.5万年間の噴出物総重量は 1.5×10^{17} gに達する。これは1,000年あたり 1.1 km^3 のマグマが地表に噴出している割合である。

降下火砕堆積物の分布は、噴煙柱の高さ、噴火時の風ベクトル、および噴煙柱の粒度組成に支配

される。粒径図上で分布軸から直交方向への最大到達距離 R_c を測定することにより、その大きさの粒子が噴煙柱内で到達した最大高度を推定できる。 R_c と噴出総重量の相関を調べると、両者には正の相関関係があることがわかる。

日本のブリー式降下火砕堆積物の92%は火山の東方に分布する。これは、日本の位置する中緯度地域の上空約 10 km 付近にほとんど常に吹いている強い西風の影響を受けたためと考えられる。西方に分布する残り 8 % は、この西風が弱まり、成層圏に東風が吹く夏季に噴火したためであろう。南部軽石について噴火時の諸因子を推定した結果は次の通りである。直径 4 mm の石質岩片は噴煙柱内で高度 15 km まで達し、その後平均風速 30 m/s の西風によって東方に運ばれ、20分後に火口から 48 km 離れた地点に着地した。

噴煙柱内の粒度組成は、全堆積物粒度組成を測定することによって知られる。中振軽石の全堆積物粒度組成は南部軽石より細粒部分に富む。すなわち噴火時の他条件が全く同一であったなら、中振軽石は南部軽石より広く拡散されたはずである。

野外観察によると、中振軽石は大部分粗粒子からなり、一方八戸火山灰は大部分細粒子からなり、両者は著しいコントラストをなす。しかし、全堆積物粒度組成を比較すると細粒子が全体に占める割合に関して両者に有意の差は見られない。八戸火山灰が野外で細粒な見かけを呈するのは、細粒火山灰が火山豆石として火山灰雲から早期に離脱したからである。八戸火山灰に代表される水蒸気マグマ噴火は、細粒物質を大量に生産することが特徴であるとこれまで考えられてきたが、むしろ水蒸気マグマ噴火においては、生産された細粒物質が火山灰雲中で凝集しやすいため火口近傍の堆積物が著しく細粒に見えるにすぎないと考えたほうがよい。